Ana Catarina Vieira Lopes

Licenciada em Genética e Biotecnologia

Sperm telomere length in patients undergoing infertility treatments: prospective study

Dissertação para obtenção do Grau de Mestre em
Genética Molecular e Biomedicina

Orientador: Professor Doutor Mário Manuel da Silva Leite Sousa, Instituto de Ciências Biomédicas Abel Salazar da Universidade do Porto
Co-orientador: Professor Doutor Carlos Pedro Fontes Oliveira, Instituto de Ciências Biomédicas Abel Salazar da Universidade do Porto

Júri:

Presidente: Professora Doutora Paula Maria Theriaga Mendes Bernardo Gonçalves
Arguente: Professora Doutora Maria de Lourdes Gomes Pereira
Vogal: Professor Doutor Mário Manuel da Silva Leite Sousa

FACULDADE DE CIÊNCIAS E TECNOLOGIA
UNIVERSIDADE NOVA DE LISBOA

Setembro de 2018

Ana Catarina Vieira Lopes

Licenciada em Genética e Biotecnologia

Sperm telomere length in patients undergoing infertility treatments: prospective study

Dissertação para obtenção do Grau de Mestre em
Genética Molecular e Biomedicina

Orientador: Professor Doutor Mário Manuel da Silva Leite Sousa, Instituto de Ciências Biomédicas Abel Salazar da Universidade do Porto

Co-orientador: Professor Doutor Carlos Pedro Fontes Oliveira, Instituto de Ciências Biomédicas Abel Salazar da Universidade do Porto

Setembro de 2018

Sperm telomere length in patients undergoing infertility treatments: prospective study

Acknowledgments

I would like to express my sincerely gratitude to all those who somehow contributed to make this project possible.

To the coordination of the master course in Molecular Genetics and Biomedicine, for enriching my scientific knowledge with a high-quality education.

To my supervisor, Professor Mário Sousa, who believed in me from the start and accepted me in his team in such a short notice. Who gave me the possibility to follow my preferences and attain my deepest expectations, trusting me with this project so promising. Thank you for your dedication and perseverance, for always being available to help and support me, for all the knowledge you transmitted me. I am surely a better professional today.

To my co-supervisor, Professor Pedro Oliveira, for all the wisdom and guidance provided, as well as for the patience and comprehension for all my doubts and delirious ideas. Your contribution was essential for me to stay focused on our goals.

To Professor Alberto Barros, who kindly accepted me in his clinic for sample collection, without which this project would not have been realizable. To the team members, Dr. Joaquina Silva, Dr. Soraia Pinto, Dr. Ana Gonçalves, Dr. Cláudia Osório, Dr. Paulo Viana, Dr. Nuno Barros and Manuela Tavares, for always finding the time to help and teach me despite your busy schedules. Mostly, thank you for receiving me so well and making me feel like a part of your family.

To Professor Rosália Sá, who provided the results from AB and TUNEL analysis, and to Dr. Maria João Pinho and Dr. Carolina Almeida, who realized the FISH analysis, enriching this project with the techniques of their expertise and making it possible for it to be completed in the given time.

To Professor Eduardo Rocha, for sharing his experience and remarkable knowledge in statistics, supporting me with the extensive data analysis.

To Professor Marco Alves and all my laboratory colleagues, Raquel, Susana, Ana Maria, Hugo, Rute, Crisóstomo, Tito, David, Bruno, Patricia and Juliana, for the mutual aid and constant good mood that created such a healthy work environment.

To all my friends, for distracting me and making me laugh even when it got arduous. Particularly, to Inês, Rodolfo and Pedro, who keep on showing me that no matter how far we are or how much time passes by, we will always look out for each other.

To Henrique, Rita and my parents, Cristina and Rui, whom I admire the most. Thank you for all the love, joy, care, support and inspiration. You always see me as someone greater than I truly am, but I definitely would not be the same without you.

Resumo

O comprimento dos telómeros em espermatozoides (STL) é um parâmetro promissor para a análise da qualidade espermática, podendo vir a elucidar os mecanismos moleculares subjacentes aos casos idiopáticos de infertilidade masculina, que representam quase metade dos casos de infertilidade masculina em todo o mundo. Os telómeros são estruturas de nucleoproteínas presentes nas extremidades dos cromossomas eucarióticos, cujas funções de proteção mantêm a estabilidade genómica. O seu papel na reprodução inclui uma intervenção ativa durante a gametogénese, fertilização e desenvolvimento pré-implantacional. Em consonância, estudos mostraram que o comprometimento da homeostase dos telómeros está associado à infertilidade masculina. Como os telómeros criticamente curtos têm a sua função afetada, a avaliação do STL poderá ser um método rápido e económico para a análise da qualidade dos espermatozoides e, assim, contribuir para melhorar o sucesso dos tratamentos de fertilidade. Esta hipótese é apoiada por vários estudos que associam o STL, de sémen em bruto, à qualidade espermática, resultados embriológicos e clínicos. Neste estudo, investigámos se essas associações são mantidas em espermatozoides purificados por *swim-up*. Para tal, avaliámos o STL relativo por Q-PCR, em espermatozoides purificados de pacientes submetidos a tratamentos de infertilidade. Não se observaram correlações significativas entre o STL e a qualidade espermática, sugerindo a importância do método de seleção de espermatozoides utilizado para isolar a população espermática de mais alta qualidade. Adicionalmente, observámos que a maioria da população apresenta um STL associado a 29,6% de taxa de gravidez, enquanto que um STL mais elevado está presente numa fração reduzida da população, mas em que as taxas de gravidez são superiores (40%). Assim, o aumento do STL parece estar relacionado ao aumento das taxas de gravidez. Estudos adicionais serão essenciais para esclarecer se o STL é um biomarcador adequado da infertilidade masculina, antes de ser rotineiramente implementado em centros de reprodução medicamente assistida.

Palavras-chave: espermatozoides; telómeros; reprodução humana; infertilidade masculina; tecnologia de reprodução assistida.

Abstract

Sperm telomere length (STL) is a promising new parameter for sperm quality analysis that may elucidate the molecular mechanisms underlying the idiopathic cases of male factor infertility, which represent almost half of all the male factor infertility cases worldwide. Telomeres consist of nucleoprotein structures present at the ends of eukaryotic chromosomes, whose protective functions maintain the genomic stability. Their role in reproduction includes an active intervention during gametogenesis, fertilization and preimplantation embryo development. In consonance, studies have shown that compromised telomere homeostasis is associated with male infertility. Since critically short telomeres have their function affected, assessing STL may be a fast and economic method for sperm quality analysis and expectantly contribute to improve the success of fertility treatments. This hypothesis is supported by several reports associating STL, in raw semen, with sperm quality, embryological and clinical outcomes. In this study we intended to investigate if these associations are maintained in swim-up purified sperm. For that, relative STL was measured by Q-PCR in purified sperm from patients undergoing infertility treatments. No significant correlations were observed between STL and sperm quality parameters, suggesting the importance of the sperm selection method used to isolate the highest quality sperm population. In addition, we observed that most of the population presents a STL associated with 29.6% of pregnancy rate, while higher STL measures are present in a reduced fraction of the population, but in which the pregnancy rates are higher (40%). Therefore, we provide insights that higher STL is related with higher pregnancy rates. Further research is essential to clarify the suitability of STL as a biomarker for male infertility, before it could be routinely implemented in medically assisted reproduction centers.

Key words: sperm; telomeres; human reproduction; male infertility; assisted reproductive technology.

Table of Contents

Figures Index

Tables Index

Abbreviations List

4-HNE	4-hydroxynoneal
AB	Aniline blue
Abs	Absorbance
$Abs_{260/230}$	Ratio between the absorbances measured at 260 nm and 230 nm
$Abs_{260/280}$	Ratio between the absorbances measured at 260 nm and 280 nm
ALT	Alternative lengthening of telomeres
AMH	Anti-müllerian hormone
ART	Assisted reproductive technology
AT	Asthenoteratozoospermia
ATM	Ataxia–telangiectasia mutated
ATR	Ataxia–telangiectasia and Rad3-related
AVR	Acrosomal vesicle region
AZ	Asthenozoospermia
B2M	Beta-2-microglobulin
BCA	Bicinchonimic acid
bFSH	Baseline follicle stimulating hormone
BP	Biochemical pregnancy
BSA	Bovine serum albumin
C	Cytosine
CO_2	Carbon dioxide
COC	Cumulus-oocyte complexes
Conc	Concentration
CP	Clinical pregnancy
C_t	Cycle threshold
Cu	Copper
DAPI	4',6-diamino-2-phenylindole
D-loop	Displacement loop
DNA	Deoxyribonucleic acid
DNP	2,4-dinitrophenyl
DNPH	2,4-dinitrophenylhydrazine
ds	Double strand
DTT	1,4-dithiothreitol
dUTP	Deoxyuridine triphosphate
ECL	Electrochemiluminescence
ER	Equatorial region
FISH	Fluorescent in situ hybridization
G	Guanine
G4	G-quadruplexes

GnRH	Gonadotropin-releasing hormone
H	Head
HDR	Homology-directed repair
HEPES	4-(2-hydroxyethyl)-1-piperazineethanesulfonic acid
HMG	Human menopausal gonadotropin
HRP	Horseradish peroxidase
hSTBP	Human sperm telomere binding protein
hTERT	Human telomerase reverse transcriptase
hTR	Human RNA component
ICSI	Intracytoplasmic sperm injection
IgG	Immunoglobulin G
IVF	In vitro fertilization
LTL	Leucocyte TL
MII	Mature oocytes at metaphase II of meiosis
M-PER	Mammalian Protein Extraction Reagent
N_2	Nitrogen
NHEJ	Nonhomologous end-joining
NM	Normal morphology
NZ	Normozoospermia
O_2	Oxygen
OA	Oligoasthenozoospermia
OAT	Oligoasthenoteratozoospermia
OP	Ongoing pregnancy
OT	Oligoteratozoospermia
OZ	Oligozoospermia
PAR	Post-acrosomal region
PB	Polar bodies
PBS	Phosphate buffered saline
PM	Progressive motility
PN	Pronuclei
POT1	Protection of telomeres protein 1
PVDF	Polyvinylidene difluoride
Q-PCR	Quantitative polymerase chain reaction
Rap1	Repressor activator protein
rFSH	Recombinant follicle stimulating hormone
rHCG	Recombinant choriogonadotropin alpha
rLH	Recombinant luteinizing hormone
RNA	Ribonucleic acid
ROS	Reactive oxygen species
RPLP0	Ribosomal protein lateral stalk subunit P

RPM	Rapid progressive motility
RT	Room temperature
S phase	Synthesis phase
sDNAfrag	Sperm DNA fragmentation
SDS	Sodium dodecyl sulfate
spH2B	Sperm variant of histone H2B
SPM	Sperm preparation medium
ss	Single strand
SSC	Saline-sodium citrate buffer
STL	Sperm TL
TA	Telomerase activity
t-circle	Telomeric circle
TdT	Terminal deoxinucleotidil transferase
TEP1	Telomerase-associated protein 1
TERRA	Telomeric repeat-containing RNA
TFA	Trifluoracetic acid
tid	Three times a day
TIN2	TRF1-interacting nuclear protein 2
TL	Telomere length
T-loop	Telomeric loop
TM	Total motility
TPP1	Tripeptidyl peptidase 1
TRF1	Telomere repeat binding factor 1
TRF2	Telomere repeat binding factor 2
TSC	Total sperm count
TUNEL	Terminal deoxynucleotidyl transferase dUTP nick end labelling
TZ	Teratozoospermia
WHO	World Health Organization

List of Statistical Symbols

%	Percentage
LOG	Logarithm
n	Sample size
p	*P*-value
Q1, Q2, Q3, Q4	First, second, third and fourth quartile
r_p	Pearson's correlation coefficient
r_s	Spearman's rank correlation coefficient
SD	Standard deviation
SQRT	Square root

List of Units

°C	Celsius degrees
h, min, sec	Hour; minute; second
IU, mIU	International units, milliinternational units
kb; bp	Kilo base pair; base pair
M, mM	Molar, millimolar
mg, µg, ng, pg	Milligram, microgram, nanogram, picogram
mL, µL	Milliliter, microliter
µm, nm	Micrometer, nanometer
rpm	Rotations per minute

The ***Introduction*** chapter was adapted from the review article entitled “Shedding light into the relevance of telomeres in human reproduction and male factor infertility”, by Ana Catarina Lopes[1,2], Pedro F. Oliveira[1,3,4], Mário Sousa[1,5], accepted for publication by the journal “Biology of Reproduction” (https://doi.org/10.1093/biolre/ioy215).

[1]Laboratory of Cell Biology, Department of Microscopy, and Multidisciplinary Unit for Biomedical Research (UMIB), Institute of Biomedical Sciences Abel Salazar (ICBAS), University of Porto, 4050-313 Porto, Portugal.

[2]Department of Life Sciences, Faculty of Science and Technology, New University of Lisbon (FCT-UNL), Campus Caparica, 2829-516 Caparica, Portugal.

[3]Department of Genetics, Faculty of Medicine, University of Porto, 4200-319 Porto, Portugal

[4]i3S- Institute of Research and Innovation in Health, University of Porto, 4200-135 Porto, Portugal.

[5]Centre for Reproductive Genetics Professor Alberto Barros, 4100-009 Porto, Portugal.

1. Introduction

1.1 Telomeric nucleoprotein complex

Telomeres, a Greek word meaning “end part”, consist of specialized nucleoprotein structures present at the ends of eukaryotic chromosomes (**Figure 1.1 A**), being essential for cell division to proceed and properly occur (Blackburn, 1991). They were first recognized early in the twentieth century as having an important role in maintaining chromosomes intact by preventing their ends to be identified as DNA breaks and trigger rearrangements and fusions that lead to genomic instability (McClintock, 1941; Muller, 1938). Further research has revealed that the telomeric DNA sequences comprise short non-coding tandem repeats (Blackburn and Gall, 1978; Szostak and Blackburn, 1982) that protect chromosomes from terminal erosion and enable progressive shortening without causing genetic information loss (Blackburn, 1984).

1.1.1 Telomeric DNA

Most eukaryotic species possess telomeres with similar sequence repeats and structures, which reveals their importance for telomeres function (McEachern et al., 2000). Human telomeric DNA, in particular, contains a variable number of the 5'-TTAGGG-3' sequence, which is conserved among vertebrates (Meyne et al., 1989; Moyzis et al., 1988).

The structure of telomeres is also conserved, being double-stranded (ds) in most of its length, but presenting a G-rich single strand (ss), referred as the 3' overhang, at their 3'-end (Henderson and Blackburn, 1989). In humans the 3' overhang contains 35-600 nucleotides (**Figure 1.1 C**) (Samassekou et al., 2010; Wright et al., 1997). The invasion of the 3' overhang into the ds region of the telomere, mediated by specific proteins, forms a folded conformation at the chromosome terminus, known as the telomeric loop (T-loop; **Figure 1.1 B, D**). In this structure, the 3' overhang complementarily binds the C-rich strand in the duplex region, forming a displacement loop (D-loop) in the invaded site (**Figure 1.1 D**) (Griffith et al., 1999; Palm and de Lange, 2008). The T-loop structure is essential to sequester the ends of chromosomes and avoid their degradation and cellular recognition as damaged DNA (Griffith et al., 1999; Karlseder et al., 1999). G-quadruplexes (G4) structures are also recognized at the 3' overhang and result from the stacking of G-tetrads (**Figure 1.1 D**), each organized in a planar structure through Hoogsteen base pairing (**Figure 1.1 E**). Similar to the T-loop, G-quadruplexes are believed to stabilize and protect the telomere ends (Henderson et al., 1987; Lin and Yang, 2017).

Additionally, telomeres exhibit a heterochromatic state which is not transcriptionally silent (Azzalin et al., 2007; Tommerup et al., 1994). A highly conserved telomere noncoding transcript, the telomeric repeat-containing RNA (TERRA), comprising UUAGGG repeats and subtelomere sequences, with a length range of 100 bp-9 kb, has been identified (Azzalin et al., 2007). TERRA associates with the telomere heterochromatin and it is believed to play a role in the establishment and maintenance of the telomere structure (Reig-Viader et al., 2016).

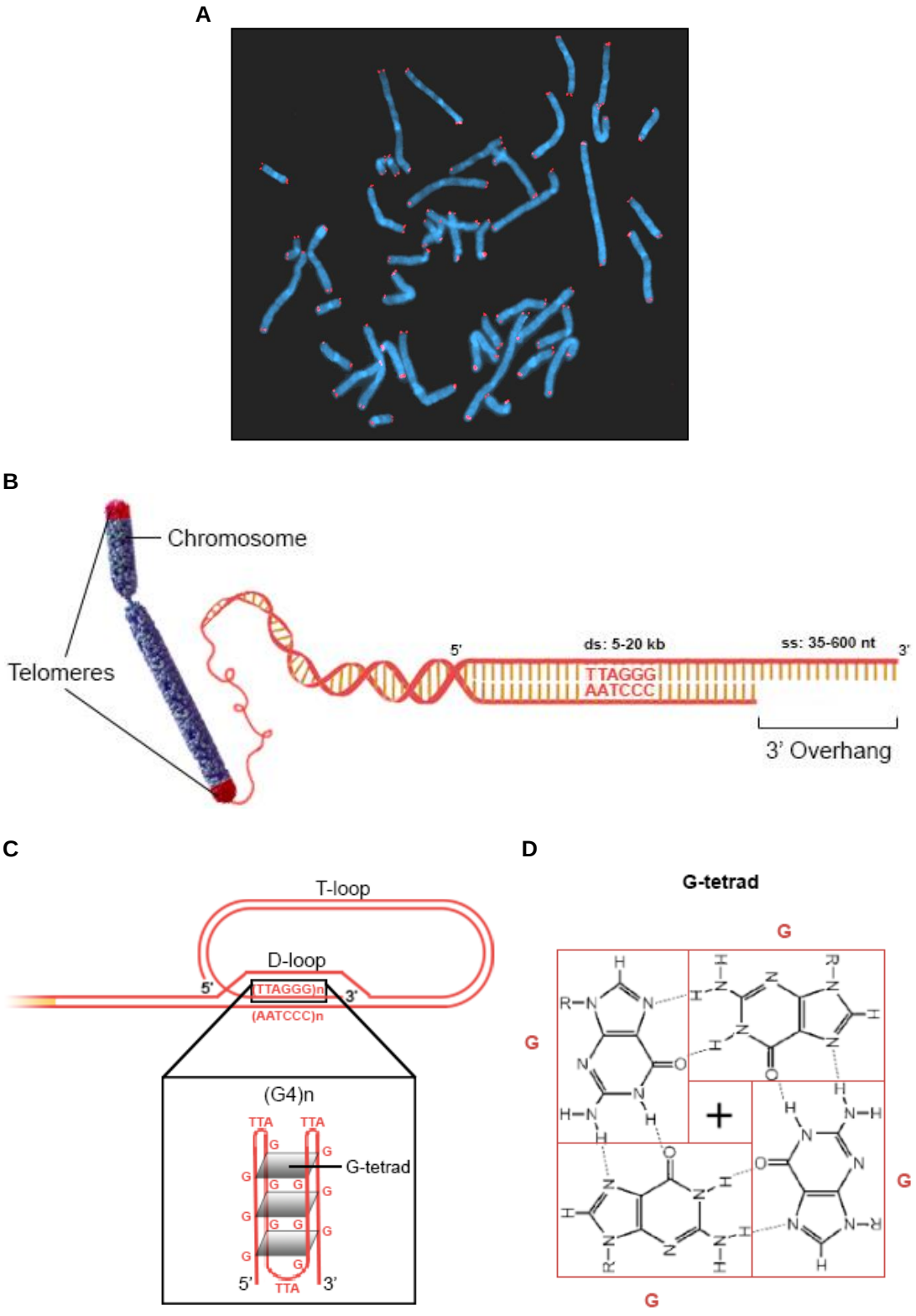

Figure 1.1 – The structure of human telomeres. (**A**) Human metaphase labeled with telomeric probes (red), evidencing the presence of telomeres in the extremity of all chromosomes, which are counterstained with DAPI (blue). (**B**) Schematic representation of the structure of human telomeres. (**C**) Schematic representation of the folding structures of the chromosome terminus: T-loop and G-quadruplexes (G4). (**E**) Schematic representation of G-tetrads, the building blocks of G4 that result from the association of four guanines by Hoogsteen hydrogen bonding, which is represented with dashed lines (N1-O6 and N2-N7). The G4 is stabilized by monovalent cations (+) present at the center of the G-tetrads. Adapted from Rhodes and Lipps, 2015. ds: double strand; ss: single strand; T-loop: telomeric loop; D-loop: displacement loop.

1.1.2 Telomeric binding proteins

The telomeric sequence repeats provide protein binding sites that allow the assembly of specific proteins, which in turn bind additional proteins to form a higher-order functional nucleoprotein complex at telomeres, the shelterin complex (de Lange, 2005). Similarly to telomeric DNA, homologous telomeric proteins are found throughout eukaryotic groups (McEachern et al., 2000).

Shelterin contains six subunits (**Figure 1.2**). The telomere repeat binding factors TRF1 and TRF2 accumulate throughout the ds region of telomeres and are both responsible for the folded conformation of the telomeric DNA, by promoting intratelomeric pairing (TRF1) and homologous ss invasion in the duplex telomeric region (TRF2) (Broccoli et al., 1997; Doksani et al., 2013; Griffith et al., 1999). In addition, TRF2 represses the Ataxia–telangiectasia mutated (ATM) kinase-dependent DNA damage signaling pathway (de Lange, 2009; Karlseder et al., 1999). On the other hand, the protection of telomeres protein 1 (POT1) binds the ss region of telomeres and it was suggested to be necessary to maintain their integrity (Baumann and Cech, 2001; Wu et al., 2006). In fact, POT1 represses the Ataxia–telangiectasia and Rad3-related (ATR) kinase-dependent DNA damage signaling pathway (de Lange, 2009; Denchi and de Lange, 2007). TRF2 and POT1 are also both responsible for repressing DNA repair mechanisms, namely nonhomologous end-joining (NHEJ) and homology-direct repair (HDR), preventing their harmful processing of telomeres (de Lange, 2009). Additionally, in the shelterin complex, the repressor activator protein (Rap1) interacts with TRF2 and the TRF1-interacting nuclear protein 2 (TIN2) interacts with TRF1 (Kim et al., 1999; Li et al., 2000). TIN2 also promotes TRF1 indirect interaction with TRF2 (Liu et al., 2004a). Most recently, the tripeptidyl peptidase 1 (TPP1), also known as TINT1, PTOP or PIP1, was identified as responsible for the interaction between TIN2 and POT1, which is thought to be crucial for POT1 telomere recruitment (de Lange, 2005; Ye et al., 2004). Therefore, TIN2 plays an essential role in the assembly of shelterin, holding together the TRF1-TIN2-TRF2 and POT1-TPP1 complexes (Nandakumar and Cech, 2013; Palm and de Lange, 2008). Other proteins (shelterin accessory factors) have been identified at telomeres and shown to be necessary to fulfill their own maintenance and function (Diotti and Loayza, 2011; Nandakumar and Cech, 2013; Palm and de Lange, 2008).

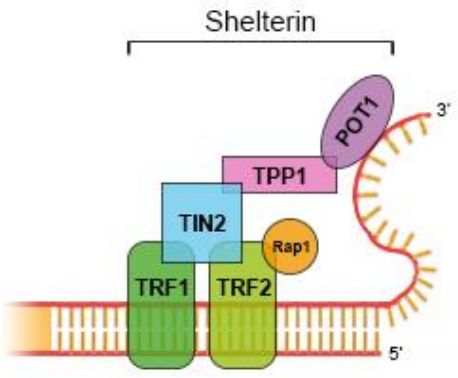

Figure 1.2 – Protein subunits of the shelterin complex.

1.2.3 Telomere capped functional state

The assembly of shelterin promotes a protective structural capped state of telomeres, through the establishment of the T-loop, in which their integrity is preserved and cell division proceeds normally, with proper chromosome segregation to daughter cells (Blackburn, 2001). Thus, telomere capping is considered a relevant factor to measure telomere function (Blackburn, 2000). On the contrary, the disruption of the telomeric nucleoprotein complex leads to an uncapped state, characterized by the unfolding of the chromosome terminus, leaving it exposed (Karlseder et al., 2002). Telomeric complexes are dynamic, being able to switch between the capped and uncapped physical states. According to this model, short telomeres that bind insufficient shelterin undergo uncapping (Blackburn, 2001; Palm and de Lange, 2008). In controlled conditions, uncapped telomeres will rapidly switch back to the capped state, but if left in the uncapped state for too long they will trigger either in cell senescence or apoptosis, mediated by the ATM or ATR kinase-dependent pathways (Blackburn, 2000; de Lange, 2009). Critically short telomeres become irreversible uncapped, which corresponds to the dysfunctional state, and may also enable NHEJ or HDR to occur, with deleterious consequences regarding genomic instability (Cesare and Reddel, 2010; de Lange, 2009; Galati et al., 2013). In sum, telomere length (TL) affects the capping state of telomeres, which regulates cell division (**Figure 1.3**). One sufficiently short telomere seems to be enough to affect the viability of the cell (Hemann et al., 2001b).

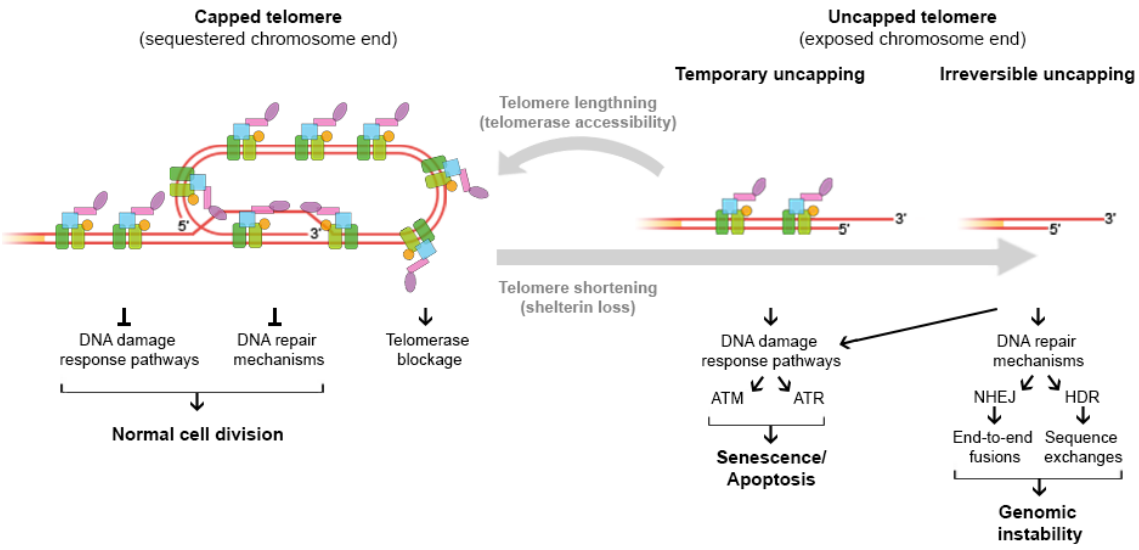

Figure 1.3 – The dynamics of telomeric complexes, switching between the capped and uncapped physical states.

1.2 The dynamics of telomere length

The number of telomeric sequence repeats present in a chromosome depends on the strictly regulated equilibrium between the shortening and lengthening processes occurring at the chromosome terminus (Blackburn, 2001). It has been shown that TL has high variability, including between individuals, cells of the same individual, chromosomes or even between the two ends of a single chromosome, which is explained by the heterogeneity of contributing factors to TL

modulation, including genetic, epigenetic, environmental and lifestyle (Samassekou et al., 2010; Thilagavathi et al., 2013c).

1.2.1 Telomere shortening

Telomeric DNA is subjected to shortening as a result of the “end-replication-problem” in which complete replication of the 3' terminus of the DNA template cannot be achieved by conventional DNA polymerases. Consequently, a blunt end and a 3' overhang are formed in the newly synthetized DNA leading and lagging strands, respectively, in each replicative round (**Figure 1.4**) (Olovnikov, 1973; Watson, 1972).

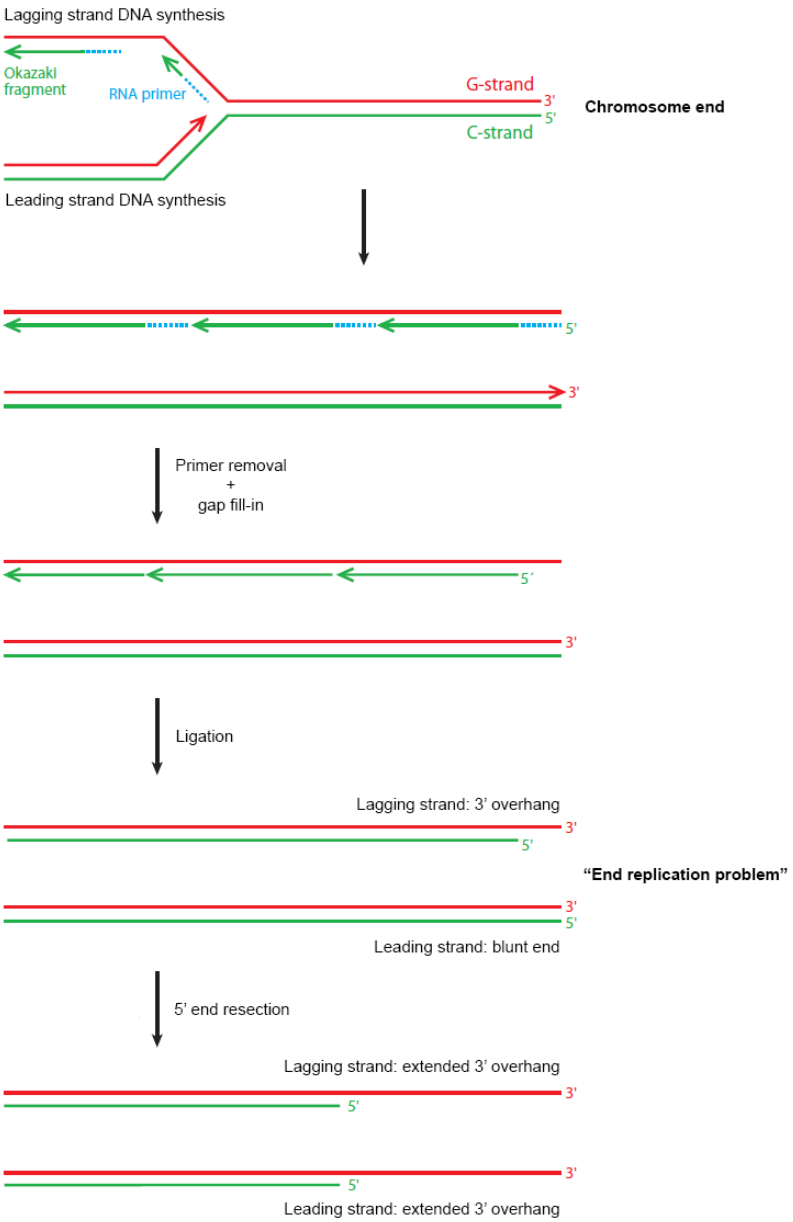

Figure 1.4 – The mechanisms of telomere shortening. The “end replication problem” forms a 3’ overhang in the lagging strand after primer removal, in each DNA replication round. 5’ end resection by the action of nucleases originates extended 3’ overhangs in both lagging and leading strands. Adapted from Palm and de Lange, 2008.

Although the “end replication problem” is the main cause of telomere progressive shortening, additional contributing factors have been identified, even in nondividing cells: the action of nucleases that digest the C-rich chromosome end and may originate extended 3' overhangs in both the DNA leading and lagging strands (**Figure 1.4**) (Chai et al., 2006); oxidative damage, to which telomeres are highly susceptible due to their G-rich repeat sequences (von Zglinicki, 2002); and rapid telomere deletion processes associated with recombination events (Pickett et al., 2009; Vidačeka et al., 2010).

It is estimated that the shortening rate of human telomeres is 50-200 bp per cell division (Samassekou et al., 2010). Without alternative replicative mechanisms, after several divisions telomeres would become progressively short and consequently uncapped, signaling the cell to stop dividing (replicative senescence) (Blackburn, 2001). Accordingly, the number of times a cell could divide would be limited by TL and thus telomeres became known as cellular mitotic clocks (Allsopp et al., 1992; Hayflick, 1965; Olovnikov, 1973).

1.2.2 Telomerase

The discovery of telomerase in 1985 revolutionized the understanding of the molecular mechanisms subjacent to telomere maintenance (Greider and Blackburn, 1985). Telomerase is a ribonucleoprotein reverse transcriptase that interacts at high affinity with telomeres and extends their 3' overhang, during the S phase (**Figure 1.5**) (Greider and Blackburn, 1987; Wright et al., 1999). The core of telomerase is conserved and contains two subunits. In humans, these subunits are referred as the human telomerase reverse transcriptase (hTERT), which is the catalytic subunit, and the human RNA component (hTR). Both are necessary but not sufficient for the activity of the enzyme in vivo (Feng et al., 1995; Nakamura et al., 1997; Weinrich et al., 1997). Additional proteins in the telomerase complex are needed to interact with the telomeric complex (Schmidt and Cech, 2015). hTR comprises the 3'-CAAUCCCAAUC-5' sequence that recognizes and complementary binds the telomeric 3' overhang, then acting as a template for DNA primer extension by hTERT. Several 5'-GGTTAG-3' sequence units are subsequently added, in successive repositioning and extension steps. Posteriorly, Okazaky-type synthesis allows the fill-in of the complementary C-rich strand (Price, 1997; Schmidt and Cech, 2015). The telomere-telomerase complex suffers continuous assembly and disassembly, dynamically maintaining a TL homeostasis (Blackburn, 2001). This process is regulated by several proteins, including the shelterin complex. This process is regulated by several proteins, including the shelterin complex. Shelterin negatively regulates TL through physical blocking of telomerase, preventing its accessibility to telomeres (Nandakumar and Cech, 2013; Samassekou et al., 2010; Stern and Bryan, 2008). Thus, telomerase preferentially binds short telomeres due to their decreased number of inhibitory bonded shelterin (Schmidt and Cech, 2015; Smogorzewska and de Lange, 2004; Stern and Bryan, 2008). Furthermore, shortened telomeres activate DNA damage signaling pathways, leading to ATM kinase recruitment, which phosphorylates TRF1, detaching it from the telomeric DNA and thus unblocking telomerase's access (Lee et al., 2015; Stern and Bryan, 2008; Wu et al., 2007). After the lengthening process, the telomere has higher probability to return to

the capped functional state (**Figure 1.3**) (Blackburn, 2001). In addition, telomerase is suggested to be a functional stabilizer of telomeres, regardless of their length, avoiding uncapped state cellular responses driven when telomeres shorten (Blackburn, 2001). Actually, it was reported that hTERT may induce the association of telomeres with the nuclear matrix, which signals gene expression to upregulate DNA repair-associated genes and down-regulate senescence-associated genes, contributing to overall genomic stability (Sharma et al., 2003).

Nevertheless, not all cell types display telomerase activity (TA). Consequently, in the absence of telomerase, telomere shortening leads to the permanent uncapped state (Blackburn, 2001). In fact, most human somatic cells do not display TA. It is only expressed in germ cells, tissues of developing embryos and stem cells. However, human adult stem cells express only a limited TA, which is able to reduce telomere shortening but it is not sufficient to avoid it (Forsyth et al., 2002). This explains why human somatic cells contain telomeres with lower length (approximately 5-10 kb) comparatively to germ cells (approximately 10-20 kb) (Thilagavathi et al., 2013c). Therefore, telomeres become progressively shortened with aging, resulting in an increase of senescent cells in a population (Forsyth et al., 2002), negatively affecting the regenerative capacity of tissues that leads to the development of age-related characteristics, such as chronic diseases (Liu, 2014; Tchkonia et al., 2013; Zhao et al., 2014). Curiously, telomere shortening is more pronounced in men than in women, which can be related to women's higher levels of estrogen, that not only has antioxidant properties but also activates telomerase (Kyo et al., 1999; Thilagavathi et al., 2013c). The shortest quartile of TL is an indicative of aberrantly short telomeres in humans (Calado and Young, 2009; Jang et al., 2008). Specifically, loss of tissue function and disease onset have been associated with TL<4 kb (Alter et al., 2007; Calado and Young, 2009; Harley et al., 2011).

Telomerase-based therapies to lengthen telomeres have been developed, aiming for a health enhancement during aging and reduction of mortality. Clinical fields such as tissue engineering, regenerative medicine and infectious diseases associated with accelerated immunosenescence could also benefit from these therapies. Different therapeutic strategies include: gene therapy with transfection of telomerase sequences, re-expression of silenced telomerase, activation of residual TA and modulation of its intracellular location (Jäger and Walter, 2016). Pharmacologic telomerase activators may be more promising in comparison with approaches such as gene therapy, due to a higher control of duration and dosage effects (Fauce et al., 2008). For example, cycloastragenol (commercialized as TA-65) is a telomerase activator derived from the root of *Astragalus membranaceus*, which was shown to be effective in immune cells, neonatal keratinocytes and fibroblasts in culture (Fauce et al., 2008; Harley et al., 2011). In vivo studies revealed an increase of leucocyte TL (LTL) in subjects taking TA-65 (Harley et al., 2011; Salvador et al., 2016). Likewise, TA-65 diet supplementation in mice promoted the elongation of critically short telomeres and the improvement of organ fitness (Bernardes de Jesus et al., 2011).

Replicative senescence is believed to be a protective mechanism against cancer. If cells with critically short telomeres continued to divide, they would induce genomic instability and thus

facilitate malignant cell transformation (Shay and Wright, 2011). Additionally, replicative senescence would prevent a tumor cell population to divide indefinitely (Forsyth et al., 2002). Telomerase is active in most cancers (85-90%) as a result of genetic mutations, thus allowing limitless cell proliferation, even when cells have short telomeres (Shay, 2016). Although TA-65 intake did not increase cancer incidence in mice (Bernardes de Jesus et al., 2011), it is still not known if systemic telomerase upregulation as a rejuvenation therapy could elicit carcinogenesis in long-lived organisms, such as humans (Jäger and Walter, 2016).

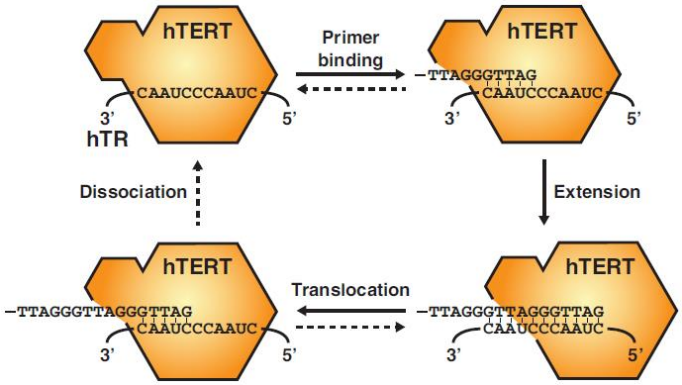

Figure 1.5 – Schematic representation of the telomerase catalytic cycle. Adapted from Schmidt and Cech, 2015.

1.2.3 Alternative lengthening of telomeres

Human cell lines and certain types of cancer (10-15%) show telomere maintenance in the absence of telomerase. This occurs through a mechanism of alternative lengthening of telomeres (ALT) (Bryan et al., 1997; Cesare and Reddel, 2010; Reddel, 2003). Whether ALT also occurs under normal physiological conditions is not yet clarified (Conomos et al., 2013).

The ALT model is based on recombination events, occurring mainly during the S phase, and in which a telomere complementary binds another telomere, used as a copy template of the telomeric DNA sequence, enabling telomere elongation by the cell machinery responsible for DNA replication. This copy template may be: another region of the same telomere, through a T-loop intermediate; the telomere of a sister chromatid or of another chromosome; or even extrachromosomal telomeric DNA, characteristically found in ALT cells (Cesare and Reddel, 2010; Min et al., 2017; Pickett and Reddel, 2015). The origin of extrachromosomal telomeric DNA repeats is still ununderstood, but possibly result from telomeric DNA fragmentation or telomere trimming, a process that has been described to maintain a TL equilibrium (Kurjanowicz et al., 2017; Pickett et al., 2009; Pickett and Reddel, 2012). In telomere trimming, overlengthened looped telomeric DNA is excised trough homologous recombination, originating extrachromosomal telomeric circles (t-circles) (Pickett et al., 2011).

Comparatively to the telomerase-dependent telomere lengthening, ALT tends to originate longer telomeres, incrementing their length by thousands of bp, while telomerase adds only 50-150 bp per cell division (Liu et al., 2007). Also, ALT generates higher TL variability, due to its preferential action at the 3' overhang of the lagging strand, whereas telomerase leads to the

formation of 3' overhangs with similar lengths in the leading and lagging strands (Chai et al., 2006; Min et al., 2017).

1.3 Telomeres in human reproduction

The importance of telomeres in maintaining genomic stability during cell division is well established. However, telomeres display additional functions in human meiosis, which implies also a role of telomeres in gametogenesis, fertility and reproduction.

While in somatic cells telomeres are associated to the nuclear matrix (de Lange, 1992), in germ cells entering meiosis telomeres attach the nuclear envelop, by protein mediation (Scherthan, 2007). During prophase I telomeres undergo polarized clustering, forming a bouquet, which promotes alignment and pairing of homologous chromosomes, synapsis, establishment of chiasma and of the functional spindle, which are necessary for proper chromosome segregation (Klutstein et al., 2015; Reig-Viader et al., 2016; Scherthan, 2007).

Telomerase is strongly activated in germ cells to ensure that a maximum TL is transmitted to the offspring trough gametes, but variable TL seems to be inherited (Baird et al., 2006; Graakjaer et al., 2006; Samassekou et al., 2010). At fertilization the inherited TL is responsible for setting an initial zero-time length mark and the replicative cell potential, from which zygote telomeres undergo progressive shortening trough successive cell divisions (Brenner et al., 1999; Kozik et al., 1998). Telomere attrition is maximum in the first year of life, due to the high division rate, decreasing in adulthood (Thilagavathi et al., 2013c). Differences observed in telomere dynamics of male and female germ cells (Keefe et al., 2015; Keefe, 2016) and in the biological effects during gametogenesis (De Meyer and Eisenberg, 2015) appear to lead to asymmetrical maternal and paternal contributions to embryo fate.

1.3.1 Telomeres in spermatogenesis and sperm

Spermatogenesis initiates in puberty and continually ensues throughout men lifespan. In the testicular seminiferous tubules, spermatogonia differentiate into sperm, whose final functional maturation occurs in the epididymis. Spermatogonia undergo mitotic proliferation and some differentiate into primary spermatocytes. Primary spermatocytes give origin to secondary spermatocytes, after the first meiotic division, and secondary spermatocytes form round spermatids after the second meiotic division. Round spermatids posteriorly maturate trough spermiogenesis into differentiated sperm (Sharma and Agarwal, 2011).

During the meiotic stages of human spermatogenesis, telomeres are reorganized in a well-defined nuclear architecture, together with the spatial disposition of functional chromosome territories (Mudrak et al., 2005; Mudrak et al., 2012). A peripheral localization of telomeres in the sperm nucleus was initially reported (Zalensky et al., 1995), although recently a more segmental reproducible distribution of telomeres throughout the sperm nucleus has been suggested, in which telomeres are found either in the nuclear periphery, interior or in an intermediate position (Ioannou et al., 2014; Ioannou et al., 2017). In addition, telomeres form clusters of dimers or tetramers, inducing looped chromosome conformations, which become more evident during

spermiogenesis (Ioannou and Tempest, 2016; Moskovtsev et al., 2010; Solov'eva et al., 2004; Zalensky et al., 1997). The interactions between telomeres and their attachment to the nuclear envelop were proposed to involve the human sperm telomere binding protein (hSTBP) complex, that only binds the telomeric region. The hSTBP complex contains a sperm variant of histone H2B (spH2B), but not the somatic shelterin proteins TRF1 and TRF2 (Gineitis et al., 2000; Zalensky et al., 1997).

During spermiogenesis, sperm chromatin is remodeled through the gradual replacement of somatic cell histones by sperm specific protamines, promoting a highly condensed transcriptionally inactive chromatin state, which is believed to have a genomic protection effect. However, 10-15% of sperm DNA remains organized in nucleosomes at non-random genomic regions that regulate embryogenesis (Rathke et al., 2014). Part of these remaining nucleosomes is found in sperm telomeres, making them readily responsive to oocyte's signals, which suggests that sperm telomeres have an essential role in male pronucleus formation and microtubule-guided movement at fertilization (Zalenskaya et al., 2000). A functional meaning was also attributed to the unique features of the human sperm nuclear architecture, whose chromosomal looping, established by telomeric interactions, and telomere position may facilitate an ordered and sequential exposure of sperm chromosomes to ooplasm components, during early fertilization. This results in a differential unpacking and activation of male's genome, believed to confer an additional level of epigenetic information for gene regulation in early development (Ioannou et al., 2017; Ioannou and Tempest, 2016; Solov'eva et al., 2004; Zalensky and Zalenskaya, 2007).

Telomere elongation during spermatogenesis may also contribute to the formation of the characteristic nuclear architecture referred (Kozik et al., 1998). Telomerase is active in fetal, newborn and adult testes (Kim et al., 1994; Wright et al., 1996). *hTR* expression, an indicator of TA, appears to increase from spermatogonia to primary spermatocytes, decreasing in secondary spermatocytes and ceasing in spermatids and sperm (**Figure 1.6**) (Yashima et al., 1998). Concordantly, TL is maximal in primary spermatocytes, further decreasing in spermatids and sperm (**Figure 1.6**) (Jørgensen et al., 2013). Collected evidence suggest that telomerase guided telomere lengthening occurs during spermatogonia proliferation or in the premeiotic S phase, but not during the remainder spermatogenesis. In this model, telomerase, along with TERRA, would only have a structural function in stabilizing telomeres during spermiogenesis, where complex chromosome reorganizations take place (Reig-Viader et al., 2016; Reig-Viader et al., 2014b). This hypothesis has also been proposed for oocytes (Reig-Viader et al., 2013).

Human sperm TL (STL) is highly heterogeneous and it appears to increase with age (Allsopp et al., 1992; Antunes et al., 2015; Aston et al., 2012; Baird et al., 2006; Kimura et al., 2008; Turner and Hartshorne, 2013; Yang et al., 2015b), while LTL undergoes age-related erosion (Allsopp et al., 1992; Aston et al., 2012; Kimura et al., 2008; Njajou et al., 2007). This phenomenon may be explained by: over-activation of telomerase in male germ cells (Aston et al., 2012); an alternative mechanism, like ALT, in male germ line, that could be induced by telomere dimers and tetramers and thus easily explaining the high STL heterogeneity (Antunes et al., 2015); selective death of germ cells, in which only those with longer telomeres would survive to the effects of aging

(Hjelmborg et al., 2015; Kimura et al., 2008); or different environment exposure (Jørgensen et al., 2013). Also, paternal age is positively associated with LTL (Broer et al., 2013; De Meyer et al., 2007; Eisenberg et al., 2012; Kimura et al., 2008; Njajou et al., 2007; Unryn et al., 2005) and STL (Ferlin et al., 2013; Yang et al., 2015b) in their offspring, thus confirming the TL heritability. The successive increase of LTL in the offspring of older males throughout multiple generations could have an adaptive effect, resulting in enhanced longevity and higher preparation for delayed reproduction (Eisenberg, 2011; Eisenberg et al., 2012). However, an alternative model has been suggested to explain the increased STL found in older men: the "birth-cohort effect". This means that males born in previous generations have longer STL comparatively to younger males as a result of "intergenerational telomere erosion" in the female germline (Stindl, 2016). Additionally, the increased heterogeneity of STL with age could be the result of environmental and thus non-inheritable factors (Nordfjall et al., 2010; Stindl, 2016).

1.3.2 Telomeres in oogenesis and oocytes

During the fetal life, oogenesis proceeds from oogonia, which undergo mitosis and originate primordial follicles that remain arrested at prophase I. After puberty, at each menstrual cycle, a selected primordial follicle evolves into a preovulatory follicle that is retained in metaphase II. Meiosis completion is only achieved after successful fertilization (Johnson, 2013). Therefore, primordial follicles can be kept in a quiescent state in the ovaries up to menopause (Reig-Viader et al., 2016).

Similarly to males, TA was detected in fetal, newborn and adult ovaries (Kim et al., 1994; Wright et al., 1996). In fact, it is present in all oogenesis states, but it decreases during oocyte maturation (**Figure 1.6**) (Wright et al., 2001). Since immature oocytes have the highest levels of TA, oocyte telomere elongation might occur during early oogenesis. However, telomeres shorten during oogenesis (**Figure 1.6**) (Turner and Hartshorne, 2013). Several factors may be responsible for oocyte telomere attrition: impaired TA, chronic exposure to reactive oxygen species (ROS) during meiotic arrest; and the "end-replication-problem" in proliferative oogonia (Keefe et al., 2006). A theory suggests that late ovulating follicles, which reinitiated meiosis last, experience more mitotic divisions in fetal oogenesis and thus present increased telomere shortening comparatively to early ovulating follicles (Henderson and Edwards, 1968; Polani and Crolla, 1991). Therefore, advanced maternal age was correlated with shorter oocyte telomeres, contributing to reproductive aging, which is characterized by declined oocyte number and function, and clarifying the female induced "intergenerational telomere erosion" mentioned above (Kalmbach et al., 2015; Keefe et al., 2006; Stindl, 2016). Consensually, and corroborating the TL heritability belief, experimental evidence has shown that telomeres in human embryos decrease with advanced maternal age (Mania et al., 2014).

1.3.3 Telomeres in embryonic development

TA decreases significantly from immature oocytes to mature oocytes and zygotes, then decreases non-significantly through cleavage stage embryos and rises significantly at the morula

stage, resuming the immature oocytes' levels at the blastocyst stage (**Figure 1.6**) (Wright et al., 2001; Wright et al., 1996). Notwithstanding, TA has not been correlated with embryo development potential (Wang et al., 2004; Wright et al., 2001). In parallel with TA, TL decreases from immature oocytes to cleavage stage embryo, varying greatly between blastomeres, and further increases at the blastocyst stage (**Figure 1.6**) (Treff et al., 2011; Turner et al., 2010). From the blastocyst stage until 16-20 weeks of gestation, most somatic tissues express high levels of telomerase, which are no longer present in the neonatal period. Thus, telomerase is repressed with increased differentiation, in a tissue specific, gestational-age dependent manner (Forsyth et al., 2002; Ulaner and Giudice, 1997; Wright et al., 1996).

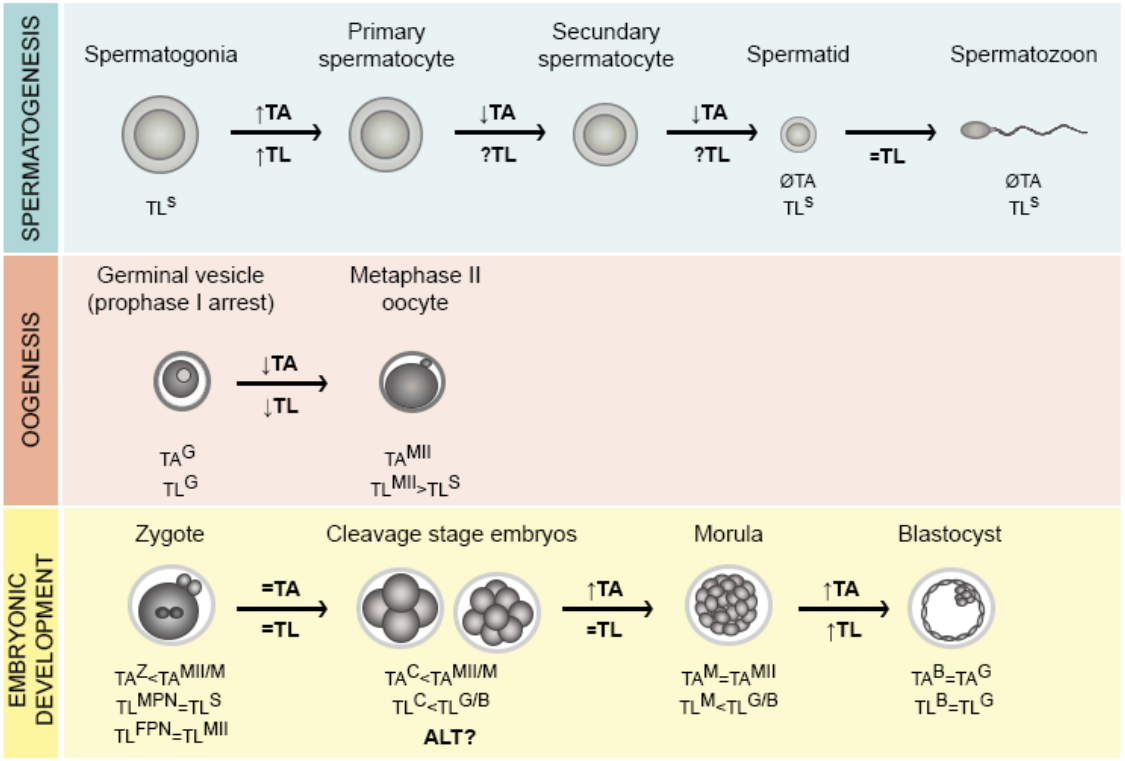

Figure 1.6 – Diagram with the relative variance of telomerase activity (TA) and telomere length (TL) throughout the different stages of spermatogenesis, oogenesis and embryonic development. In **spermatogenesis**, TA increases from the spermatogonia to the primary spermatocyte, decreases in the secondary spermatocyte and ceases (ØTA) in the spermatid and spermatozoon (Yashima et al., 1998), while TL increases from the spermatogonia to the primary spermatocyte and again decreases to the same TL of the spermatogonia in both the spermatid and spermatozoon (TL^S) (Jørgensen et al., 2013). In **oogenesis**, TA and TL decreases from the germinal vesicle to the metaphase II oocyte (Turner and Hartshorne, 2013; Wright et al., 2001). The TL of metaphase II oocytes (TL^{MII}) is usually higher than the TL of sperm (Turner and Hartshorne, 2013). TA further decreases from the metaphase II oocyte (TA^{MII}) to the zygote (TA^Z) (Wright et al., 2001). In zygotes, the TL of female pronucleus (TL^{FPN}) does not change from TL^{MII}, the same happening to the TL of male PN (TL^{MPN}), which is equal to TL^S. Thus, TL^{FPN} is higher than TL^{MPN} (Turner and Hartshorne, 2013). During **embryonic development**, TA does not alter significantly from the zygote to the different cleavage stage embryos (TA^C), but increases at the morula stage (TA^M), equalizing TA^{MII}. TA further increases at the blastocyst stage (TA^B), in which the TA of the germinal vesicle (TA^G) is resumed (Wright et al., 2001). TL decreases from the germinal vesicle (TL^G) to cleavage stage embryos (TL^C), in which alternative lengthening of telomeres (ALT) can possible occur to maintain telomere stability, explaining the high variability of TL between blastomeres. TL is maintained at the morula stage (TL^M) and then increases to TL^G level at the blastocyst stage (TL^B) (Turner et al., 2010).

Telomerase seems to be responsible for establishing the maximum embryo TL and a theory of TL reset at the morula-blastocyst transition was stablished (Schaetzlein et al., 2004; Treff et al., 2011). However, differences in the inherited TL, transmitted by gametes at fertilization, may still have a long-lasting effect in the final embryo TL (Simpson and Wells, 2014). Additionally, oocytes were shown to have longer TL than sperm, a proportion that is maintained in the female and male pronuclei (**Figure 1.6**). This suggests that oocytes could modify sperm telomeres by sister chromatid exchange (ALT), until telomerase ensues at the blastocyst stage (Turner and Hartshorne, 2013). Thus, questions regarding the differential parental TL inheritance are also still to be answered (De Meyer and Eisenberg, 2015).

The ALT pathway has been referred to promote telomere lengthening in early mice embryos, contributing to TL heterogeneity at the cleavage stages, and ceasing at the blastocyst stage, in which and from onwards TL would only be maintained by telomerase (Liu et al., 2007; Schaetzlein et al., 2004). This suggested that two telomere lengthening mechanisms act at different times, during preimplantation embryo development (**Figure 1.6**) (Keefe, 2016; Liu et al., 2007). TL maintenance by telomerase, after an initial elongation phase, was actually recently reported in human embryonic stem cells, from the inner mass of the blastocyst, whose ALT pathway was suppressed (Zeng et al., 2014). However, to our knowledge, no evidence has so far confirmed that ALT induces telomere lengthening during the cleavage stages of human embryo development.

1.4 Telomeres and sperm pathology

Sperm pathology refers to the structural and functional defects in sperm, whose incidence is higher in infertile men (Chemes and Rawe, 2003). The causes of defective spermatozoa are multifactorial, including genetic, lifestyle and environmental factors, that often act in combination (Aitken et al., 2014; Gomes et al., 2015).

Male factor infertility is present in 50% of all infertility cases worldwide (Agarwal et al., 2015), but it is still idiopathic in almost half of the cases (Cram et al., 2001), in which no physical or endocrine parameters explain the reduced semen quality. Despite idiopathic infertility, infertility of unknown origin also comprises unexplained infertility, in which standard semen analysis fails in identifying infertile sperm subpopulations (Hamada et al., 2011). Thus, questions regarding the molecular mechanisms underlying male infertility are still being raised (Reig-Viader et al., 2016). Endocrine disorders (Oliveira et al., 2017), chromosomal abnormalities (Chatziparasidou et al., 2015; Gonçalves et al., 2017; Harton and Tempest, 2012; Madureira et al., 2014; Shah et al., 2003), gene mutations (Grangeia et al., 2008; Pereira et al., 2015; Pereira et al., 2017; Shah et al., 2003), sperm apoptosis (Almeida et al., 2005; Almeida et al., 2011), mitochondrial dysfunction (Sharbatoghli et al., 2012), imprinting disorders (Laqqan et al., 2017; Marques et al., 2011; Marques and Sousa, 2013), DNA damage (Barratt et al., 2010; Bucar et al., 2015; Sá et al., 2015) and altered DNA packing (Hammoud et al., 2009) have been identified as contributing factors. In recent years, reports showing that telomeric instability compromises the viability of gametes,

eventually affecting fertility, have been gaining importance and pinpoint telomere homeostasis as a novel human infertility biomarker (Reig-Viader et al., 2016).

The lengthening of telomeres occurring during spermatogenesis was proposed to contribute to the maintenance of a critical TL during embryo cleavage, resulting in a species-specific TL preservation in the newborn (Achi et al., 2000). The presence of variations in human STL was reported, which suggested that truncated telomeres could induce genomic instability, severely affecting the development of the zygote (Baird et al., 2006). In accordance, decreased STL in idiopathic male infertility (Thilagavathi et al., 2013a) and decreased LTL in couples with recurrent pregnancy loss (Thilagavathi et al., 2013b) were found. Studies in mice also revealed that short STL contributed to a compromised fertilization of gametes and abnormal early embryo development (Liu et al., 2002; Liu et al., 2004b). It was thus proposed that critical short telomeres in sperm would impair their response to oocyte signaling during fertilization, consequently disturbing the development and implantation of the embryo (Thilagavathi et al., 2013a).

A critical TL was shown to be necessary for chromosome pairing, synapsis, recombination and spindle formation in mice (Keefe and Liu, 2009). Spermatocytes, unlike oocytes, seem to have a regulatory mechanism that prevents the accumulation of meiotic errors and the transmission of genetic abnormalities to the offspring, which explains the low incidence of aneuploid spermatocytes comparing to oocytes (Hemann et al., 2001a; Liu et al., 2004b; Nagaoka et al., 2012). Instead, these defective spermatocytes are eliminated, leading to a reduction of mature sperm, which contributes to infertility (Reig-Viader et al., 2014a). In concordance, azoospermic men with an altered distribution of crossovers (decreased in the usual subtelomeric region and increased in telomeres and centromeres, where they are usually inhibited) has been reported, suggesting that a telomere impairment was in the origin of the infertile phenotype (Ren et al., 2016).

Concerning telomere structure, the disruption of telomeric interactions, associated with human sperm DNA damage, has been reported in infertile men (Moskovtsev et al., 2010). This loss of telomere interactions possibly impairs chromosomal looping and arrangement in the nucleus, thus affecting the ordered remodeling and activation of paternal DNA during fertilization and, consequently, proper gene expression at early embryo development (Millan et al., 2012; Moskovtsev et al., 2010; Mudrak et al., 2012). Therefore, altered sperm nuclear organization may impair sperm viability. Alterations in the structure of telomeres may also contribute to a higher susceptibility to oxidative damage in sperm, which promotes DNA fragmentation and loss of telomeric sequence repeats (Rocca et al., 2016). In addition, decreased TERRA levels and alterations in its association with telomeres, as well as decreased localization of telomerase at telomeres, were reported in primary spermatocytes from men with idiopathic infertility. A decrease in chromosome recombination rates was also observed, possibly as a result of abnormal synapsis. Thus, the impaired equilibrium of these telomere stabilizers could disrupt telomere structure and affect meiotic chromosome dynamics and DNA repair (Reig-Viader et al., 2014a). Finally, mutations in *hTERT* and in the telomerase-associated protein 1 gene (*TEP1*) were identified in idiopathic infertile men (Yan et al., 2014), and alterations in the expression of *hTERT*

were shown to predict spermatogenesis disorders (Schrader et al., 2002). In these two last studies, both TL and telomere structure could be impaired. Together, these findings demonstrate that alterations in TL and/or telomere structure in the male germ line impair telomere homeostasis in infertile men.

1.5 Sperm telomere length, seminal parameters and assisted reproductive technology outcomes

Characterizing sperm pathologies that negatively affect fertility and establishing a diagnosis allows a prediction of the outcomes in assisted reproductive technology (ART) and the establishment of a suitable clinical treatment. The selection of viable subpopulations of sperm is important not only to improve the success of ART but also to avoid the transmission of abnormal characteristics to future generations (Chemes and Rawe, 2003). Since a variable STL has been reported between individuals and even within the same individual (Antunes et al., 2015; Cariati et al., 2016; Ferlin et al., 2013; Turner and Hartshorne, 2013; Yang et al., 2015a), and given the impact of STL in male infertility, the selection of sperm with longer telomeres could be crucial for successful ART in fertility treatments (Yang et al., 2015a). In addition, it would prevent the transmission of infertile men short telomeres that may affect the child health (Aitken et al., 2014). In fact, TL has been considered a risk factor for genetic damage in newborns (Moreno-Palomo et al., 2014).

The semen processing procedures (swim-up and density gradient centrifugation) simulate genital tract sperm selection and are widely used to isolate a more functional population of spermatozoa for ART treatments. This population typically shows higher motility and decreased DNA fragmentation relatively to raw semen. Recent studies have reported this sperm population also contains longer telomeres (Santiso et al., 2010; Yang et al., 2015a). These results suggested that sperm with longer telomeres have higher quality and may be naturally selected in the female genital tract (Santiso et al., 2010), emphasizing their importance in fertilization and early embryonic development.

Additional studies have analyzed the associations between STL and semen parameters in raw semen, including sperm concentration, vitality, morphology and motility. Mean STL was shown to be higher in patients with normal semen parameters, except in relation to sperm morphology (Antunes et al., 2015). In addition, positive correlations between STL and progressive sperm motility (Rocca et al., 2016; Zhao et al., 2016) and vitality (Rocca et al., 2016) were reported. Also, a positive correlation between STL and sperm count was reported by many (Cariati et al., 2016; Ferlin et al., 2013; Yang et al., 2015a; Yang et al., 2015b; Zhao et al., 2016), with STL being lower in oligozoospermic than in normozoospermic men. A decreased sperm count may reflect the apoptotic events induced by short telomeres in the male germline, as shown in telomerase knockout mice (Hemann et al., 2001a; Lee et al., 1998; Liu et al., 2002; Liu et al., 2004b).

It was also observed in raw semen a positive correlation between STL and sperm chromatin maturity (Rocca et al., 2016), and a negative correlation between STL and sperm DNA

fragmentation (sDNAfrag) (Rocca et al., 2016; Zhao et al., 2016). A negative correlation between STL and sperm ROS content was also reported in raw semen (Zhao et al., 2016). It is possible that lower chromatin protamination that cause altered DNA packing may increase the vulnerability of DNA to damaging factors, such as ROS, promoting DNA fragmentation, which in turn induces telomere shortening (Rocca et al., 2016). Thus, telomere shortening could result from factors that impair spermatogenesis rather than causing this impairment (Rocca et al., 2016; Thilagavathi et al., 2013c; Zhao et al., 2016). From a different perspective, dysfunctional short telomeres could also induce sDNAfrag (Moskovtsev et al., 2010), possibly related with triggered apoptosis. Whether sDNAfrag is the cause or the consequence of telomere shortening needs further investigation.

A relation between STL in raw semen and pregnancy rates was reported, with no pregnancy ensuing from cases presenting abnormal STLs, either critically short or atypically long (Cariati et al., 2016). This result strengthens the need of a TL equilibrium for telomere function. In another study, STL of purified sperm was positively correlated with good quality and transplantable embryos in in vitro fertilization (IVF) (Yang et al., 2015b). Furthermore, TL in embryos seems to be related with their viability since short telomeres were reported in chromosomally abnormal blastomeres from slow developing embryos and from embryo cells in patients with recurrent miscarriage (Mania et al., 2014). Embryo aneuploidy is the leading cause of embryo development delay and miscarriage (Hassold and Hunt, 2001), and short telomeres have actually been associated with aneuploid embryos (Treff et al., 2011). Although no direct association has been reported between STL and sperm aneuploidies, there is a substantial overlap between these two parameters in raw semen. Also, a negative correlation between STL and diploid sperm was stated in raw semen (Cariati et al., 2016).

Table A.1 in **Appendix A** resumes the associations reported concerning STL. Even though additional confirmations are needed, STL assessment has become a promising fast and economical method for sperm quality analysis, which is extremally informative, as it not only associates with the most important semen quality parameters, but also provides information regarding paternal genomic stability and clinical outcomes. STL may thus be a suitable new biomarker for male infertility (Cariati et al., 2016; Rocca et al., 2016; Zhao et al., 2016). However, it remains unclear whether specific treatments could be applied to men with atypical STL (Cariati et al., 2016). In addition, contradictory results arise from studies in which STL from raw semen did not correlate with seminal parameters (Thilagavathi et al., 2013a; Turner and Hartshorne, 2013), sperm ROS content (Thilagavathi et al., 2013a) or sDNAfrag (Cariati et al., 2016; Thilagavathi et al., 2013a; Turner and Hartshorne, 2013). Absence of correlation of STL with clinical outcomes was also observed either in raw or purified sperm outcome or treatment outcome (Turner and Hartshorne, 2013; Yang et al., 2015b). In one study, sDNAfrag did not also relate with the disruption of telomere interactions, as previously reported (Moskovtsev et al., 2010). It was proposed that the TL resetting after fertilization, through the lengthening mechanisms occurring until the blastocyst stage of development, resumes the inherited TL into a

normal set point, turning STL unfit to diagnose male infertility (Mania et al., 2014; Turner and Hartshorne, 2013).

1.6 Objectives

It is of major interest to elucidate the molecular mechanisms underlying telomere function and how their disruption may affect sperm quality, to provide insights into the pathways that may influence clinical outcomes. The main goal of this study was to clarify whether STL, in swim-up purified sperm, is related to sperm quality and the embryological and clinical outcomes, in order to ascertain if STL is a suitable biomarker of male infertility, that could be routinely implemented in medically assisted reproduction centers. The originality of this study resides on the broad panoply of associations analyzed. In the first instance it is expected to determine whether STL is related with sperm quality parameters (total count, concentration, total motility, progressive motility, rapid progressive motility, morphology, oxidative profile, chromatin maturity, DNA fragmentation and aneuploidy), demographic characteristics (male age and time of infertility), embryologic outcomes (rates of fertilization, embryo cleavage, high-quality embryos, low-quality embryos and blastocyst formation) and clinical outcomes (rates of biochemical pregnancy, implantation, clinical pregnancy and ongoing pregnancy). After disclosing the parameters that are strongly correlated with STL, clinicians may choose the STL measurement test to further evaluate the reproductive potential of the male patient. Additionally, it is expected that with the results obtained the clinician may predict the success and guide infertility treatments more accurately.

2. Materials and Methods

2.1 Ethical approval

The procedures of the IVF clinic Centre for Reproductive Genetics A. Barros (CGR) are under the determinations of the National Law on Medically Assisted Procreation (Law of 2017) and supervised by the National Council on Medically Assisted Procreation (CNPMA-2015). According to these rules, the use of clinic databases and patient biological material for diagnostic and research can be used without further ethical approval, under strict individual anonymity and after patient informed and written consent.

2.2 Patients

This research study was performed on swim-up sperm samples retrieved from 78 consecutive treatment cycles, happening between October and December of 2017, that used ejaculated sperm for IVF or intracytoplasmic sperm injection (ICSI) procedures. All ART treatments were performed at CGR.

2.3 Karyotype analysis

At CGR, all couples undergoing ART treatments perform karyotype analysis. Karyotypes were evaluated using G-banding with analysis of at least 30 metaphases from peripheral blood lymphocytes, according to general protocols.

2.4 Sperm preparation

For spermiogram analysis, semen samples were collected by masturbation into sterile cups following 2-4 days of sexual abstinence. Samples were left to liquefy for 30 min over a thermal plate at 37ºC and subsequently used for assessment of seminal parameters. For IVF/ICSI treatments, semen samples were left to liquefy at 33ºC, 5% CO_2 in humidified air and then submitted to discontinuous gradient centrifugation (PureSperm System 90-45%; Nidacon, Sweden). After centrifugation at 1500 rpm, for 20 min, at room temperature (RT), the bottom gradient layer was recovered. The pellet was thereafter washed two times (1500 rpm, 10 min, RT) in Sperm preparation medium (SPM; Origio, Denmark) containing 4-(2-hydroxyethyl)-1-piperazineethanesulfonic acid (HEPES) buffer. The pellet was then layered with 100-1000 µL of sequential Fert medium (Origio) and incubated (1 h, 33ºC, 6% CO_2 in humidified air) to collect the swim-up fraction containing rapid progressive motile sperm that actively migrated from the pellet to the upper aqueous phase. After ART, the remainder patient sample was used for the research analyses.

2.5 Ovarian controlled hyperstimulation

Women underwent controlled ovarian hyperstimulation in 75 (96.2%) of the cases with a gonadotropin-releasing hormone (GnRH) antagonist protocol (0.25 mg cetrorelix, Cetrotide; Merck-Serono, Germany; or 0.25 mg ganirelix, Orgalutran; Organon, USA) and in 3 (3.8%) of the

cases with the long agonist protocol (0.1 mg triptorelin, Decapeptyl; Ipsen Pharma Biotech, France). For stimulation, in 30 (38.5.%) of the cases recombinant follicle stimulating hormone (rFSH, folitropin beta, IU/mL, Puregon; Organon; rFSH, folitropin alfa, IU/mL, Gonal-F; Merck-Serono) was used; in 34 (43.6%) of the cases human menopausal gonadotropin (HMG, IU/mL, Menopur; Ferring, Switzerland) was added to rFSH; in 2 (2.6%) of the cases HMG was used alone; and in 12 (15.4%) of the cases rFSH was used in combination with recombinant luteinizing hormone (folitropin alfa + lutropin alfa rFSH+rLH, IU/mL, Pergoveris, Merck-Serono; rLH, IU/mL, Luveris, Merck-Serono). Ovulation trigger was performed in 30 (38.5%) of the cases with recombinant choriogonadotropin alpha (rHCG, 250 µg, Ovitrelle; Merck-Serono); in 23 (29.5%) of the cases with a GnRH agonist (0.2 mg triptorelin); and in 12 (15.4%) of the cases a dual trigger was used, with triptorelin (0.2 mg) and rHCG (250 µg). Estradiol serum levels were assayed at the day of HCG or one day before (Huirne et al., 2007; Pinto et al., 2009).

2.6 Gamete and embryo handling

For IVF, cumulus-oocyte complexes (COC) were collected in SynVitro Flush medium (without heparin, Origio). All media are devoid of phenol red. After this step all procedures were performed under paraffin oil (Ovoil-100, Vitrolife, Sweden). COC were washed with SynVitro Flush in 1-well culture dishes (Falcon, USA). They were then transferred to an ESCO incubator (EscoMedical, Denmark, MRI-6A10, 37ºC, 5% O_2, 6% CO_2, 89% N_2, in a humidified atmosphere) in 5-well culture dishes (Vitrolife) with Sequential Fert medium (Origio), 500 µL/well (up to 4 COC/well), and inseminated (4-5h after oocyte pick-up) with 50000-100000 sperm/mL. About 16-19h after insemination, COC were mechanically denuded in wells, to observe oocyte maturity and fertilization. They were then transferred individually to 12-well microdoplet culture dishes (Vitrolife) with Sequential Cleavage medium (Origio), 30 µL/droplet, up to day 3. Thereafter, oocytes were transferred to new dishes with Sequential Blast medium (Origio), up to day 5.

For ICSI, COC allocated in 1-well culture dishes with Sequential Fert were incubated in the ESCO for 2h. Thereafter, they were denuded, for 30 sec, with recombinant hyaluronidase (ICSI Cumulase, Origio), washed with Sperm Prep medium and then mechanically dissociated from granulosa cells in Sperm Prep medium (Origio), with oocyte denudation micropipettes (Vitrolife). Denudation was performed at 37ºC (thermic laminar flow base). Denuded oocytes were then incubated in 5-well culture dishes up to microinjection (1-2 h) in Sequential Cleavage. Microinjection was performed in an inverted microscope (Nikon, Japan) equipped with Hoffman optics and Narishige micromanipulators (Narishige, Japan), using microinjection and holding micropipettes (Vitrolife), under a described technique (Tesarik and Sousa, 1995). After ICSI, oocytes were transferred individually to 12-well microdoplet culture dishes with Sequential Cleavage, up to day 3, and then transferred to new dishes with Sequential Blast, up to day 5. When incubated in Embryoscope (FertiliTech, Vitrolife), injected oocytes were transferred to 12-well Embryo Slide culture dishes (Vitrolife) with Sequential Cleavage (25 µL/well), up to day 3, and then in Sequential Blast. In this case, the medium is replaced (20 µL) but not the culture dish.

Embryo quality was graded according to described methods at day 3 (Vandervorst et al., 1998) and day 5 (Gardner et al., 2000). Ultrasound-guided embryo transfer used a Sure View Wallace Embryo Replacement Catheter or Wallace malleable stylet (Smiths Medical Int, UK).

2.7 Luteal supplementation

All patients had luteal supplementation with intravaginal administration of natural-micronized progesterone (Utrogestan; Jaba, France; Projeffik; Effik, Netherlands), 200 mg (tid), from the day of oocyte retrieval. Implantation was confirmed by a rise in β-HCG serum, 12 days after embryo transfer. Clinical pregnancy was established by ultrasound at 7 weeks of gestation. When a GnRH agonist was used for triggering final oocyte maturation, progesterone luteal support was associated with oral estradiol (Estrofen; Novo Nordisk, Denmark), and a bolus of rHCG (Ovitrelle, 250 µg) was given at the day of oocyte pick-up (Radesic and Tremellen, 2011).

2.8 Sperm DNA fragmentation evaluation

The incidence of morphological normal spermatozoa displaying nuclear DNA strand breaks was identified by the terminal deoxynucleotidyl transferase dUTP nick end labelling (TUNEL) assay using the In Situ Cell Death Detection kit, Fluorescein (Roche Diagnostics, USA), according to manufacturer's instructions for in situ technique, as previously described (Gomes et al., 2015). The evaluation of only morphologically normal spermatozoa is related to the fact that those are the ones selected by embryologists for the ICSI procedure. The TUNEL assay measures the actual damage, the spontaneous or accidental breaking of DNA strands into nucleosomal fragments, by a direct way. From the swim-up retrieved fraction, 10 µL were spread onto adhesion microscope slides (Waldemar Knittel, Germany), left to air dry at RT and then stored at -20ºC until use. Sperm cells were fixed for 1 h, at RT, with 4% paraformaldehyde (Merck, Germany) in phosphate buffered saline (PBS). The slides were then washed in PBS and permeabilized with 0.1% Triton X-100 (Sigma, USA) in 0.1% sodium citrate (Sigma), for 2 min at 4°C. After washing twice with PBS, the slides were incubated in 50 µL of labeling solution containing the terminal deoxinucleotidil transferase (TdT) enzyme, for 1 h at 37ºC, in a dark moist chamber. After incubation, the slides were washed and cells were counterstained with Vectashield antifade medium containing 4',6-diamino-2-phenylindole (DAPI; Vector Laboratories, USA). On each slide, a minimum of 200 morphological normal spermatozoa (Sá et al., 2015), without head, mid-piece or tail abnormalities, were scored under the x100 objective of a Nikon Eclipse E400 fluorescence microscope fitted with a CCD camera and NIS-Elements BR V.4.60 software (Nikon). For each experiment, a negative (TdT enyme omitted and replaced by distilled water) and a positive (deoxyribonuclease treatment) control were performed to ensure the reproducibility of the assay. A double-blind procedure was employed. Each spermatozoon was assigned as apoptotic (if displaying intense green fluorescence) or normal (blue staining only). The percentage of TUNEL-positive sperm was expressed as the percentage of cells exhibiting sDNAfrag.

2.9 Sperm chromatin maturity evaluation

Chromatin maturity was evaluated by acidic aniline blue (AB) staining. Immature sperm chromatin contains more histones, which are rich in lysine and arginine and bind AB (AB+). Sperm with mature chromatin contain more protamines, which are rich in cysteines that do not bind AB (AB-). Thus, AB+ cells reveal sperm with immature chromatin and AB- cells reveal sperm with mature chromatin (Asmarinah et al., 2016). From the swim-up retrieved fraction, 10 µL were spread onto adhesion microscope slides (Waldemar Knittel), left to air dry at RT and then stored at -20ºC until use. Sperm cells were fixed in 3% glutaraldehyde (Merck) in 0.2 M PBS, for 30 min at RT. Cells were then stained with 5% aqueous AB (Merck), mixed with 4% acetic acid (Merck) pH 3.5, for 5 min at RT. On each slide, 200 spermatozoa were evaluated and the percentage of sperm heads stained dark blue (AB+) and not stained (AB-) was calculated.

2.10 Sperm chromosomic alterations evaluation

The percentage of sperm cells with euploidy, diploidy and overall aneuploidy in each sample was obtained by fluorescent in situ hybridization (FISH). Retrieved swim-up samples were washed twice in PBS (2x 10 min, 1500 rpm) and then fixed with methanol/acetic acid, 3:1 (VWR International, USA; Panreac, Germany). After two washes with this fixative solution (2x 10 min, 1500 rpm) the samples were kept at -20ºC until the FISH procedure execution. FISH was performed using a probe mixture containing CEPX (Spectrum Green), CEPY (Spectrum Orange) and CEP18 (Spectrum Aqua) from the AneuVysion Multicolour DNA Probe Kit (Abbott Molecular, USA). Briefly, 10 µL of fixed semen sample was spread on a slide, washed in saline-sodium citrate buffer (SSC), 1:10 (Invitrogen, USA), dehydrated in ethanol series and the sperm heads were decondensed with 1,4-dithiothreitol (DTT; Roche Applied Systems, USA). Sperm cells and the probe mixture were denatured separately and the hybridization occurred overnight, at 37ºC in a humidified chamber. In order to counterstain the DNA (blue), 5 µL of DAPI (Abbott Molecular) was applied. Sperm cells were observed and analyzed in a fluorescence microscope Axio Imager Z1 (Carl Zeiss MicroImaging, Inc, Germany) fitted with a CCD camera AxioCam MRm (Zeiss) and an automated image software FISH Imaging System, version 5.1 (MetaSystems GmbH, Germany). Aneuploid sperm included disomy 18, disomy X, disomy Y, disomy XY or diploidies. Diploid sperm cases were considered those with disomy 18 simultaneously with disomy X or disomy Y or disomy XY.

2.11 Sperm telomere length measurement

2.11.1 Sperm DNA extraction and quantification

DNA was extracted from retrieved swim-up samples using the NZY Tissue gDNA Isolation Kit (NZYtech, Portugal), according to manufacturer's instructions. The DNA samples were then quantified in NanoDrop 1000 spectrophotometer (Thermo Scientific, USA), software version 3.7.0. DNA concentration was obtained with the absorbance at 260 nm, knowing that 1 absorbance corresponds to 50 µg of dsDNA/mL. The purity of each DNA sample was analyzed

by the Abs_{260}/Abs_{280} and Abs_{260}/Abs_{230} ratios. The DNA samples were then stored at -20ºC until use.

2.11.2 Specific sperm DNA amplification by quantitative polymerase chain reaction

Relative STL was measured by quantitative polymerase chain reaction (Q-PCR), as previously described (O'Callaghan et al., 2008). In the CFX Connect Real-Time PCR Detection System (Bio-Rad, UK), with the Bio-Rad CFX Manager 3.1 software, two PCRs were performed in separate plates for each sample (which maintained the same position in each plate), one for telomere (T) amplification and the other one for single copy (S) control gene amplification. The single copy control gene used was beta-2-microglobulin (*B2M*), which encodes for a serum protein that associates with the major histocompatibility complex class I and has been tested for gene-dosage studies (Covault et al., 2003). Each DNA sample was run in triplicate. Each plate included a no template control and serial dilutions of DNA from the positive control HT-1376 cell line (ATCC® CRL-1472™, USA), generating a reference curve to compensate for inter-plate PCR efficiency variations. Each PCR was performed with Green Master Mix NZY qPCR (2×) (NZYtech) and 20 ng of DNA. The specific primer nucleotide sequences used and **t**he thermocycler conditions are listed in **Table 2.1.** A melting curve was obtained for each sample to access primer specificity.

Table 2.1 – Nucleotide sequences of the primers used for telomere and *B2M* amplification, with the expected amplicon size, and the respective quantitative polymerase chain reaction (Q-PCR) thermocycler conditions.

	Sequence (5'-3')	Amplicon size (bp)	Annealing temperature (°C)	Amplification cycles
Telomere				
Primer forward	CGG TTT GTT TGG GTT TGG GTT TGG GTT TGG GTT TGG GTT	>78	60	40
Primer reverse	GGC TTG CCT TAC CCT TAC CCT TAC CCT TAC CCT TAC CCT			
B2M (AN: NG_012920.2)				
Primer forward	GAG GCT ATC CAG CGT GAG TC	306	58	40
Primer reverse	GAC GCT TAT CGA CGC CCT AA			

The principle of TL measurement by Q-PCR is represented in **Figure 2.1**. The shortest PCR product possible (the sum of the lengths of the two telomere primers) is expected from telomeric DNA amplification, with a copy number proportional to the number of primer binding sites at the beginning of the PCR, rather than products with the same length as the telomere (Cawthon, 2002). The mean cycle threshold (C_t) values obtained in each sample were used to calculate their T/S ratio (relative STL), which is normalized against a common reference sample and it is proportional to the sample average TL (from all the sperm cells present therein) (Cawthon, 2002), according to the following formulas: $\Delta C_t(\text{sample}) = \Delta C_t(\text{telomere}) - \Delta C_t(\text{control})$;

ΔC_t(reference curve) = ΔC_t(telomere) - ΔC_t(control); $\Delta\Delta C_t$ = ΔC_t(sample) - ΔC_t(reference curve); T/S = $2^{-\Delta\Delta Ct}$.

Figure 2.1 – Schematic representation of telomere length (TL) measurement by quantitative polymerase chain reaction (Q-PCR). Two pairs of chromosomes are shown in blue, with their respective telomeres distinguished in red. Primers for telomere amplification are represented as red arrows and primers for single copy gene amplification are represented as green arrows. Variable sized telomeres are represented. TL can be measured based on PCR signal, as the number of primers that bind the telomeric DNA (T) in the beginning of the PCR is proportional to the total summed length of all the telomeres in the cell. The single copy gene (S) is a measure of the number of cells present in a given sample, as exactly two pairs of primer copies of the single copy gene are expected to bind the DNA of a single cell, in the beginning of the PCR. The ratio of the PCR signals (T/S) is thus proportional to the average telomere length per cell, in a given sample. Adapted from Lan et al., 2009.

2.12 Sperm oxidative profile characterization

2.12.1 Sperm total protein extraction and quantification

Total protein was extracted from retrieved swim-up samples using the Mammalian Protein Extraction Reagent (M-PER), which contains a mild, non-denaturing detergent that dissolves cell membranes. 50 µL of M-PER (Thermo Scientific) were added to sperm cells, which were then mixed during 15 min, 300 rpm, at RT. Thereafter, cells were sonicated during 20 min, at 4° C. The lysate was centrifuged at 12300 rpm for 20 min, at RT, leaving the total protein extracted on the supernatant. Protein samples were stored at -20°C until use.

Sperm total protein extracted was quantified with bicinchonimic acid (BCA), using the BCA Protein Assay Kit (Thermo Scientific). In alkaline conditions, proteins reduce Cu^{2+} to Cu^{1+}, which reacts with BCA to form a purple-colored complex, passible of being quantified by spectrophotometry. Serial dilutions of bovine serum albumin (BSA; Sigma-Aldrich, USA) in PBS were included in the assay, to obtain a calibration curve. 10 µL of each dilution and 1 µL of each sample's total protein extract, diluted in 9 µL of PBS, were pipetted into a 96-well plate. The kit manufacturer's instructions were then followed. Lastly, absorbance at 570 nm was measured with the Multiskan FC Microplate Photometer (Thermo Scientific), software version 1.00.79.

2.12.2 Protein carbonylation, protein nitration and lipid peroxidation evaluation by slot blot

To characterize the oxidative profile of the swim-up samples, protein carbonylation, protein nitration and lipid peroxidation, which are commonly used biomarkers for oxidation, were evaluated by the quantification of their resulting products: 2,4-dinitrophenyl (DNP) for protein

carbonylation, 3-nitrotyrosine for protein nitration and 4-hydroxynoneal (4-HNE) for lipid peroxidation, as previously described (Dias et al., 2015).

Sperm total protein extracts were derivatized with 2,4-dinitrophenylhydrazine (DNPH) (Levine et al., 1990), which is converted to DNP in the presence of protein carbonyl groups. Briefly, 5 µL of total protein extract were diluted in filtered PBS, up to 20 µL, to which 20 µL of 12% sodium dodecyl sulfate (SDS) were added. Subsequently, 40 µL of 20 mM DNPH (Sigma-Aldrich), diluted in 10% trifluoracetic acid (TFA; Thermo Scientific) were added to the suspension. Following homogenization, samples were incubated 30 min in the dark, at RT. After incubation, 30 µL of a stop solution with 2 M Tris (NZYTech) and 18% β-mercaptoethanol (Sigma-Aldrich) were added.

The derivatized samples were diluted to the final concentration of 0,004 µg/mL and transferred to a polyvinylidene difluoride (PVDF) blotting membrane (0.45 PVDF, Amersham Hybond, GE Healthcare, Life Sciences, Germany) with the Hybri-slot Manifold System (Biometra, Germany), which were then incubated overnight at 4°C with a rabbit anti-DNP (1:1000, D9656, Sigma-Aldrich). Posteriorly, a conjugation with a mouse anti-rabbit IgG-HRP (1:5000, sc-2357, Santa Cruz Biotechnology, Germany) was performed during 90 min, at RT.

In parallel, sperm total protein extracts were diluted to the final concentration of 0,2 µg/mL and transferred to another PVDF membrane with the Hybri-slot Manifold System (Biometra), which were then incubated overnight at 4°C with a rabbit anti nitro-tyrosine (1:1000, 96915, Cell Signaling Technology, Netherlands). Posteriorly, a conjugation with a mouse anti-rabbit IgG-HRP (1:5000, sc-2357, Santa Cruz Biotechnology) was performed during 90 min, at RT.

Equivalently, sperm total protein extracts were diluted to the final concentration of 0,05 µg/mL and transferred to another PVDF membrane with the Hybri-slot Manifold System (Biometra), which were then incubated overnight at 4°C with a goat anti 4-HNE (1:5000, AB5605, Merck Millipore, USA). Posteriorly, a conjugation with a donkey anti-goat IgG-HRP (1:5000, sc-2020, Santa Cruz Biotechnology) was performed during 90 min, at RT.

Finally, all membranes were revealed in the ChemiDoc™ XRS+ System (Bio-Rad), and the densities of each obtained band were quantified using the Image Lab software, version 5.2 (Bio-Rad).

2.13 Statistical analysis

Shapiro-Wilk test was used to evaluate the normality of the data. Different normalization transformations were tested according to the data distribution, including negative reciprocal, logarithm, square root, cube root, forth root and arcsine. For correlation analysis between relative STL and different parameters, Pearson's (r_p) or Spearman's rank (r_s) correlation coefficients were used according to the distribution of the variables. Correlation coefficients were interpreted according to the rule of Thumb (Mukaka, 2012). In addition, parametric/ non-parametric tests were used for comparison of relative STL between two groups (Student's *t*-test/ Mann-Whitney *U* test) and between more than two groups (One-way ANOVA/ Kruskal-Wallis), as appropriate. F test or Levene's were used for analysis of the homogeneity of variances. All statistical analysis was

carried out using the Past 3 software (version 3.20). Graphics were obtained using GraphPad Prism 6 (GraphPad software, USA). *P*-value<0.05 was considered statically significant.

3. Results

3.1 Sperm telomere length frequency distribution

The measurement of relative STL was performed in 73 of the total 78 patients, as five samples provided insufficient DNA for analysis. Relative STL revealed high inter-individual variations, ranging from 1.65 to 19.67, with mean 5.22, standard deviation ± 3.26, median 4.56 and interquartile range of 2.25. As represented in **Figure 3.1**, the relative STL of all the patients analyzed had a non-normal, logarithmic distribution (Shaphiro-Wilk, $p<0.001$). Three samples were identified as outliers (14.69, 19.60 and 19.67). Since high STL heterogeneity has been previously reported (Antunes et al., 2015) we had no reason to exclude these samples from the statistical analysis.

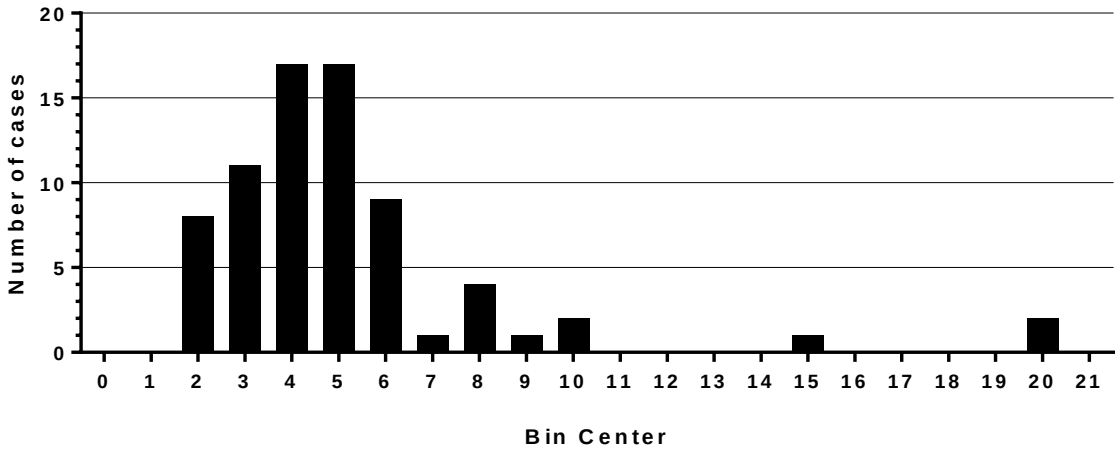

Figure 3.1 – Frequency distribution histogram of relative sperm telomere length in 73 patients.

3.2 Sperm telomere length and sperm quality associations

We evaluated six seminal parameters reported in the spermiograms of the 78 patients, which are described in **Table 3.1.** No statistically significant correlations were found between relative STL and any of the seminal parameters (**Table 3.2**).

For further statistical analysis, we used World of Health (WHO) 2010 guidelines (World Health Organization, 2010) concerning: total sperm count (TSC: $\geq 39\times10^6$/ejaculate, sperm concentration (Conc: $\geq 15\times10^6$/mL), sperm total motility (TM: ≥40%), sperm progressive motility (PM: ≥32%) and sperm normal morphology (NM: ≥4%). Sperm rapid progressive motility (RPM: ≥25%) was also included, as described in WHO 1999 (World Health Organization, 1999). The following **groups** were analyzed: normozoospermia (NZ; Conc: $\geq 15\times10^6$/mL + PM: ≥32% + NM: ≥4%); oligozoospermia (OZ; Conc: $<15\times10^6$/mL); asthenozoospermia (AZ; PM: <32%); teratozoospermia (TZ; NM: <4%); oligoasthenozoospermia (OA; Conc: $<15\times10^6$/mL + PM: <32%); oligoteratozoospermia (OT; Conc: $<15\times10^6$/mL + NM: <4%); asthenoteratozoospermia (AT; PM: <32% + NM: <4%); and oligoasthenoteratozoospermia (OAT; Conc $<15\times10^6$/mL + PM: <32% + NM: <4%). **Table 3.3** indicates the patients' clinical classifications accordingly.

Table 3.1 – Seminal parameters analyzed in the 78 patient sperm samples.

Seminal parameters	Mean ± SD	Range
Total count (×10^6/ejaculate)	199.52 ± 196.42	0.07-971.3
Concentration (×10^6/mL)	67.2 ± 65.65	0.02-296
Total motility (%)	60 ± 14.68	19-84
Progressive motility (%)	48.2 ± 15.15	6-75
Rapid progressive motility (%)	26.7 ± 15.48	0-58
Normal morphology (%)	4.7 ± 3.75	0-17

Table 3.2 – Correlation of relative sperm telomere length with seminal parameters.

Seminal parameters	n	r_s	p
Total count (×10^6/ejaculate)	73	0.064	0.59
Concentration (×10^6/mL)	73	0.006	0.957
Total motility (%)	73	-0.11	0.354
Progressive motility (%)	73	-0.04	0.736
Rapid progressive motility (%)	72	0.017	0.886
Normal morphology (%)	71	0.165	0.169

r_s: Spearman's rank correlation coefficient.

Table 3.3 – Distribution of patients' clinical classification following semen analysis.

Patient clinical classification	n	Rate (%)
Normozoospermic	33/73	45.2
Oligozoospermic	13/78	16.7
Asthenozoospermic	9/73	12.3
Teratozoospermic	35/76	46.1
Oligoasthenozoospermic	4/73	5.5
Oligoteratozoospermic	8/76	10.5
Asthenoteratozoospermic	7/73	9.6
Oligoasthenoteratozoospermic	3/73	4.1

The seminal parameters were also divided into **subgroups** to better characterize the association between relative STL and seminal parameters. We selected the following intervals: for TSC: ≥39 and <39×10^6/ejaculate; for Conc: ≥15, <15, ≤10, 10-20 and ≥20×10^6/mL; for TM: ≥40% and <40%; for PM: ≥32% and <32%; for RPM: ≤5%, 5-15%, 15-25% and ≥25%; for NM: ≥4%, <4%, < 1%, 1-4%, 4-10% and ≥ 10%. These intervals were chosen because the number of cases was too low to use standard intervals (Almeida et al., 2005). The comparison of relative STL between samples in the referred intervals, for each seminal parameter, did not show statistically significant differences (**Table B.1** in **Appendix B**).

The comparison of relative STL of patients with NZ and the relative STL of the remaining clinical classifications (OZ, AZ, TZ, OA, OT, AT and OAT) revealed that there was a modest decrease of relative STL in all pathological groups, except for OAT, in which the "n" was extremely small (n=3), although these decreases did not reach statistical significance (**Table 3.4**).

Table 3.4 – Comparison of relative sperm telomere length between normozoospermic patients and the remaining clinical groups.

Clinical classification	n	Mean±SD	Median	Test	p
NZ	33	6.04±4.36	4.76		
OZ	11	5.38±1.90	4.99	*t*-test	0.6
AZ	9	5.31±1.83	5.64	*t*-test	0.724
TZ	32	4.45±1.72	4.46	Mann-Whitney *U*	0.240
OA	4	5.69±2.47	5.83	*t*-test	0.747
OT	6	5.34±2.01	4.78	*t*-test	0.765
AT	7	5.47±2.02	6.16	*t*-test	0.717
OAT	3	6.30±2.63	7.80	Mann-Whitney *U*	0.567

NZ: normozoospermia; OZ: oligozoospermia; AZ: asthenozoospermia; TZ: teratozoospermia; OA: oligoasthenozoospermia; OT: oligoteratozoospermia; AT: asthenoteratozoospermia OAT: oligoasthenoteratozoospermia.

Correlation analysis of relative STL with sperm oxidative profile, sDNAfrag, sperm chromatin maturity, sperm chromosomic alterations, seminal parameters and male age, within the different clinical groups were performed, when "n" was ≥3 (**Table C.1** in **Appendix C**). Among patients with NZ, relative STL was significantly positively correlated with TSC (**Figure 3.2 A**). Surprisingly, in the OT group relative STL was significantly negatively correlated with TSC and Conc (**Figure 3.2 B and C**), and in the AZ, TZ and OA groups relative STL was significantly negatively correlated and with PM (**Figure 3.2 D-F**).

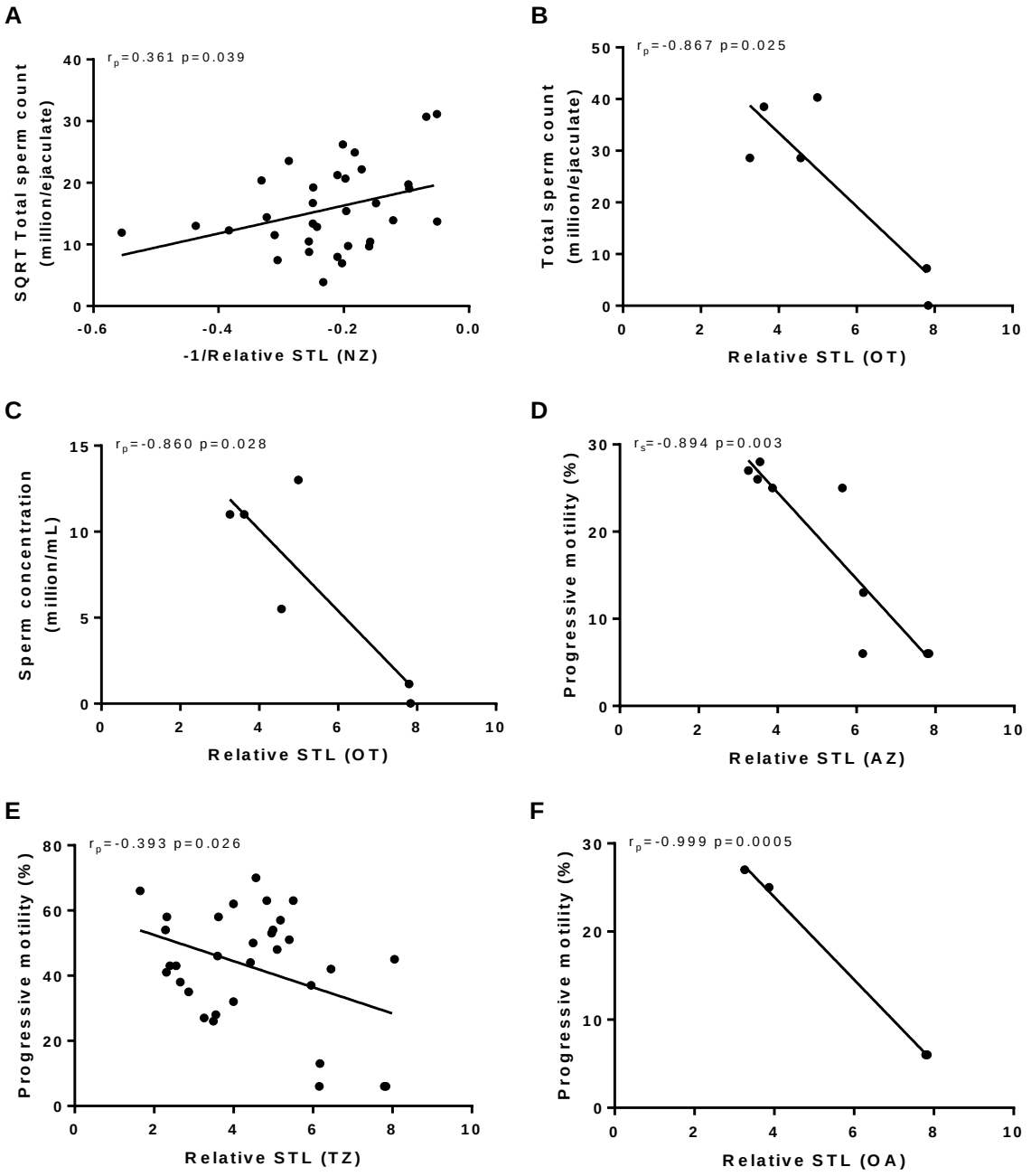

Figure 3.2 – Statistically significant correlations between relative sperm telomere length (STL) and seminal parameters, in different clinical groups. (**A**) Correlation between relative STL and total sperm count, in patients with normozoospermia (NZ). (**B**) Correlation between relative STL and total sperm count, in patients with oligoteratozoospermia (OT). (**C**) Correlation between relative STL and sperm concentration, in patients with OT. (**D**) Correlation between relative STL and progressive motility, in patients with asthenozoospermia (AZ). (**E**) Correlation between relative STL and progressive motility, in patients with teratozoospermia (TZ). (**F**) Correlation between relative STL and progressive motility, in patients with oligoasthenozoospermia (OA). Pearson's (r_p) or Spearman's rank (r_s) correlation coefficients and *P*-value are shown. SQRT: square root.

Additional information regarding patients' sperm quality was analyzed by evaluation of sDNAfrag, sperm chromatin maturity, sperm chromosomic alterations and oxidative profile, with the correlations between these parameters and relative STL being performed.

Of the 78 patients, 47 samples had enough sperm for characterization of the oxidative profile regarding protein carbonylation. The results from protein nitration and lipid peroxidation

could not be obtained in the given time. Relative STL and protein carbonylation did not show a statistically significant correlation (**Table 3.5**).

Of the 78 patients, 39 samples (38 with relative STL measurement) had enough remaining sperm for sDNAfrag analysis. In total, 8022 sperm were evaluated, with a mean of 206 sperm per patient. The mean of sDNAfrag was 23.2% (3.3-83.9%). The established cut-off for sDNAfrag is ≥30.6% (Majzoub et al., 2017). There were 8 (20.5%) cases with sDNAfrag above the cutoff (mean 51.3%; range 31.4-83.9%), which indicates that the majority of the samples (n 31; rate 79.5%) had normal sDNAfrag values (mean 15.9%, range 3.3-30.5%). No significant correlations were found between relative STL and sDNAfrag (**Table 3.5**).

Table 3.5 – Correlation of relative sperm telomere length with sperm quality parameters. *P*-value <0.05 is presented in bold.

Sperm quality parameter	**n**	**r_p**	**r_s**	**p**
Chromatin maturity (AB-, %)	40		-0.197	0.223
DNA fragmentation (TUNEL+, %)	38	-0.045		0.788
Staining patterns				
H+ (%)	38	0.348		**0.032**
AVR+ (%)	38	0.05		0.763
ER+ (%)	38	-0.25		0.137
PAR+ (%)	38	-0.371		**0.022**
Euploidy rate (%)	43		-0.108	0.49
Diploidy rate (%)	6		0.015	0.924
Aneuploidy rate (%)	43		0.507	0.333
Protein carbonylation (protein expression)	46		-0.075	0.62

H: head; AVR: acrosomal vesicle region; ER: equatorial region; PAR: post-acrosomal region.

Recently, patterns of DNA fragmentation staining were described in sperm (Sá et al., 2015), as shown in **Figure 3.3**: the acrosomal vesicle region (AVR), which is gene rich; the equatorial region (ER), that is protamine rich and presents a compact chromatin; the post-acrosomal region (PAR), which is gene poor and presents lower protamine content and higher histone content; and the head (H), that corresponds to a whole staining of the sperm head. In the 39 analyzed cases, pattern H had a mean of 40.6% (6.7-100%), with pattern H+ ≥30.6% being observed in 24 cases (17 pure, 3 associated with the PAR pattern, 3 associated with the ER pattern and 1 associated with the AVR pattern); pattern AVR had a mean of 16.8% (0-72.73%), with pattern AVR+ ≥30.6% being observed in 4 cases (3 pure); pattern ER had a mean of 20.1% (0-50%), with pattern ER+ ≥30.6% being observed in 8 cases (3 pure and 2 associated with the PAR pattern); pattern PAR had a mean of 22.6% (0-62.16%), with pattern PAR+ ≥30.6% being observed in 10 cases (5 pure). Thus, the majority of sperm with DNA fragmentation above the cut-off showed a predominance of the H pattern, followed by PAR, ER and, lastly, AVR. The correlations of the different sDNAfrag patterns with relative STL are included in **Table 3.5**. Relative STL was significantly negatively correlated with the PAR pattern and significantly positively correlated with the H pattern (**Figure 3.4 A and B**).

The comparison of relative STL in samples with the different sDNAfrag patterns bellow and above the cut-off did not show statistically significant differences (**Table B.1** in **Appendix B**). For deeper correlation analysis, relative STL was correlated with sDNAfrag in the <30.6% and ≥30.6% **subgroups** regarding the different staining patterns (**Table 3.6**), revealing a significant and negative correlation with PAR <30.6% (**Figure 3.5 A**). Relative STL also presented a significant negative correlation with PAR in patients with NZ (**Figure 3.5 B**).

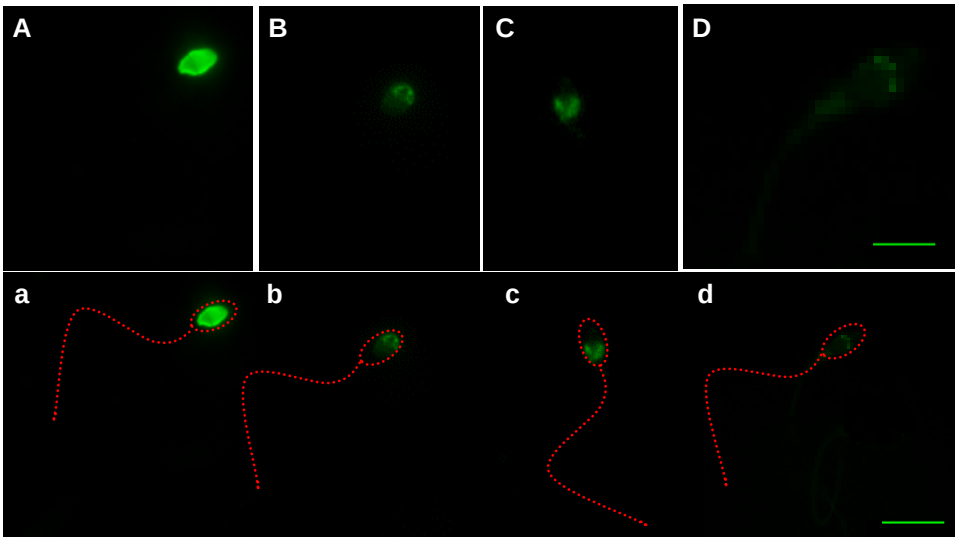

Figure 3.3 – Representative observations of the TUNEL assay for sperm DNA fragmentation evaluation, considering the different staining patterns. Evaluation was performed in morphologically normal spermatozoa. Upper panel: **(A)** sperm head; **(B)** acrosome vesicle region; **(C)** post-acrosome region; **(D)** equatorial region. Lower-panel: schematic representation of the same images of the upper panel (with the corresponding letters) to facilitate interpretation. Scale bar=10 µm.

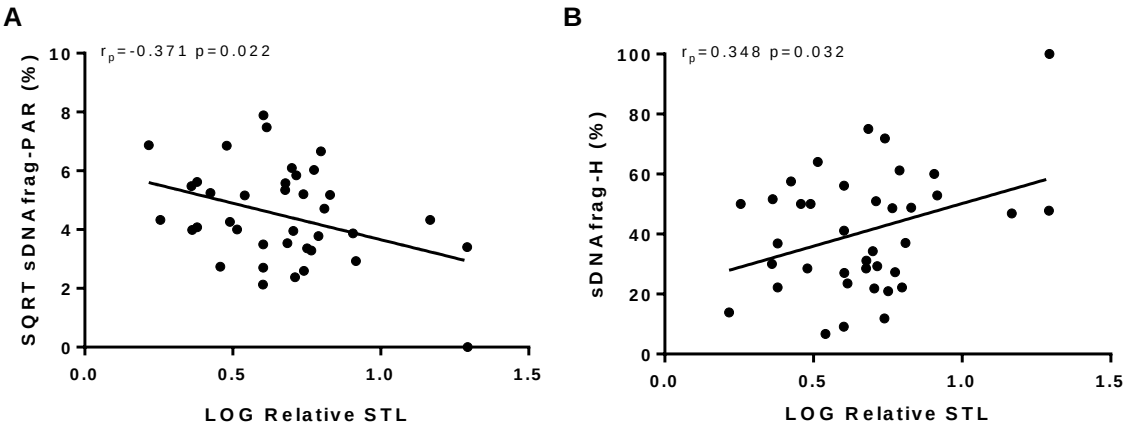

Figure 3.4 – Statistically significant correlations between relative sperm telomere length (STL) and sperm DNA fragmentation (sDNAfrag), in different staining patterns. (**A**) Correlation between relative STL and sDNAfrag in the post-acrosomal region (PAR). (**B**) Correlation between relative STL and sDNAfrag in the Head (H). Pearson's correlation coefficient (r_p) and *P*-value are shown. SQRT: square root; LOG: logarithm.

Table 3.6 – Correlation of relative sperm telomere length with sperm DNA fragmentation subgroups. *P*-value <0.05 is presented in bold.

Sperm quality parameter	Intervals	n	r_p	r_s	p
DNA fragmentation (TUNEL+, %)	<30.6	30		0.139	0.463
	≥30.6	8	-0.306		0.461
Staining patterns					
H+ (%)	<30.6	15	0.102		0.716
	≥30.6	23	0.282		0.193
AVR+ (%)	<30.6	34		0.119	0.502
	≥30.6	4	0.121		0.879
ER+ (%)	<30.6	30		-0.048	0.8
	≥30.6	8	0.386		0.346
PAR+ (%)	<30.6	28	-0.398		**0.036**
	≥30.6	10	-0.196		0.588

H: head; AVR: acrosomal vesicle region; ER: equatorial region; PAR: post-acrosomal region.

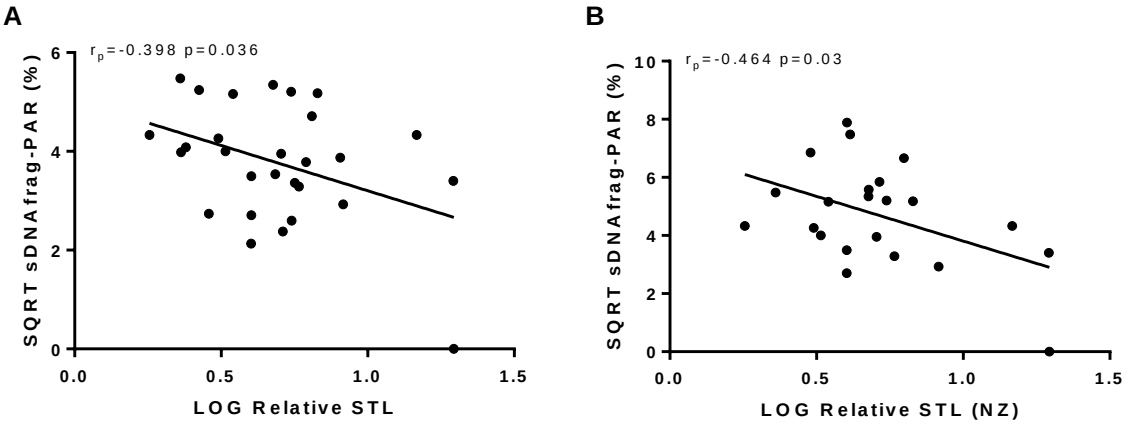

Figure 3.5 – Statistically significant correlations between relative sperm telomere length (STL) and sperm DNA fragmentation (sDNAfrag) in the post-acrosomal region (PAR), within subgroups. (**A**) Cases with <30.6 % sDNAfrag-PAR. (**B**) Patients with normozoospermia (NZ). Pearson's correlation coefficient (r_p) and *P*-value are shown. SQRT: square root; LOG: logarithm.

Of the 78 patients, 41 samples (40 with relative STL measurement) had enough remaining sperm for AB analysis (**Figure 3.6**). In total, 9259 sperm were evaluated, with a mean of 226 sperm per patient. The mean AB- was 57% (19-97%) in all the patients analyzed. The mean AB+ was 42.8% (2.9-80.9%). No statistically significant correlation was found between relative STL and the AB- percentage, indicator of sperm chromatin maturity (**Table 3.5**). There were 2 (4.9%) cases (mean: 93.8%, range: 90.5-97%) above the AB cut-off (≥87%) (Asmarinah et al., 2016). Therefore, 39 (95.1%) cases (mean: 55.3%, range: 19-86.8%) of the sperm evaluated revealed low sperm chromatin maturity. For deeper analysis of the association between relative STL and AB- we stablished the following **subgroups**, as an adaptation to our results: AB- <50%, with 14 (34.1%) cases; AB- 50-70%, with 17 (41.5%) cases; AB- 70-80%, with 6 (14.6%) cases; and AB- ≥80%, with 4 (9.8%) cases. No statistically significant correlation was found between relative STL and chromatin maturity in any of these subgroups (**Table 3.7**). The comparison of relative STL between the established AB- subgroups did not also reveal statistically

significant differences (**Table B.1** in **Appendix B**). However, there was a clear significant decrease of relative STL from the AB- <50% subgroup to the AB- ≥80% subgroup (**Figure 3.7 A**). In addition, a significant negative correlation was found between relative STL and chromatin maturity in patients with TZ (**Table C.1** in **Appendix C**), as shown in **Figure 3.7 B**. In this correlation, the 13 samples included (TZ with relative STL and AB evaluation) had predominantly alterations in the head and midpiece, as shown in **Table 3.8**)

Figure 3.6 – Representative observations of the AB assay for sperm chromatin maturity evaluation. On the left: an AB- spermatozoon, revealing sperm chromatin fully condensed; on the right: an AB+ spermatozoon, revealing sperm immature chromatin condensation. Scale bar=20 µm.

Table 3.7 – Correlation of relative sperm telomere length with sperm chromatin maturity subgroups.

Sperm quality parameter	Intervals	n	r_p	r_s	p
Chromatin maturity (AB-, %)	<50	14		-0.073	0.805
	≥50-<70	17	0.323		0.206
	≥70-<80	6	-0.481		0.334
	≥80	3	0.052		0.967

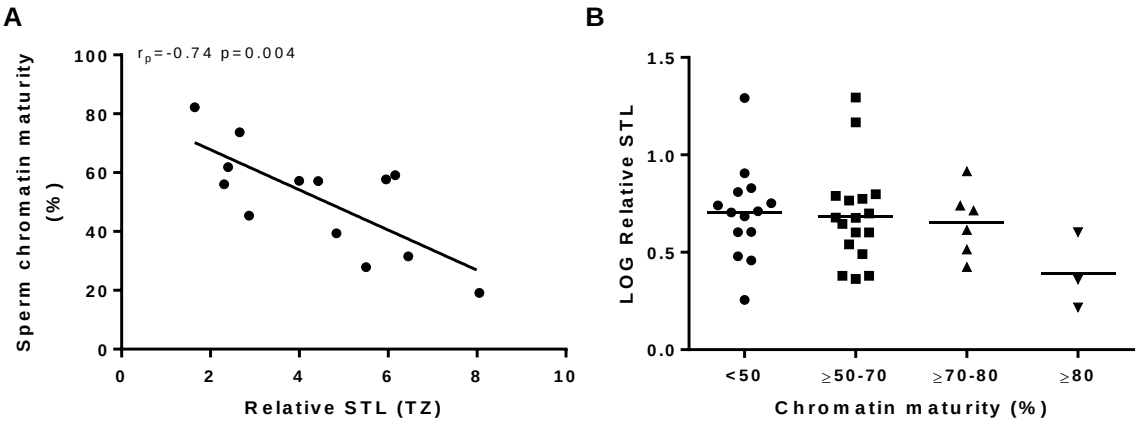

Figure 3.7 – Statistically significant associations between relative sperm telomere length (STL) and sperm chromatin maturity (AB-). (**A**) Correlation between relative STL and sperm chromatin maturity in patients with teratozoospermia (TZ). (**B**) Comparison of relative STL between the different chromatin maturity subgroups. Mann-Whitney pairwise between AB- <50% and AB- ≥80%: p= 0.044.

Table 3.8 – Characterization of sperm morphology in the teratozoospermic patients with relative sperm telomere length and sperm chromatin maturity evaluation. The head, midpiece and tail regions are not mutually exclusive.

Normal morphology (%)	Altered morphology		
	Head (%)	Midpiece (%)	Tail (%)
2	96	58	51
2	98	53	35
3	94	46	61
2	97	24	8
3	97	39	10
2	98	42	8
1	99	51	11
2	97	49	24
0	100	44	15
3	97	29	17
0	100	53	26
2	98	42	21
2	96	46	15

In order to ascertain the origin of the correlation found between relative STL and sDNAfrag-H in the totality of the population, we compared the relative STL with sDNAfrag-H in the different sperm chromatin maturity subgroups (**Table 3.9**). A significant and positive correlation was found in the AB- ≥50-<70% subgroup (**Figure 3.8**).

Table 3.9 – Correlation of relative sperm telomere length with sperm DNA fragmentation in the head (H) pattern, within the chromatin maturity subgroups. *P*-value <0.05 is presented in bold.

Sperm quality parameter	Chromatin maturity intervals	n	r_p	p
DNA fragmentation (H+)	<50	14	0.085	0.774
	≥50-<70	15	0.556	**0.03**
	≥70-<80	6	-0.199	0.705
	≥80	3	0.935	0.230

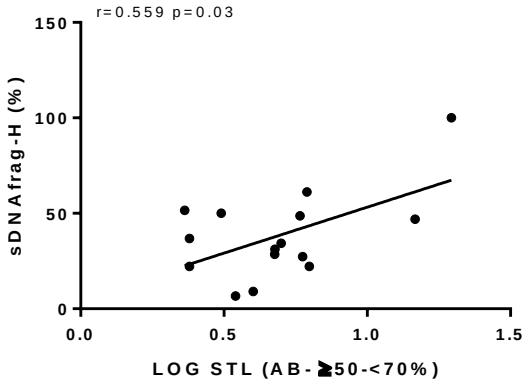

Figure 3.8 – Statistically significant associations between relative sperm telomere length (STL) and sperm DNA fragmentation (sDNAfrag) in the head (H), within the chromatin maturity (AB-) ≥50-<70% subgroup.

Of the 78 patients, 44 samples had enough remaining sperm to detect sperm aneuploidies by FISH (**Figure 3.9**). In total, 22165 sperm were evaluated, with a mean of 504 sperm per patient. Sperm euploidy (mean 98.9%, range 95.9-99.8%) was observed in all 44 patients, with haploid X sperm in 53.1% and haploid Y sperm in 46.9% of the euploid cases. Globally, 99.6% of sperm were haploid and 0.4% of sperm were aneuploid. Disomy 18 (mean 0.33%, range 0.19-0.99%) was observed in 15 patients, 3 of which (0.59%, 0.77%, and 0.99%) were above the cut-off for chromosome 18 (0.0-0.39%) (Vegetti et al., 2000). Disomy X (mean 0.28%, range 0.19-0.79%) was observed in 12 patients, with 1 case (0.79%) above the cut-off for chromosome X (0.018-0.7%) (Vegetti et al., 2000). Disomy Y (mean 0.21%, range 0.19-0.39%) was observed in 13 patients, none of which was above the cut-off for chromosome Y (0.009-0.6%) (Vegetti et al., 2000). Disomy XY (mean 0.46%, range 0.19-1.97%) was observed in 19 patients, with 3 cases (0.59%, 0.6%, and 1.97%) above the cut-off for disomy XY (0.062-0.42%) (Vegetti et al., 2000). Diploidy was observed in 6 patients (mean 0.20%, range 0.19-0.2%), none of which was above the cut-off for diploidy (0.06-0.97%) (Vegetti et al., 2000). No statistically significant correlation was found between relative STL and the rate of euploidies, aneuploidies or diploidies (**Table 3.6**). In addition, the comparison of relative STL between pure euploid samples and samples with aneuploidies did not reveal statistically significant differences (**Table B.1** in **Appendix B**).

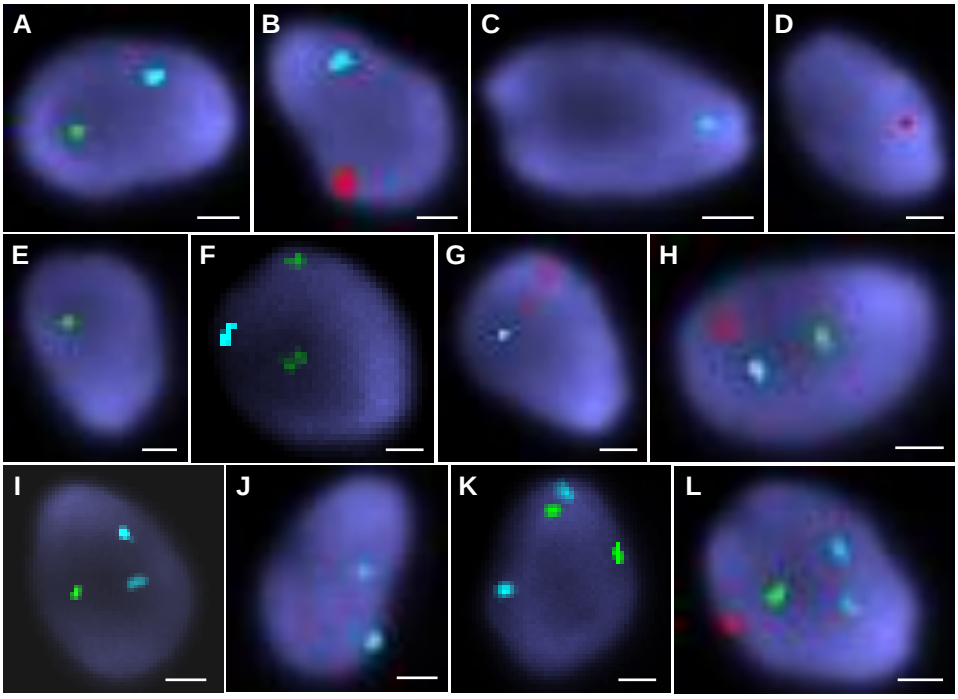

Figure 3.9 – Representative observations of the FISH assay for sperm chromosomic numeric alterations evaluation: (**A**) haploid (X,18); (**B**) haploid (Y,18); (**C**) sex chromosome nulisomy (18+); (**D**) chromosome 18 nulisomy (Y+); 3E chromosome 18 nulisomy (X+); 3F sex chromosome disomy (XX/18); (**G**) sex chromosome disomy (YY/18); (**H**) sex chromosome disomy (XY/18); (**I**) chromosome 18 disomy (X/18,18); (**J**) chromosome 18 disomy (Y/18,18); (**K**) sexual and autosomic disomy (XX/18,18); (**L**) sexual and autosomic disomy (XY/18,18). Color legends: X chromosome (green); Y chromosome (orange); chromosome 18 (aqua-blue); nucleus (DAPI-blue). Scale bar=1 µm.

3.3 Sperm telomere length and reproductive characteristics associations

From the 78 ART treatment cycles studied, 26 (33.3%) were IVF and 52 (66.7%) were ICSI. **Table 3.10** specifies the patients' demographic and stimulation characteristics.

Table 3.10 – Demographic and stimulation characteristics.

	n	Mean ± SD	Range	Rate (%)
Age				
Female age (years)	78	38.3 ± 4.3	27-49	
Male age (years)	78	39.3 ± 4.1	29-48	
Karyotype				
Normal male karyotype	68/71			95.8
Abnormal male karyotype	3/71			4.2
Normal female karyotype	69/72			95.8
Abnormal female karyotype	3/72			4.2
Infertility				
Time of infertility (years)	77	2.8 ± 2.1	1-13	
Male factor only	31/78			39.7
Female factor only	32/78			41
Mixed factors (male + female)	6/78			7.7
Mixed factors (female + female)	9/78			11.5
Stimulation				
bFSH (mIU/mL)	73	9.2 ± 4.9	2.4-31.5	
AMH (ng/mL)	72	2.4 ± 2.2	0.1-13.5	
Follicles	77	9.5 ± 4.5	1-20	
GnRH antagonist	75/78			96.2
GnRH agonist	3			3.8
Total GnRH dose	78	2647.1 ± 1239.2		
rFSH	31/78			38.5
rFSH + HMG	33/78			43.6
rFSH + rLH	12/78			15.4
HMG	2/78			2.6
Time stimulation (days)	78	9.0 ± 1.9		
Estradiol (pg/mL)	74	1596.8 ± 930.6		
Ovulation trigger				
rHCG	30/78	6500 ± 0		38.5
GnRH agonist	23/78	0.2 ± 0		29.5
Dual trigger (rHCG + agonist)	25/78			32.1

Male abnormal karyotypes: 46Xinv(Y)(p11,2q11,22); 46XY,inv(3)(p26.1q13.1); 47XYY.
Female abnormal karyotypes: 45X(3)/47XXX(2)/46XX(53); 46XX,t(10;12); 45X(3)46XX(55).
bFSH: baseline follicle stimulating hormone; rFSH; recombinant FSH; AMH: anti-müllerian hormone; GnRH: gonadotropin releasing hormone; HMG: human menopausal gonadotropin; rLH: recombinant luteinizing hormone; rHCG: recombinat human chroriogonadotropin.

No statistically significant correlations were found between relative STL and male age or time of infertility of isolated male factor infertility cases (**Table 3.11**). To further investigate a

possible effect of age on STL we categorized male age as <35 and ≥35 years, a cut-off determined in previous studies (Bray et al., 2006). No statistically significant difference was found between the relative STL of the two age groups (**Table B.1** in **Appendix B**). However, a negative significant correlation was observed between relative STL and male age in patients with AZ (**Figure 3.10 A**), OA (**Figure 3.10 B**) and AT (**Figure 3.10 C**), as stated in **Table C.1**, **Appendix C**. No statistically significant difference was found in the relative STL of cases with isolated male factor infertility, isolated female factor infertility and mixed factor infertility (**Table B.1** in **Appendix B**).

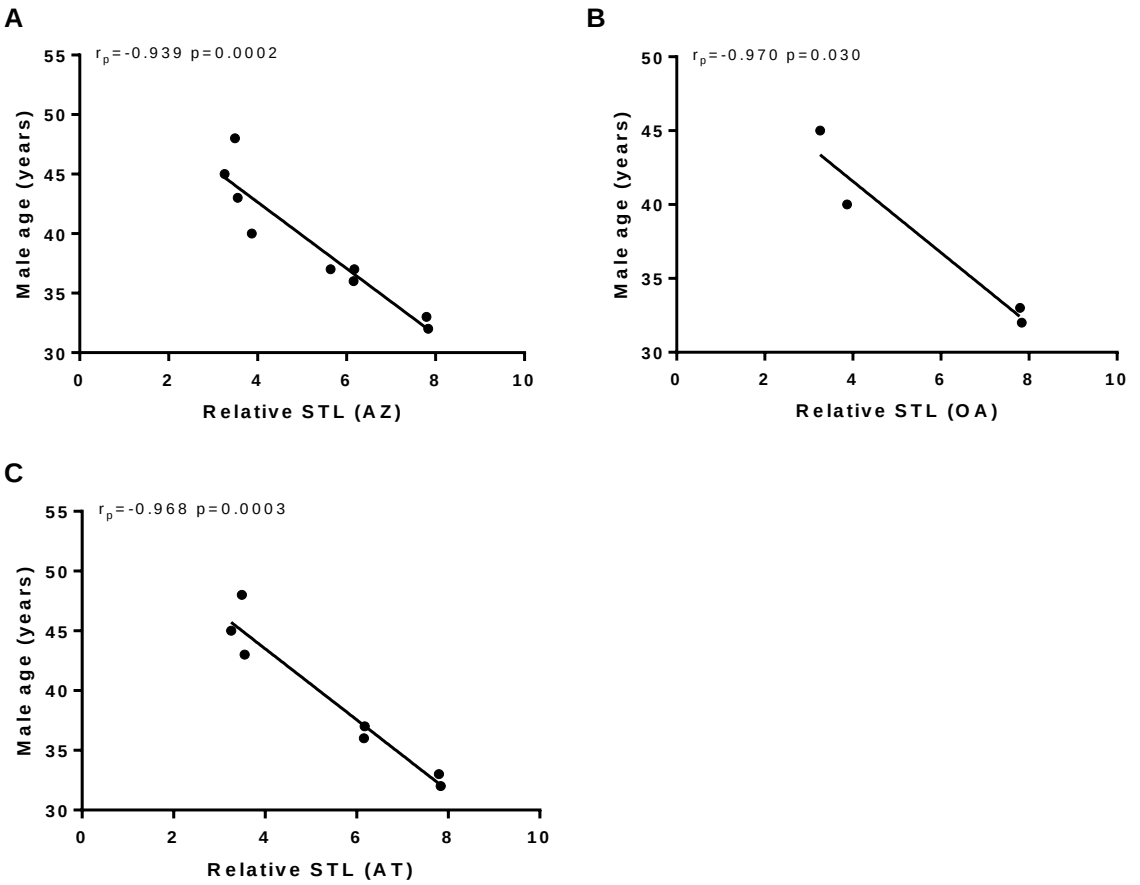

Figure 3.10 – Statistically significant correlations between relative sperm telomere length (STL) and male age, in different clinical groups. (**A**) Patients with asthenozoospermia (AZ). (**B**) Patients with oligoasthenozoospermia (OA). (**C**) Patients with asthenoteratozoospermia (AT). Pearson's correlation coefficient (r_p) and *P*-value are shown.

Table 3.11 – Correlation of relative sperm telomere length with patients' demographic parameters.

Demographic parameter	n	r_s	p
Male age (years)	73	0.03	0.821
Time of infertility (years)	27	-0.06	0.765

3.4 Sperm telomere length and embryological/ clinical outcomes associations

The embryological and clinical outcomes are described in **Table 3.12**. These results only intend to present the population study, since the total number of cycles (n=78) is too low for

comprehensive studies. For this reason, this is a prospective study, intending to analyze possible relationships with STL. Also due to the short time of the study, there are no newborn data.

No correlation was found between relative STL and the rates of fertilization, embryo cleavage, high-quality embryo, low-quality embryo, blastocyst and implantation, in couples with isolated male factor infertility (**Table 3.13**). As reported in **Table B.1** in **Appendix B**, no significant difference was found between the relative STL of couples achieving ongoing pregnancy (OP), clinical pregnancy (CP) or biochemical pregnancy (BP). In this comparison, only isolated male factor infertility cases were included. The CP cases corresponded to those that did not reach OP (abortion cases). Likewise, the BP cases included did not reach CP. The non-pregnancy group included only ECT cases.

The comparison of the frequency distribution histograms of relative STL in the totality of the samples, in the cases with embryo transfer cycles, BP, CP and OP are presented in **Figure 3.11**, in which all factors of infertility were included, and in **Figure 3.12**, in which only the isolated male factor infertility cases were included.

When including all infertility factors, 61 couples with ECT had relative STL measurement (**Table 3.14**). In 89% of the cases, relative STL was distributed around the mean value (mean±SD) and 11% cases had a higher deviation from the mean value (<mean-SD, >mean+SD). The 61 ECT originated 18 OP, in which the minimum relative STL was 2.29 and the maximum was 19.60. A pregnancy rate ($OP_{interval}/ECT_{interval}$) of 29.6% occurred in the highest sample size, that had lower relative STL, in comparison with the pregnancy rate of 40.0% obtained in a lower sample size, having the highest relative STL. When analyzing the distribution of OP throughout relative STL quartiles, Q2 and Q4 revealed the highest pregnancy rates and Q3 the lowest.

When excluding the female factor infertility cases (**Table 3.15**), 24 couples with ETC had relative STL measurement, with 92% being distributed around the mean value (mean±SD) and 8% having a higher deviation from the mean value (<mean-SD, >mean+SD). The 24 ETC originated 5 OP, whose relative STL ranged from 3.22 to 19.60. A pregnancy rate of 18.2% occurred in the highest sample size, that had lower relative STL, in comparison with the pregnancy rate of 100% (n=1) obtained in a lower sample size, with the highest relative STL. When analyzing the distribution of OP throughout relative STL quartiles, Q4 had a clear predominance of pregnancy rate (50.0%), with Q3 originating no OP.

Table 3.12 – Embryological and clinical outcomes.

	n	Mean ± SD	Range	Rate (%)
Cycles	78			
Embryo transfer cycles (ETC)	65			
Canceled cycles	13/78			16.7
Oocytes				
COC	621	8.0 ± 4.6	1-20	
MII	470	6.0 ± 3.5	0-15	
Maturation rate (MII/COC)	470/621			75.7
Normal fertilized oocytes (2PN+2PB)	388	5.0 ± 3.3	0-15	
Fertilization rate (2PN/MII)	388/470			82.6
Embryos				
Embryos cleaved-day 2	378	5.0 ± 3.0	1-12	
Embryo cleavage rate (day 2 embryos/2PN)	378/388			97.4
Day 3 embryos	338	5.4 ± 2.7	1-12	
Day 3 grade A/B embryos	332	5.3 ± 2.3	1-12	
Day 3 grade A/B rate	332/338			98.2
Day 4 embryos	268	5.2 ± 2.4	1-11	
Day 5 embryos	208	4.3 ± 2.1	1-11	
Blastocyst rate	151/245			61.6
nº of transferred embryos (TE)	97	1.5 ± 0.5	1-2	
Day of embryo transfer				
Day 1	1/65			1.5
Day 2	12/65			18.5
Day 3	9/65			13.8
Day 4	4/65			6.2
Day 5	39/65			60.0
Pregnancy				
BP (/ETC)	30/65			46.2
Sacs	27			
Implantation rate (Sacs/TE)	27/97			27.8
CP (/ETC)	25/65			38.5
Singletons (/CP)	23/25			92.0
Twins (/CP)	2/25			8.0
Triplets (/CP)	0			0
Ectopic pregnancy (/CP)	0			0
Abortion (/CP)	6/25			24.0
OP (/ETC)	19/65			29.2
OP singletons (/OP)	17/19			89.5
OP twins (/OP)	2/19			10.5

COC: cumulus-oocyte complexes; **MII**: mature oocytes at metaphase II of meiosis; **PN:** pronuclei; **PB**: polar bodies; **BP**: biochemical pregnancy; **CP**: clinical pregnancy; **OP**: ongoing pregnancy.

Table 3.13 – Correlation of relative sperm telomere length with embryological outcomes.

Embryological parameter	n	r_s	p
Fertilization rate	27	0.051	0.801
Embryo cleavage rate	27	0.227	0.256
High-quality embryo	23	-0.289	0.181
Low-quality embryo	27	0.277	0.162
Blastocyst rate	15	<-0.001	>0.999
Implantation rate	24	-0.075	0.62

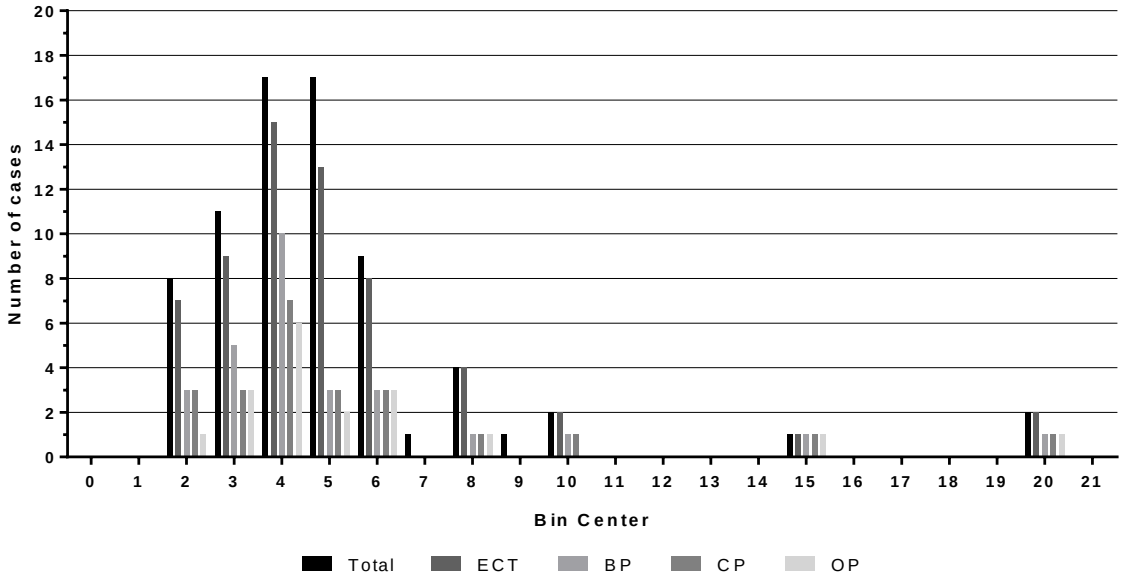

Figure 3.11 – Frequency distribution histogram of relative sperm telomere length in the totality of the samples, in the cases with embryo transfer cycles (ECT), biochemical pregnancy (BP), clinical pregnancy (CP) and ongoing pregnancy (OP). All factors of infertility were included.

Table 3.14 – Rates of ongoing pregnancy within relative STL intervals, with all factors of infertility included.

Relative STL intervals	$OP_{interval}/OP_{total}$		$OP_{interval}/ETC_{interval}$		$OP_{interval}/ETC_{total}$	
	n	Rate (%)	n	Rate (%)	n	Rate (%)
Quartiles						
Q1: 1.6-3.5	4/18	22.2	4/15	26.7	4/61	6.6
Q2: 3.5-4.5	6/18	33.3	6/16	37.5	6/61	9.8
Q3: 4.5-5.7	3/18	16.7	3/15	20.0	3/61	4.9
Q4: 5.7-19.7	5/18	27.8	5/15	33.3	5/61	8.2
Mean ± SD						
5.3 ± 3.5	16/18	88.9	16/54	29.6	16/61	26.0
<Mean - SD						
<5.3 - 3.5	0/18	0.0	0/2	0.0	0/61	0.0
>Mean + SD						
>5.3 + 3.5	2/18	11.1	2/5	40.0	2/61	3.3

STL: sperm telomere length; OP: ongoing pregnancy; ECT: embryo transfer cycles.

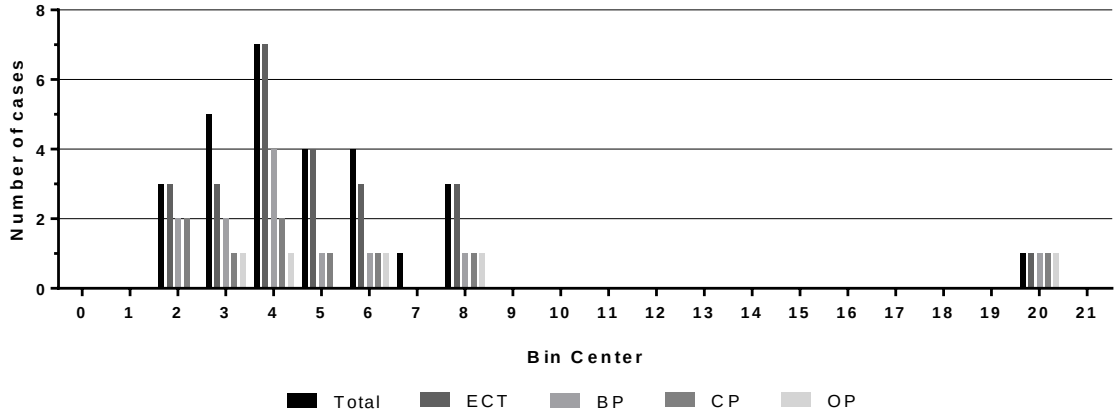

Figure 3.12 – Frequency distribution histogram of relative sperm telomere length in the totality of the samples, in the cases with embryo transfer cycles (ECT), biochemical pregnancy (BP), clinical pregnancy (CP) and ongoing pregnancy (OP). Only isolated male factor infertility cases were included.

Table 3.15 – Rates of ongoing pregnancy within relative STL intervals, including the isolated male factor infertility cases only.

Relative STL intervals	$OP_{interval}/OP_{total}$		$OP_{interval}/ETC_{interval}$		$OP_{interval}/ETC_{total}$	
	n	Rate (%)	n	Rate (%)	n	Rate (%)
Quartiles						
Q1: 1.6-3.3	1/5	20.0	1/6	16.7	1/24	4.2
Q2: 3.3-4.3	1/5	20.0	1/6	16.7	1/24	4.2
Q3: 4.3-6.1	0/5	0.0	0/6	0	0/24	0.0
Q4: 6.1-19.6	3/5	60.0	3/6	50.0	3/24	12.5
Mean ± SD						
5.2 ± 3.5	4/5	80.0	4/22	18.2	4/24	16.7
<Mean - SD						
<5.2 - 3.5	0/5	0.0	0/1	0.0	0/24	0.0
>Mean + SD						
>5.2+ 3.5	1/5	20.0	1/1	100.0	1/24	4.2

STL: sperm telomere length; OP: ongoing pregnancy; ECT: embryo transfer cycles.

4. Discussion

It is widely known that sperm quality plays an essential role in determining the success of ART treatments, which has encouraged research studies concerning efficient sperm selection methods. In recent years, studies have demonstrated a potential effect of STL, when evaluated in raw semen, in sperm quality and male infertility, temptingly pinpointing STL measurement as a new test to predict the outcomes of ART treatments and contribute to improve their success rates. In addition, STL was consensually shown to increase from raw semen to swim-up purified sperm (Santiso et al., 2010; Yang et al., 2015a; Zhao et al., 2016). Therefore, we analyzed STL in purified sperm in order to ascertain if the relations of STL with sperm quality and male infertility are maintained in a high-quality selected sperm population. We provide a complete analysis of sperm quality, including standard seminal parameters, sperm oxidative profile, DNA fragmentation, chromatin maturity and chromosomic alterations. Furthermore, we included sDNAfrag staining patterns to better characterize the relation of STL with sDNAfrag. In addition, for the first time we provide a full analyzes of the effect of STL in embryological and clinical outcomes, including the rates of fertilization, embryo cleavage, embryo quality, blastocyst formation, implantation, BP, CP and OP.

We applied the Q-PCR method for measurement of relative STL in couples undergoing infertility treatments. In recent years, Q-PCR has been adopted by several research studies to measure relative STL (**Table A.1**, **Appendix A**). Its main advantage is the requirement of small amounts of DNA, an aspect particularly important in the analysis of sperm, which has low DNA yield. In addition, since we intended to analyze the relation of STL with clinical parameters, using sperm retrieved from swim-up, which are the ones selected for ART treatments, was demanding, which diminished the sperm count available for TL measurement and thus enhanced the low DNA yield. Q-PCR is faster, cheaper and has higher-throughput in comparison with other technologies that access TL (Montpetit et al., 2014). However, TL measured by Q-PCR is not comparable between studies, due to inter-assay variation and deviations introduced by differential DNA extraction methods or amplification efficiency (Aviv et al., 2011; Kurjanowicz et al., 2017; Raschenberger et al., 2016).

We obtained a logarithmic relative STL distribution, indicating that sperm samples with longer telomeres are under-represented in a given population, which has been previously demonstrated (Kimura et al., 2008). We found no significant correlations of relative STL with seminal parameters, sperm protein carbonylation, total sDNAfrag, sperm chromatin maturity or sperm euploidy/aneuploidy rate, which emphasizes the efficacy of the sperm purification method used in selecting a high-quality sperm population to be used in ART treatments. However, when performing the statistical analysis in different clinical groups, significant correlations were revealed. We, therefore, attribute the contradictory results reported in the literature to the heterogenicity of characteristics and size of the samples under analysis.

A significant positive correlation of relative STL with sperm PM was previously reported in the raw semen of normozoospermic patients: r=0.46, p=0.004 (Rocca et al., 2016) and r=0.42,

p=0.03 (Zhao et al., 2016), but not in studies that included patients with altered seminal parameters (Thilagavathi et al., 2013a; Turner and Hartshorne, 2013), indicating that factors related to impaired PM are independent of STL. In our purified sperm samples, no significant correlation was found between relative STL and PM, either in the totality of the population or in the normozoospermic group, which may be explained by the fact that purified sperm, which is known to have, besides higher STL, better PM (Zhao et al., 2016), is not representative of the STL-PM relation in raw semen.

A significant positive correlation between relative STL and TSC was also previously reported in the raw semen of normozoospermic patients: r=0.44, p=0.002 (Zhao et al., 2016). It was proposed that short telomeres induce apoptosis in sperm and therefore a reduced sperm count (Reig-Viader et al., 2014a). However, a relation between sperm concentration and apoptotic index has only been reported in patients with normal seminal parameters, indicating an apoptosis dysregulation in patients with low-quality sperm (Ricci et al., 2002). In line with these findings, although we did not find a relation between relative STL and TSC in the totality of the population, we observed a significant positive correlation between relative STL and TSC in normozoospermic patients (r=0.361, p=0.039), corroborating the previous finding (Zhao et al., 2016). In addition, human sperm apoptosis decreases with age, indicating a decline of the natural sperm selection process with aging (Singh et al., 2003). Thus, the relation between sperm count with STL in a population may depend on the percentage of normozoospermic patients included and on the prevailing age set of the patients under analysis. This may explain why discordant results have been reported, regarding the association between STL and sperm concentration in raw semen, with some studies revealing a significant positive correlation: r=0.53, p<0.01 (Yang et al., 2015a); r=0.33, p=0.0064 (Cariati et al., 2016); and other studies reporting the absence of correlation between these parameters (Rocca et al., 2016; Thilagavathi et al., 2013a; Turner and Hartshorne, 2013). Note that, although STL may contribute to altered sperm count, additional causes of OZ are probably independent of STL, explaining why we did not see significant differences in the relative STL of patients with NZ or OZ.

Finally, within seminal parameters, we found no association between relative STL and sperm NM, either in the totality of the population or in the normozoospermic group, which is in accordance with the literature (Rocca et al., 2016; Thilagavathi et al., 2013a; Turner and Hartshorne, 2013; Zhao et al., 2016).

Seminal parameters in additional clinical groups, analyzed for the first time, revealed unexpected significant negative correlations with relative STL, namely: TSC (n=6, r=-0.87, p=0.025) and Conc (n=6, r=-0.86, p=0.027) in OT, PM in AZ (n=9, r=-0.89, p=0.003), TZ (n=32, r=-0.39, p=0.026) and OA (n=4, r=-1, p<0.001). The population subdivision in groups led to a drastic decrease in the number of evaluated cases. Although the correlation coefficients obtained reveal a high/very high correlation, a higher “r” appears to coincide with a lower “n”, possibly indicating the absence of biological significance. To confirm the importance of these results it would be necessary to increase the sample size in the future, so that the “n” wouldn’t be excessively small in the different clinical groups.

Previous studies demonstrated a significant and negative correlation between sDNAfrag and relative STL in the raw semen of normozoospermic patients: r=-0.44, p=0.001 (Rocca et al., 2016). Although we did not find this correlation in the totality of the population or in the different clinical groups, we found for the first time a negative significant correlation of relative STL with the specific PAR sDNAfrag pattern (r=-0.371, p=0.022). In a previous study, PAR was the only pattern shown to increase from raw semen to swim-up selected sperm, in which it was the second most frequent sDNAfrag region, a result we replicated (Sá et al., 2015). It was suggested that since the PAR is a gene poor region, with lower content of protamines, it has higher susceptibility to oxidative damage than the other regions of sperm head, which have more compact chromatin. It seems likely that a higher content of ROS in sperm promotes PAR sDNAfrag and triggers telomere shortening, rather than telomere shortening promoting sDNAfrag specifically in PAR as a result of triggered apoptosis. Although we did not find a correlation between relative STL and protein carbonylation, one study evaluating the superoxide content in sperm of 150 patients reported a negative significant correlation between STL and ROS production: r=-0.40, p=0.004 (Zhao et al., 2016). Furthermore, when subdividing PAR sDNAfrag in subgroups, we detected a significant negative correlation in the <30.6% subgroup (r=-0.398, p=0.036) and in the normozoospermic group (r=-0.464, p=0.03); which suggests that in pathological groups the high levels of sDNAfrag may reflect apoptotic events that are independent of STL. This hypothesis is supported by the fact that no relation was found between STL and sDNAfrag in reports that included the raw semen of patients with altered seminal parameters in the analysis (Cariati et al., 2016; Santiso et al., 2010; Thilagavathi et al., 2013a; Turner and Hartshorne, 2013). Moreover, we found a significant positive correlation between relative STL and the sDNAfrag H pattern, the most common pattern observed in swim-up purified sperm (Sá et al., 2015), in the totality of the population (r=0.348, p=0.032). sDNAfrag is related with increased overall aneuploidy rate (Muriel et al., 2007), in which there is a higher DNA content, possible explaining higher TL measures in sperm fragmented DNA, when analyzing the most severe sDNAfrag pattern, in which DNA fragmentation is spread all over the sperm head. However, no correlation was found between relative STL and the sDNAfrag-H≥30.6% subgroup. In order to find the origin of the correlation found in the totality of the population we analyzed the correlations between relative STL and sDNAfrag-H within different chromatin maturity intervals, because immature sperm is related with increased fragmentation and aneuploidy rates, as a mechanism to eliminate sperm with genomic defects (Balasuriya et al., 2011; Kovanci et al., 2001). Although we did not find a correlation in the most immature sperm subgroup (AB- <50%), possibly because additional factors are contributing to the sDNAfrag-H, besides the high aneuploidy rate, we did find a correlation between relative STL and sDNAfrag-H (r=0.559, p=0.03), in low chromatin maturity conditions (AB- ≥50-<70%). Therefore, we conclude that both decreased sperm chromatin maturity and increased sDNAfrag-H are simultaneously contributing for a higher STL, possibly due to increased sperm aneuploidy rate. These results emphasize the importance of quantifying the different staining patterns when performing a sDNAfrag analysis.

Chromatin maturity was not significantly and positively correlated with relative STL in the

totality of our population or in the normozoospermic group, unlike previously reported in the raw semen of normozoospermic patients: r=0.41, p=0.002 (Rocca et al., 2016). However, we observed an increased relative STL in the most immature sperm subgroup (AB- <50%) in comparison with the most mature (AB- ≥80). When differentiating the different clinical groups, a significant negative correlation was found between relative STL and chromatin maturity (r=0.74, p=0.004), in patients with TZ. Since most of the morphological alterations in this TZ subgroup occurred in the head and midpiece and there is a relation between abnormal head shape, increased aneuploidy rate and chromatin immaturity in sperm (Calogero et al., 2003; Härkönen et al., 2001; Kovanci et al., 2001; Mehdi et al., 2012), we conclude that a higher DNA content is inducing a higher relative STL in this particular morphological abnormal sperm population, that has low chromatin maturity.

Although telomeres are vital for the maintenance of genomic stability, no correlation was found between relative STL and chromosomic abnormalities in sperm, in agreement with a previous report (Cariati et al., 2016). This may be explained by the regulatory mechanism in spermatocytes believed to promote the elimination of aneuploid spermatocytes (Hemann et al., 2001a; Liu et al., 2004b). It is important to note that the presumable association between increased relative STL and increased aneuploidy rate referred above was applied to pathological sperm subpopulations.

Male fertility and sperm quality is known to decrease with age (Hassan and Killick, 2003; Kidd et al., 2001). Surprisingly, many studies have reported a positive association between STL and male age, which we did not observe, as did not other reports (Rocca et al., 2016; Thilagavathi et al., 2013a; Zhao et al., 2016). This could be explained by our limited age range, having only one patient bellow 30 years and none above 50 years. However, even in studies reported in the literature with a higher number of samples and a larger age range, the correlations obtained with STL were low or negligible: r=0.34, p<0.02 (Baird et al., 2006); r=0.32, p=0.0002 (Aston et al., 2012); r=0.32, p=0.01 (Allsopp et al., 1992); r=0.1, p=0.04 (Yang et al., 2015b); which calls into question their relevance. In addition, we found a significant negative correlation between relative STL and male age in several clinical groups: r= -0.939, p=0.0002, in AZ; r=-0.970, p=0.03, in OA; and r=-0.968, p=0.0003 in AT. OAT is the only clinical group with asthenozoospermic patients that did not reveal a significant correlation between these parameters, probably because the “n” was dramatically low (n=3). It appears that in asthenozoospermic patients, relative STL decreases with age, possibly because the factor affecting PM is also affecting STL and accumulating with age. DNA damage in male germ line increases with age, possibly as a result of ROS, which also accumulate with age (Schmid et al., 2007; Singh et al., 2003). In addition, ROS are known to impair seminal parameters (Agarwal et al., 1994) and sperm motility, in particular (Guthrie and Welch, 2012; Pereira et al., 2017). Thus, the accumulation of ROS with age could promote both STL shortening and impairment of PM.

To date, only one study has evaluated the effect of STL in the embryological outcomes of ART treatments, in which STL was measured in purified sperm (Yang et al., 2015b). In this study no relation was found between relative STL and fertilization rate, in conformity with our

results. However, we did not also obtain a relation between relative STL and embryo cleavage, embryo quality or blastocyst formation rates, while in the referred study the authors show a positive association between STL and good quality embryo rate (regression coefficient: 1.63, $p<0.001$) and transplantable embryo rate (regression coefficient: 1.57, $p<0.001$), conferring STL a predictive value of embryonic quality. This transplantable embryo rate corresponded to our high-quality embryo rate, including embryos with <25% fragmentation. The discrepant results may result from the different rates of embryo quality obtained, as we had 98% of high-quality embryos and the authors had only 75%.

In line with a previous report measuring STL in raw semen, in which there were no differences between the STL of couples with BP and CP (Turner and Hartshorne, 2013), we found no differences between relative STL of OP, CP and BP. In addition, one study using purified sperm did not also obtain an association between STL and CP (Yang et al., 2015b). In a different report the authors determined a relative STL interval in which the pregnancy rate (OP) was 35.7%, and outside which the pregnancy rate was null (Cariati et al., 2016). However, the STL measurement in this study was performed in sperm from raw semen, which are not normally used in ART treatments and whose STL-sperm quality relations do not represent the ones observed in purified sperm, according to our results.

The relative STL of the majority of our sperm purified population occurred within an interval that originated a pregnancy rate of 29.6%. Less frequently, STL had a higher deviation from the mean value, presenting longer STL, that originated a pregnancy rate of 40.0%. When removing the female factor infertility cases from the analysis, the pregnancy rate for STL around the mean value was 18.2%, while longer STL revealed 100% pregnancy rate. Although in clinical practice isolated male factor infertility cases are very rare, this analysis allows us to determine a possible interference of female factor infertility in the potentiality of STL to originate an OP. To further evaluate this effect, we differentiated our STL in quartiles. OP appeared to be evenly distributed within the different relative STL quartiles in the totality of the population. Curiously, when removing the female factor infertility cases, even though this criterium reduced the sample size dramatically, there was a clear predominance of OP in the Q4 (50%). Therefore, we provide insights that higher STL, although underrepresented in a population, may have higher success rates in originating OP, possibly related with an active role during early embryo development.

5. Conclusions and Future Perspectives

This is the most comprehensive study realized to date regarding the effect of STL in sperm quality and clinical outcomes. STL was measured in purified sperm, in which there was no correlation between relative STL and sperm quality, confirming that the methods currently used for sperm selection in ART treatments are already isolating the highest quality sperm. The analysis of the correlations reported in the literature, regarding STL in raw semen and sperm quality, suggest that pathological clinical cases may have interfering factors that disassociate STL from sperm quality. Since normozoospermic patients represent a reduced group in general population, STL may not be appropriate to evaluate sperm quality. Nevertheless, due to the importance of telomeres in meiosis, fertilization and early embryo development, STL may still be a useful parameter to predict clinical outcomes, whose measurement could be requested not in altered seminal parameters cases, but in idiopathic infertility or recurrent pregnancy loss cases. Although we cannot fully conclude that STL is related with clinical outcomes, we provide insights that higher STL is related with higher pregnancy rates. It seems plausible that, independently of the lengthening mechanisms occurring during early development, the TL transmitted through sperm to the embryo could has a decisive effect right after fertilization. In addition, we cannot exclude the influence of oocyte's telomeres, which were proposed to guide the telomere lengthening mechanisms occurring in early development until the blastocyst stage, in the embryo's final TL. Since TL in women is higher than in men and TL in oocytes was shown to be higher than in sperm (Thilagavathi et al., 2013c; Turner and Hartshorne, 2013), the female contribution to the embryo's final TL seems to be quite relevant, perhaps even more than STL in determining the clinical outcome. In addition, TL is an indicator of telomere structure, which is the triggering factor in all the signaling pathways related to telomere function (Stewart et al., 2003). Therefore, a disruption in telomere structure, independently of TL, could impair the telomere function in sperm and early embryos. In the future, the expansion of the sample size for consolidation of the results and the application of complementary methodologies, such as Western Blot for shelterin evaluation in the sperm samples, are paths to explore in order to clarify the suitability of STL as a biomarker of male infertility, whose measurement could be implemented in medically assisted reproduction centers to contribute to improve the success of ART treatments.

6. References

Achi, M.V., Ravindranath, N., Dym, M., 2000. Telomere length in male germ cells is inversely correlated with telomerase activity. Biol Reprod 63, 591-598.

Agarwal, A., Ikemoto, I., Loughlin, K.R., 1994. Relationship of sperm pParameters with levels of reactive oxygen species in semen specimens. J Urol 152, 107-110.

Agarwal, A., Mulgund, A., Hamada, A., Chyatte, M., 2015. A unique view on male infertility around the globe. Reprod Biol Endocrinol 13, 37.

Aitken, R.J., Smith, T.B., Jobling, M.S., Baker, M.A., De Iuliis, G.N., 2014. Oxidative stress and male reproductive health. Asian J Androl 16, 31-38.

Allsopp, R.C., Vaziri, H., Patterson, C., Goldstein, S., Younglai, E.V., Futcher, A.B., Greider, C.W., Harley, C.B., 1992. Telomere length predicts replicative capacity of human fibroblasts. Proc Natl Acad Sci U S A 89, 10114-10118.

Almeida, C., Cardoso, M.F., Sousa, M., Viana, P., Goncalves, A., Silva, J., Barros, A., 2005. Quantitative study of caspase-3 activity in semen and after swim-up preparation in relation to sperm quality. Hum Reprod 20, 1307-1313.

Almeida, C., Cunha, M., Ferraz, L., Silva, J., Barros, A., Sousa, M., 2011. Caspase-3 detection in human testicular spermatozoa from azoospermic and non-azoospermic patients. Int J Androl 34, e407-e414.

Alter, B.P., Baerlocher, G.M., Savage, S.A., Chanock, S.J., Weksler, B.B., Willner, J.P., Peters, J.A., Giri, N., Lansdorp, P.M., 2007. Very short telomere length by flow fluorescence in situ hybridization identifies patients with dyskeratosis congenita. Blood 110, 1439-1447.

Antunes, D.M., Kalmbach, K.H., Wang, F., Dracxler, R.C., Seth-Smith, M.L., Kramer, Y., Buldo-Licciardi, J., Kohlrausch, F.B., Keefe, D.L., 2015. A single-cell assay for telomere DNA content shows increasing telomere length heterogeneity, as well as increasing mean telomere length in human spermatozoa with advancing age. J Assist Reprod Genet 32, 1685-1690.

Asmarinah, Syauqy, A., Umar, L.A., Lestari, S.W., Mansyur, E., Hestiantoro, A., Paradowszka-Dogan, A., 2016. Sperm chromatin maturity and integrity correlated to zygote development in ICSI program. Syst Biol Reprod Med 62, 309-316.

Aston, K.I., Hunt, S.C., Susser, E., Kimura, M., Factor-Litvak, P., Carrell, D., Aviv, A., 2012. Divergence of sperm and leukocyte age-dependent telomere dynamics: implications for male-driven evolution of telomere length in humans. Mol Hum Reprod 18, 517-522.

Aviv, A., Hunt, S.C., Lin, J., Cao, X., Kimura, M., Blackburn, E., 2011. Impartial comparative analysis of measurement of leukocyte telomere length/DNA content by Southern blots and qPCR. Nucleic Acids Res 39, e134.

Azzalin, C.M., Reichenbach, P., Khoriauli, L., Giulotto, E., Lingner, J., 2007. Telomeric repeat containing RNA and RNA surveillance factors at mammalian chromosome ends. Science 318, 798-801.

Baird, D.M., Britt-Compton, B., Rowson, J., Amso, N.N., Gregory, L., Kipling, D., 2006. Telomere instability in the male germline. Hum Mol Genet 15, 45-51.

Balasuriya, A., Speyer, B., Serhal, P., Doshi, A., Harper, J.C., 2011. Sperm chromatin dispersion test in the assessment of DNA fragmentation and aneuploidy in human spermatozoa. Reprod Biomed Online 22, 428-436.

Barratt, C.L.R., Aitken, R.J., Björndahl, L., Carrell, D.T., de Boer, P., Kvist, U., Lewis, S.E.M., Perreault, S.D., Perry, M.J., Ramos, L., Robaire, B., Ward, S., Zini, A., 2010. Sperm DNA: organization, protection and vulnerability: from basic science to clinical applications—a position report. Hum Reprod 25, 824–838.

Baumann, P., Cech, T.R., 2001. Pot1, the putative telomere end-binding protein in fission yeast and humans. Science 292, 1171-1175.

Bernardes de Jesus, B., Schneeberger, K., Vera, E., Tejera, A., Harley, C.B., Blasco, M.A., 2011. The telomerase activator TA-65 elongates short telomeres and increases health span of adult/old mice without increasing cancer incidence. Aging Cell 10, 604-621.

Blackburn, E.H., 1984. Telomeres: do the ends justify the means? Cell 37, 7-8.

Blackburn, E.H., 1991. Structure and function of telomeres. Nature 350, 569-573.

Blackburn, E.H., 2000. Telomere states and cell fates. Nature 408, 53-56.

Blackburn, E.H., 2001. Switching and signaling at the telomere. Cell 106, 661-673.

Blackburn, E.H., Gall, J.G., 1978. A tandemly repeated sequence at the termini of the extrachromosomal ribosomal RNA genes in Tetrahymena. J Mol Biol 120, 33-53.

Bray, I., Gunnell, D., Davey Smith, G., 2006. Advanced paternal age: how old is too old? J Epidemiol Community Health 60, 851-853.

Brenner, C.A., Wolny, Y.M., Adler, R.R., Cohen, J., 1999. Alternative splicing of the telomerase catalytic subunit in human oocytes and embryos. Mol Hum Reprod 5, 845-850.

Broccoli, D., Smogorzewska, A., Chong, L., de Lange, T., 1997. Human telomeres contain two distinct Myb-related proteins, TRF1 and TRF2. Nat Genet 17, 231-235.

Broer, L., Codd, V., Nyholt, D.R., Deelen, J., Mangino, M., Willemsen, G., Albrecht, E., Amin, N., Beekman, M., de Geus, E.J., Henders, A., Nelson, C.P., Steves, C.J., Wright, M.J., de Craen, A.J., Isaacs, A., Matthews, M., Moayyeri, A., Montgomery, G.W., Oostra, B.A., Vink, J.M., Spector, T.D., Slagboom, P.E., Martin, N.G., Samani, N.J., van Duijn, C.M., Boomsma, D.I., 2013. Meta-analysis of telomere length in 19713 subjects reveals high heritability, stronger maternal inheritance and a paternal age effect. Eur J Hum Genet 21, 1163-1168.

Bryan, T.M., Marusic, L., Bacchetti, S., Namba, M., Reddel, R.R., 1997. The telomere lengthening mechanism in telomerase-negative immortal human cells does not involve the telomerase RNA subunit. Hum Mol Genet 6, 921-926.

Bucar, S., Goncalves, A., Rocha, E., Barros, A., Sousa, M., Sá, R., 2015. DNA fragmentation in human sperm after magnetic-activated cell sorting. J Assist Reprod Genet 32, 147-154.

Calado, R.T., Young, N.S., 2009. Telomere diseases. N Engl J Med 361, 2353-2365.

Calogero, A.E., Burrello, N., De Palma, A., Barone, N., D'Agata, R., Vicari, E., 2003. Sperm aneuploidy in infertile men. Reprod Biomed Online 6, 310-317.

Cariati, F., Jaroudi, S., Alfarawati, S., Raberi, A., Alviggi, C., Pivonello, R., Wells, D., 2016. Investigation of sperm telomere length as a potential marker of paternal genome integrity and semen quality. Reprod Biomed Online 33, 404-411.

Cawthon, R.M., 2002. Telomere measurement by quantitative PCR. Nucleic Acids Res 30, e47.

Cesare, A.J., Reddel, R.R., 2010. Alternative lengthening of telomeres: models, mechanisms and implications. Nat Rev Genet 11, 319-330.

Chai, W., Du, Q., Shay, J.W., Wright, W.E., 2006. Human telomeres have different overhang sizes at leading versus lagging strands. Mol Cell 21, 427-435.

Chatziparasidou, A., Christoforidis, N., Samolada, G., Nijs, M., 2015. Sperm aneuploidy in infertile male patients: a systematic review of the literature. Andrologia 47, 847-860.

Chemes, H.E., Rawe, V.Y., 2003. Sperm pathology: a step beyond descriptive morphology. Origin, characterization and fertility potential of abnormal sperm phenotypes in infertile men. Hum Reprod Update 9, 405-428.

Conomos, D., Pickett, H.A., Reddel, R.R., 2013. Alternative lengthening of telomeres: remodeling the telomere architecture. Front Oncol 3, 27.

Covault, J., Abreu, C., Kranzler, H., Oncken, C., 2003. Quantitative real-time PCR for gene dosage determinations in microdeletion genotypes. Biotechniques 35, 594-396, 598.

Cram, D.S., O'Bryan, M.K., de Kretser, D.M., 2001. Male infertility genetics-the future. J Androl 22, 738-746.

de Lange, T., 1992. Human telomeres are attached to the nuclear matrix. EMBO J 11, 717-724.

de Lange, T., 2005. Shelterin: the protein complex that shapes and safeguards human telomeres. Genes Dev 19, 2100-2110.

de Lange, T., 2009. How telomeres solve the end-protection problem. Science 326, 948-952.

De Meyer, T., Eisenberg, D.T., 2015. Possible technical and biological explanations for the 'parental telomere length inheritance discrepancy' enigma. Eur J Hum Genet 23, 3-4.

De Meyer, T., Rietzschel, E.R., De Buyzere, M.L., De Bacquer, D., Van Criekinge, W., De Backer, G.G., Gillebert, T.C., Van Oostveldt, P., Bekaert, S., 2007. Paternal age at birth is an important determinant of offspring telomere length. Hum Mol Genet 16, 3097-3102.

Denchi, E.L., de Lange, T., 2007. Protection of telomeres through independent control of ATM and ATR by TRF2 and POT1. Nature 448, 1068-1071.

Dias, T.R., Alves, M.G., Bernardino, R.L., Martins, A.D., Moreira, A.C., Silva, J., Barros, A., Sousa, M., Silva, B.M., Oliveira, P.F., 2015. Dose-dependent effects of caffeine in human Sertoli cells metabolism and oxidative profile: relevance for male fertility. Toxicology 328, 12-20.

Diotti, R., Loayza, D., 2011. Shelterin complex and associated factors at human telomeres. Nucleus 2, 119-135.

Doksani, Y., Wu, J.Y., de Lange, T., Zhuang, X., 2013. Super-resolution fluorescence imaging of telomeres reveals TRF2-dependent T-loop formation. Cell 155, 345-356.

Eisenberg, D.T., 2011. An evolutionary review of human telomere biology: the thrifty telomere hypothesis and notes on potential adaptive paternal effects. Am J Hum Biol 23, 149-167.

Eisenberg, D.T., Hayes, M.G., Kuzawa, C.W., 2012. Delayed paternal age of reproduction in humans is associated with longer telomeres across two generations of descendants. Proc Natl Acad Sci U S A 109, 10251-10256.

Fauce, S.R., Jamieson, B.D., Chin, A.C., Mitsuyasu, R.T., Parish, S.T., Ng, H.L., Kitchen, C.M., Yang, O.O., Harley, C.B., Effros, R.B., 2008. Telomerase-based pharmacologic enhancement of antiviral function of human CD8+ T lymphocytes. J Immunol 181, 7400-7406.

Feng, J., Funk, W., Wang, S., Weinrich, S., Avilion, A., Chiu, C., Adams, R., Chang, E., Allsopp, R., Yu, J., Le, S., West, M.D., Harley, C.B., Andrews, W.H., Greider, C.W., Villeponteau, B., 1995. The RNA component of human telomerase. Science 269, 1236-1241.

Ferlin, A., Rampazzo, E., Rocca, M.S., Keppel, S., Frigo, A.C., De Rossi, A., Foresta, C., 2013. In young men sperm telomere length is related to sperm number and parental age. Hum Reprod 28, 3370-3376.

Forsyth, N.R., Wright, W.E., Shay, J.W., 2002. Telomerase and differentiation in multicellular organisms: turn it off, turn it on, and turn it off again. Differentiation 69, 188-197.

Galati, A., Micheli, E., Cacchione, S., 2013. Chromatin structure in telomere dynamics. Front Oncol 3, 46.

Gardner, D.K., Lane, M., Stevens, J., Schlenker, T., Schoolcraft, W.B., 2000. Blastocyst score affects implantation and pregnancy outcome: towards a single blastocyst transfer. Fertil Steril 73, 1155-1158.

Gineitis, A.A., Zalenskaya, I.A., Yau, P.M., Bradbury, E.M., Zalensky, A.O., 2000. Human sperm telomere-binding complex involves histone H2B and secures telomere membrane attachment. J Cell Biol 151, 1591-1598.

Gomes, M., Gonçalves, A., Rocha, E., Sá, R., Alves, A., Silva, J., Barros, A., Pereira, M.L., Sousa, M., 2015. Effect of in vitro exposure to lead chloride on semen quality and sperm DNA fragmentation. Zygote 23, 384-393.

Gonçalves, C., Cunha, M., Rocha, E., Fernandes, S., Silva, J., Ferraz, L., Oliveira, C., Barros, A., Sousa, M., 2017. Y-chromosome microdeletions in nonobstructive azoospermia and severe oligozoospermia. Asian J Androl 19, 338-345.

Graakjaer, J., Der-Sarkissian, H., Schmitz, A., Bayer, J., Thomas, G., Kolvraa, S., Londono-Vallejo, J.A., 2006. Allele-specific relative telomere lengths are inherited. Hum Genet 119, 344-350.

Grangeia, A., Barro-Soria, R., Carvalho, F., Damas, A.M., Maurício, A.C., Kunzelmann, K., Barros, A., Sousa, M., 2008. Molecular and functional characterization of CBAVD-causing mutations located in CFTR nucleotide-binding domains. Cell Physiol Biochem 22, 79-92.

Greider, C.W., Blackburn, E.H., 1985. Identification of a specific telomere terminal transferase activity in Tetrahymena extracts. Cell 43, 405-413.

Greider, C.W., Blackburn, E.H., 1987. The telomere terminal transferase of Tetrahymena is a ribonucleoprotein enzyme with two kinds of primer specificity. Cell 51, 887-898.

Griffith, J.D., Comeau, L., Rosenfield, S., Stansel, R.M., Bianchi, A., Moss, H., de Lange, T., 1999. Mammalian telomeres end in a large duplex loop. Cell 97, 503-514.

Guthrie, H.D., Welch, G.R., 2012. Effects of reactive oxygen species on sperm function. Theriogenology 78, 1700-1708.

Hamada, A., Esteves, S.C., Agarwal, A., 2011. Unexplained male infertility: potential causes and management. Hum. Androl. 1, 2-16.

Hammoud, S.S., Nix, D.A., Zhang, H., Purwar, J., Carrell, D.T., Cairns, B.R., 2009. Distinctive chromatin in human sperm packages genes for embryo development. Nature 460, 473-478.

Härkönen, K., Suominen, J., Lähdetie, J., 2001. Aneuploidy in spermatozoa of infertile men with teratozoospermia. Int J Androl. 24, 197-205.

Harley, C.B., Liu, W., Blasco, M., Vera, E., Andrews, W.H., Briggs, L.A., Raffaele, J.M., 2011. A natural product telomerase activator as part of a health maintenance program. Rejuvenation Res 14, 45-56.

Harton, G.L., Tempest, H.G., 2012. Chromosomal disorders and male infertility. Asian J Androl 14, 32-39.

Hassan, M.A.M., Killick, S.R., 2003. Effect of male age on fertility: evidence for the decline in male fertility with increasing age. Fertil Steril 79, 1520-1527.

Hassold, T., Hunt, P., 2001. To err (meiotically) is human: the genesis of human aneuploidy. Nat Rev Genet 2, 280-291.

Hayflick, L., 1965. The limited in vitro lifetime of human diploid cell strains. Exp Cell Res 37, 614-636.

Hemann, M.T., Rudolph, K.L., Strong, M.A., DePinho, R.A., Chin, L., Greider, C.W., 2001a. Telomere dysfunction triggers developmentally regulated germ cell apoptosis. Mol Biol Cell 12, 2023-2030.

Hemann, M.T., Strong, M.A., Hao, L.Y., Greider, C.W., 2001b. The shortest telomere, not average telomere length, is critical for cell viability and chromosome stability. Cell 107, 67-77.

Henderson, E., Hardin, C.C., Walk, S.K., Tinoco Jr, I., Blackburn, E.H., 1987. Telomeric DNA oligonucleotides form novel intramolecular structures containing guanine-guanine base pairs. Cell 51, 899-908.

Henderson, E.R., Blackburn, E.H., 1989. An overhanging 3' terminus is a conserved feature of telomeres. Mol Cell Biol 9, 345-348.

Henderson, S.A., Edwards, R.G., 1968. Chiasma frequency and maternal age in mammals. Nature 218, 22-28.

Hjelmborg, J.B., Dalgård, C., Mangino, M., Spector, T.D., Halekoh, U., Möller, S., Kimura, M., Horvath, K., Kark, J.D., Christensen, K., Kyvik, K.O., Aviv, A., 2015. Paternal age and telomere length in twins: the germ stem cell selection paradigm. Aging Cell 14, 701–703.

Huirne, J.A., Homburg, R., Lambalk, C.B., 2007. Are GnRH antagonists comparable to agonists for use in IVF? Hum Reprod 22, 2805-2813.

Ioannou, D., Millan, N., Jordan, E., Tempest, H.G., 2014. Global telomere organisation in the 3D human sperm nucleus: a new arrangement and inferences for fertilization and embryogenesis. Fertil Steril 102, e111.

Ioannou, D., Millan, N.M., Jordan, E., Tempest, H.G., 2017. A new model of sperm nuclear architecture following assessment of the organization of centromeres and telomeres in three-dimensions. Sci Rep 7, 41585.

Ioannou, D., Tempest, H.G., 2016. Segmented hairpin-loop organization of chromosomes in sperm nuclei: implications for fertilization and embryogenesis. Fertil Steril 106, e303.

Jäger, K., Walter, M., 2016. Therapeutic targeting of telomerase. Genes (Basel) 7, 39.

Jang, J.S., Choi, Y.Y., Lee, W.K., Choi, J.E., Cha, S.I., Kim, Y.J., Kim, C.H., Kam, S., Jung, T.H., Park, J.Y., 2008. Telomere length and the risk of lung cancer. Cancer Sci 99, 1385-1389.

Johnson, M.H., 2013. Making eggs, Essential reproduction, 7th ed. John Wiley and Sons, Chichester, pp. 133-150.

Jørgensen, P.B., Fedder, J., Koelvraa, S., Graakjaer, J., 2013. Age-dependence of relative telomere length profiles during spermatogenesis in man. Maturitas 75, 380-385.

Kalmbach, K.H., Antunes, D.M., Kohlrausch, F., Keefe, D.L., 2015. Telomeres and female reproductive aging. Semin Reprod Med 33, 389-395.

Karlseder, J., Broccoli, D., Dai, Y., Hardy, S., de Lange, T., 1999. p53- and ATM-dependent apoptosis induced by telomeres lacking TRF2. Science 283, 1321-1325.

Karlseder, J., Smogorzewska, A., de Lange, T., 2002. Senescence induced by altered telomere state, not telomere loss. Science 295, 2446-2449.

Keefe, D., Kumar, M., Kalmbach, K., 2015. Oocyte competency is the key to embryo potential. Fertil Steril 103, 317-322.

Keefe, D.L., 2016. Telomeres, reproductive aging, and genomic instability during early development. Reprod Sci 23, 1612-1615.

Keefe, D.L., Liu, L., 2009. Telomeres and reproductive aging. Reprod Fertil Dev 21, 10-14.

Keefe, D.L., Marquard, K., Liu, L., 2006. The telomere theory of reproductive senescence in women. Curr Opin Obstet Gynecol 18, 280-285.

Kidd, S.A., Eskenazi, B., Wyrobek, A.J., 2001. Effects of male age on semen quality and fertility: a review of the literature. Fertil Steril 75, 237-248.

Kim, N., Piatyszek, M., Prowse, K., Harley, C., West, M., Ho, P., Coviello, G., Wright, W., Weinrich, S., Shay, J., 1994. Specific association of human telomerase activity with immortal cells and cancer. Science 266, 2011-2015.

Kim, S.H., Kaminker, P., Campisi, J., 1999. TIN2, a new regulator of telomere length in human cells. Nat Genet 23, 405-412.

Kimura, M., Cherkas, L.F., Kato, B.S., Demissie, S., Hjelmborg, J.B., Brimacombe, M., Cupples, A., Hunkin, J.L., Gardner, J.P., Lu, X., Cao, X., Sastrasinh, M., Province, M.A., Hunt, S.C., Christensen, K., Levy, D., Spector, T.D., Aviv, A., 2008. Offspring's leukocyte telomere length, paternal age, and telomere elongation in sperm. PLoS Genet 4, e37.

Klutstein, M., Fennell, A., Fernandez-Alvarez, A., Cooper, J.P., 2015. The telomere bouquet regulates meiotic centromere assembly. Nat Cell Biol 17, 458-469.

Kovanci, E., Kovacs, T., Moretti, E., Vigue, L., Bray-Ward, P., Ward, D.C., Huszar, G., 2001. FISH assessment of aneuploidy frequencies in mature and immature human spermatozoa classified by the absence or presence of cytoplasmic retention. Hum Reprod 16, 1209–1217.

Kozik, A., Bradbury, E.M., Zalensky, A., 1998. Increased telomere size in sperm cells of mammals with long terminal (TTAGGG)n arrays. Mol Reprod Dev 51, 98-104.

Kurjanowicz, P., Moskovtsev, S., Librach, C., 2017. Genomic fragmentation and extrachromosomal telomeric repeats impact assessment of telomere length in human spermatozoa: quantitative experiments and systematic review. Hum Reprod 32, 2170-2177.

Kyo, S., Takakura, M., Kanaya, T., Zhuo, W., Fujimoto, K., Nishio, Y., Orimo, A., Inoue, M., 1999. Estrogen activates telomerase. Cancer Res 59, 5917-5921.

Lan, Q., Cawthon, R., Shen, M., Weinstein, S.J., Virtamo, J., Lim, U., Hosgood 3rd, H.D., Albanes, D., Rothman, N., 2009. A prospective study of telomere length measured by monochrome multiplex quantitative PCR and risk of non-Hodgkin lymphoma. Clin Cancer Res 15, 7429-7433.

Laqqan, M., Tierling, S., Alkhaled, Y., LoPorto, C., Hammadeh, M.E., 2017. Alterations in sperm DNA methylation patterns of oligospermic males. Reprod Biol 17, 396-400.

Lee, H.W., Blasco, M.A., Gottlieb, G.J., Horner, J.W., Greider, C.W., DePinho, R.A., 1998. Essential role of mouse telomerase in highly proliferative organs. Nature 392, 569-574.

Lee, S.S., Bohrson, C., Pike, A.M., Wheelan, S.J., Greider, C.W., 2015. ATM kinase is required for telomere elongation in mouse and human cells. Cell Rep 13, 1623-1632.

Levine, R.L., Garland, D., Oliver, C.N., Amici, A., Climent, I., Lenz, A.G., Ahn, B.W., Shaltiel, S., Stadtman, E.R., 1990. Determination of carbonyl content in oxidatively modified proteins. Methods Enzymol 186, 464-478.

Li, B., Oestreich, S., de Lange, T., 2000. Identification of human Rap1: implications for telomere evolution. Cell 101, 471-483.

Lin, C., Yang, D., 2017. Human telomeric G-quadruplex structures and G-quadruplex-interactive compounds. Methods Mol Biol 1587, 171-196.

Liu, D., O'Connor, M.S., Qin, J., Songyang, Z., 2004a. Telosome, a mammalian telomere-associated complex formed by multiple telomeric proteins. J Biol Chem 279, 51338-51342.

Liu, J.P., 2014. Molecular mechanisms of ageing and related diseases. Clin Exp Pharmacol Physiol 41, 445-458.

Liu, L., Bailey, S.M., Okuka, M., Munoz, P., Li, C., Zhou, L., Wu, C., Czerwiec, E., Sandler, L., Seyfang, A., Blasco, M.A., Keefe, D.L., 2007. Telomere lengthening early in development. Nat Cell Biol 9, 1436-1441.

Liu, L., Blasco, M.A., Trimarchi, J.R., Keefe, D.L., 2002. An essential role for functional telomeres in mouse germ cells during fertilization and early development. Dev Biol 249, 74-84.

Liu, L., Franco, S., Spyropoulos, B., Moens, P.B., Blasco, M.A., Keefe, D.L., 2004b. Irregular telomeres impair meiotic synapsis and recombination in mice. Proc Natl Acad Sci U S A 101, 6496-6501.

Madureira, C., Cunha, M., Sousa, M., Neto, A.P., Pinho, M.J., Viana, P., Gonçalves, A., Silva, J., Teixeira da Silva, J., Oliveira, C., Ferraz, L., Doria, S., Carvalho, F., Barros, A., 2014. Treatment by testicular sperm extraction and intracytoplasmic sperm injection of 65 azoospermic patients with non-mosaic Klinefelter syndrome with birth of 17 healthy children. Andrology 2, 623-631.

Majzoub, A., Agarwal, A., Cho, C.L., Esteves, S.C., 2017. Sperm DNA fragmentation testing: a cross sectional survey on current practices of fertility specialists. Transl Androl Urol 6, S710-S719.

Mania, A., Mantzouratou, A., Delhanty, J.D., Baio, G., Serhal, P., Sengupta, S.B., 2014. Telomere length in human blastocysts. Reprod Biomed Online 28, 624-637.

Marques, C.J., Barros, A., Sousa, M., 2011. Sperm epigenetic profile, in: Zini, A., Agarwal, A. (Eds.), Sperm chromatin: biological and clinical applications in male infertility and assisted reproduction. Springer, New York, p. 243.

Marques, C.J., Sousa, M., 2013. Imprinted gene anomalies in sperm, in: Carrell, D.T. (Ed.), Paternal influences on human reproductive success. Cambridge University Press, Cambridge, p. 27.

McClintock, B., 1941. The stability of broken ends of chromosomes in Zea mays. Genetics 26, 234–282.

McEachern, M.J., Krauskopf, A., Blackburn, E.H., 2000. Telomeres and their control. Annu Rev Genet 34, 331-358.

Mehdi, M., Gmidene, A., Brahem, S., Guerin, J.F., Elghezal, H., Saad, A., 2012. Aneuploidy rate in spermatozoa of selected men with severe teratozoospermia. Andrologia 44 Suppl 1, 139-143.

Meyne, J., Ratliff, R.L., Moyzis, R.K., 1989. Conservation of the human telomere sequence (TTAGGG)n among vertebrates. Proc Natl Acad Sci U S A 86, 7049-7053.

Millan, N.M., Lau, P., Hann, M., Ioannou, D., Hoffman, D., Barrionuevo, M., Maxson, W., Ory, S., Tempest, H.G., 2012. Hierarchical radial and polar organisation of chromosomes in human sperm. Chromosome Res 20, 875-887.

Min, J., Wright, W.E., Shay, J.W., 2017. Alternative lengthening of telomeres can be maintained by preferential elongation of lagging strands. Nucleic Acids Res 45, 2615-2628.

Montpetit, A.J., Alhareeri, A.A., Montpetit, M., Starkweather, A.R., Elmore, L.W., Filler, K., Mohanraj, L., Burton, C.W., Menzies, V.S., Lyon, D.E., Jackson-Cook, C.K., 2014. Telomere length: a review of methods for measurement. Nurs Res 63, 289-299.

Moreno-Palomo, J., Creus, A., Marcos, R., Hernández, A., 2014. Genomic instability in newborn with short telomeres. PLoS One 9, e91753.

Moskovtsev, S.I., Willis, J., White, J., Mullen, J.B., 2010. Disruption of telomere-telomere interactions associated with DNA damage in human spermatozoa. Syst Biol Reprod Med 56, 407-412.

Moyzis, R.K., Buckingham, J.M., Cram, L.S., Dani, M., Deaven, L.L., Jones, M.D., Meyne, J., Ratliff, R.L., Wu, J.R., 1988. A highly conserved repetitive DNA sequence, (TTAGGG)., present at the telomeres of human chromosomes. Proc Natl Acad Sci U S A 85, 6622-6626.

Mudrak, O., Tomilin, N., Zalensky, A., 2005. Chromosome architecture in the decondensing human sperm nucleus. J Cell Sci 118, 4541-4550.

Mudrak, O.S., Nazarov, I.B., Jones, E.L., Zalensky, A.O., 2012. Positioning of chromosomes in human spermatozoa is determined by ordered centromere arrangement. PLoS One 7, e52944.

Mukaka, M.M., 2012. Statistics corner: a guide to appropriate use of correlation coefficient in medical research. Malawi Med J 24, 69-71.

Muller, H.J., 1938. The remaking of chromosomes. Collect Net 13, 181-198.

Muriel, L., Goyanes, V., Segrelles, E., Gosalvez, J., Alvarez, J.G., Fernandez, J.L., 2007. Increased aneuploidy rate in sperm with fragmented DNA as determined by the sperm chromatin dispersion (SCD) test and FISH analysis. J Androl 28, 38-49.

Nagaoka, S.I., Hassold, T.J., Hunt, P.A., 2012. Human aneuploidy: mechanisms and new insights into an age-old problem. Nat Rev Genet 13, 493-504.

Nakamura, T.M., Morin, G.B., Chapman, K.B., Weinrich, S.L., Andrews, W.H., Lingner, J., Harley, C.B., Cech, T.R., 1997. Telomerase catalytic subunit homologs from fission yeast and human. Science 277, 955-959.

Nandakumar, J., Cech, T.R., 2013. Finding the end: recruitment of telomerase to telomeres. Nat Rev Mol Cell Biol 14, 69-82.

Njajou, O.T., Cawthon, R.M., Damcott, C.M., Wu, S.H., Ott, S., Garant, M.J., Blackburn, E.H., Mitchell, B.D., Shuldiner, A.R., Hsueh, W.C., 2007. Telomere length is paternally inherited and is associated with parental lifespan. Proc Natl Acad Sci U S A. 104, 12135–12139.

Nordfjall, K., Svenson, U., Norrback, K.F., Adolfsson, R., Roos, G., 2010. Large-scale parent-child comparison confirms a strong paternal influence on telomere length. Eur J Hum Genet 18, 385-389.

O'Callaghan, N., Dhillon, V., Thomas, P., Fenech, M., 2008. A quantitative real-time PCR method for absolute telomere length. Biotechniques 44, 807-809.

Oliveira, P.F., Sousa, M., Silva, B.M., Monteiro, M.P., Alves, M.G., 2017. Obesity, energy balance and spermatogenesis. Reproduction 153, R173-R185.

Olovnikov, A.M., 1973. A theory of marginotomy. The incomplete copying of template margin in enzymic synthesis of polynucleotides and biological significance of the phenomenon. J Theor Biol 41, 181-190.

Palm, W., de Lange, T., 2008. How shelterin protects mammalian telomeres. Annu Rev Genet 42, 301-334.

Pereira, R., Oliveira, J., Ferraz, L., Barros, A., Santos, R., Sousa, M., 2015. Mutation analysis in patients with total sperm immotility. J Assist Reprod Genet 32, 893–902.

Pereira, R., Sá, R., Barros, A., Sousa, M., 2017. Major regulatory mechanisms involved in sperm motility. Asian J Androl 19, 5-14.

Pickett, H.A., Cesare, A.J., Johnston, R.L., Neumann, A.A., Reddel, R.R., 2009. Control of telomere length by a trimming mechanism that involves generation of t-circles. EMBO J 28, 799-809.

Pickett, H.A., Henson, J.D., Au, A.Y., Neumann, A.A., Reddel, R.R., 2011. Normal mammalian cells negatively regulate telomere length by telomere trimming. Hum Mol Genet 20, 4684-4692.

Pickett, H.A., Reddel, R.R., 2012. The role of telomere trimming in normal telomere length dynamics. Cell Cycle 11, 1309-1315.

Pickett, H.A., Reddel, R.R., 2015. Molecular mechanisms of activity and derepression of alternative lengthening of telomeres. Nat Struct Mol Biol 22, 875-880.

Pinto, F., Oliveira, C., Cardoso, M.F., Teixeira-da-Silva, J., Silva, J., Sousa, M., Barros, A., 2009. Impact of GnRH ovarian stimulation protocols on intracytoplasmic sperm injection outcomes. Reprod Biol Endocrinol 7, 5.

Polani, P.E., Crolla, J.A., 1991. A test of the production line hypothesis of mammalian oogenesis. Hum Genet 88, 64-70.

Price, C.M., 1997. Synthesis of the telomeric C-strand. A review. Biochemistry (Mosc) 62, 1216-1223.

Radesic, B., Tremellen, K., 2011. Oocyte maturation employing a GnRH agonist in combination with low-dose hCG luteal rescue minimizes the severity of ovarian hyperstimulation syndrome while maintaining excellent pregnancy rates. Hum Reprod 26, 3437-3442.

Raschenberger, J., Lamina, C., Haun, M., Kollerits, B., Coassin, S., Boes, E., Kedenko, L., Kottgen, A., Kronenberg, F., 2016. Influence of DNA extraction methods on relative telomere length measurements and its impact on epidemiological studies. Sci Rep 6, 25398.

Rathke, C., Baarends, W.M., Awe, S., Renkawitz-Pohl, R., 2014. Chromatin dynamics during spermiogenesis. Biochim Biophys Acta 1839, 155-168.

Reddel, R.R., 2003. Alternative lengthening of telomeres, telomerase, and cancer. Cancer Lett 194, 155-162.

Reig-Viader, R., Brieno-Enriquez, M.A., Khoriauli, L., Toran, N., Cabero, L., Giulotto, E., Garcia-Caldes, M., Ruiz-Herrera, A., 2013. Telomeric repeat-containing RNA and telomerase in human fetal oocytes. Hum Reprod 28, 414-422.

Reig-Viader, R., Capilla, L., Vila-Cejudo, M., Garcia, F., Anguita, B., Garcia-Caldes, M., Ruiz-Herrera, A., 2014a. Telomere homeostasis is compromised in spermatocytes from patients with idiopathic infertility. Fertil Steril 102, 728-738.e721.

Reig-Viader, R., Garcia-Caldes, M., Ruiz-Herrera, A., 2016. Telomere homeostasis in mammalian germ cells: a review. Chromosoma 125, 337-351.

Reig-Viader, R., Vila-Cejudo, M., Vitelli, V., Busca, R., Sabate, M., Giulotto, E., Caldes, M.G., Ruiz-Herrera, A., 2014b. Telomeric repeat-containing RNA (TERRA) and telomerase are components of telomeres during mammalian gametogenesis. Biol Reprod 90, 103.

Ren, H., Ferguson, K., Kirkpatrick, G., Vinning, T., Chow, V., Ma, S., 2016. Altered crossover distribution and frequency in spermatocytes of infertile men with azoospermia. PLoS One 11, e0156817.

Rhodes, D., Lipps, H.J., 2015. G-quadruplexes and their regulatory roles in biology. Nucleic Acids Res 43, 8627-8637.

Ricci, G., Perticarari, S., Fragonas, E., Giolo, E., Canova, S., Pozzobon, C., Guaschino, S., Presani, G., 2002. Apoptosis in human sperm: its correlation with semen quality and the presence of leukocytes. Hum Reprod 17, 2665-2672.

Rocca, M.S., Speltra, E., Menegazzo, M., Garolla, A., Foresta, C., Ferlin, A., 2016. Sperm telomere length as a parameter of sperm quality in normozoospermic men. Hum Reprod 31, 1158-1163.

Sá, R., Cunha, M., Rocha, E., Barros, A., Sousa, M., 2015. Sperm DNA fragmentation is related to sperm morphological staining patterns. Reprod Biomed Online 31, 506-515.

Salvador, L., Singaravelu, G., Harley, C.B., Flom, P., Suram, A., Raffaele, J.M., 2016. A natural product telomerase activator lengthens telomeres in humans: a randomized, double blind, and placebo controlled study. Rejuvenation Res 19, 478-484.

Samassekou, O., Gadji, M., Drouin, R., Yan, J., 2010. Sizing the ends: normal length of human telomeres. Ann Anat 192, 284-291.

Santiso, R., Tamayo, M., Gosalvez, J., Meseguer, M., Garrido, N., Fernandez, J.L., 2010. Swim-up procedure selects spermatozoa with longer telomere length. Mutat Res 688, 88-90.

Schaetzlein, S., Lucas-Hahn, A., Lemme, E., Kues, W.A., Dorsch, M., Manns, M.P., Niemann, H., Rudolph, K.L., 2004. Telomere length is reset during early mammalian embryogenesis. Proc Natl Acad Sci U S A 101, 8034-8038.

Scherthan, H., 2007. Telomere attachment and clustering during meiosis. Cell Mol Life Sci 64, 117-124.

Schmid, T.E., Eskenazi, B., Baumgartner, A., Marchetti, F., Young, S., Weldon, R., Anderson, D., Wyrobek, A.J., 2007. The effects of male age on sperm DNA damage in healthy non-smokers. Hum Reprod 22, 180-187.

Schmidt, J.C., Cech, T.R., 2015. Human telomerase biogenesis, trafficking, recruitment, and activation. Genes Dev 29, 1095–1105.

Schrader, M., Müller, M., Schulze, W., Heicappell, R., Krause, H., Straub, B., Miller, K., 2002. Quantification of the expression level of the gene encoding the catalytic subunit of telomerase in testicular tissue specimens predicts successful sperm recovery. Hum Reprod 17, 150-156.

Shah, K., Sivapalan, G., Gibbons, N., Tempest, H., Griffin, D.K., 2003. The genetic basis of infertility. Reproduction 126, 13-25.

Sharbatoghli, M., Valojerdi, M.R., Amanlou, M., Khosravi, F., Jafar-abadi, M.A., 2012. Relationship of sperm DNA fragmentation, apoptosis and dysfunction of mitochondrial membrane potential with semen parameters and ART outcome after intracytoplasmic sperm injection. Arch Gynecol Obstet 286, 1315-1322.

Sharma, G.G., Gupta, A., Wang, H., Scherthan, H., Dhar, S., Gandhi, V., Iliakis, G., Shay, J.W., Young, C.S., Pandita, T.K., 2003. hTERT associates with human telomeres and enhances genomic stability and DNA repair. Oncogene 22, 131-146.

Sharma, R., Agarwal, A., 2011. Spermatogenesis: an overview, in: Zini, A., Agarwal, A. (Eds.), Sperm chromatin: biological and clinical applications in male infertility and assisted reproduction. Springer, New York, p. 19.

Shay, J.W., 2016. Role of Telomeres and Telomerase in Aging and Cancer. Cancer Discov 6, 584-593.

Shay, J.W., Wright, W.E., 2011. Role of telomeres and telomerase in cancer. Semin Cancer Biol 21, 349-353.

Simpson, J.L., Wells, D., 2014. Telomere length and aneuploidy: clinical and biological insights into human preimplantation embryos. Reprod Biomed Online 28, 531-532.

Singh, N.P., Muller, C.H., Berger, R.E., 2003. Effects of age on DNA double-strand breaks and apoptosis in human sperm. Fertil Steril 80, 1420-1430.

Smogorzewska, A., de Lange, T., 2004. Regulation of telomerase by telomeric proteins. Annu Rev Biochem 73, 177-208.

Solov'eva, L., Svetlova, M., Bodinski, D., Zalensky, A.O., 2004. Nature of telomere dimers and chromosome looping in human spermatozoa. Chromosome Res 12, 817-823.

Stern, J.L., Bryan, T.M., 2008. Telomerase recruitment to telomeres. Cytogenet Genome Res 122, 243-254.

Stewart, S.A., Ben-Porath, I., Carey, V.J., O'Connor, B.F., Hahn, W.C., Weinberg, R.A., 2003. Erosion of the telomeric single-strand overhang at replicative senescence. Nat Genet 33, 492-496.

Stindl, R., 2016. The paradox of longer sperm telomeres in older men's testes: a birth-cohort effect caused by transgenerational telomere erosion in the female germline. Mol Cytogenet 9, 12.

Szostak, J.W., Blackburn, E.H., 1982. Cloning yeast telomeres on linear plasmid vectors. Cell 29, 245-255.

Tchkonia, T., Zhu, Y., van Deursen, J., Campisi, J., Kirkland, J.L., 2013. Cellular senescence and the senescent secretory phenotype: therapeutic opportunities. J Clin Invest 123, 966-972.

Tesarik, J., Sousa, M., 1995. Key elements of a highly efficient intracytoplasmic sperm injection technique: Ca2+ fluxes and oocyte cytoplasmic dislocation. Fertil Steril 64, 770-776.

Thilagavathi, J., Kumar, M., Mishra, S.S., Venkatesh, S., Kumar, R., Dada, R., 2013a. Analysis of sperm telomere length in men with idiopathic infertility. Arch Gynecol Obstet 287, 803-807.

Thilagavathi, J., Mishra, S.S., Kumar, M., Vemprala, K., Deka, D., Dhadwal, V., Dada, R., 2013b. Analysis of telomere length in couples experiencing idiopathic recurrent pregnancy loss. J Assist Reprod Genet 30, 793-798.

Thilagavathi, J., Venkatesh, S., Dada, R., 2013c. Telomere length in reproduction. Andrologia 45, 289-304.

Tommerup, H., Dousmanis, A., de Lange, T., 1994. Unusual chromatin in human telomeres. Mol Cell Biol 14, 5777-5785.

Treff, N.R., Su, J., Taylor, D., Scott, R.T., Jr., 2011. Telomere DNA deficiency is associated with development of human embryonic aneuploidy. PLoS Genet 7, e1002161.

Turner, S., Hartshorne, G.M., 2013. Telomere lengths in human pronuclei, oocytes and spermatozoa. Mol Hum Reprod 19, 510-518.

Turner, S., Wong, H.P., Rai, J., Hartshorne, G.M., 2010. Telomere lengths in human oocytes, cleavage stage embryos and blastocysts. Mol Hum Reprod 16, 685-694.

Ulaner, G.A., Giudice, L.C., 1997. Developmental regulation of telomerase activity in human fetal tissues during gestation. Mol Hum Reprod 3, 769-773.

Unryn, B.M., Cook, L.S., Riabowol, K.T., 2005. Paternal age is positively linked to telomere length of children. Aging Cell 4, 97-101.

Vandervorst, M., Liebaers, I., Sermon, K., Staessen, C., De Vos, A., Van de Velde, H., Van Assche, E., Joris, H., Van Steirteghem, A., Devroey, P., 1998. Successful preimplantation genetic diagnosis is related to the number of available cumulus-oocyte complexes. Hum Reprod 13, 3169-3176.

Vegetti, W., Van Assche, E., Frias, A., Verheyen, G., Bianchi, M.M., Bonduelle, M., Liebaers, I., Van Steirteghem, A., 2000. Correlation between semen parameters and sperm aneuploidy rates investigated by fluorescence in-situ hybridization in infertile men. Hum Reprod 15, 351-365.

Vidačeka, N.Š., Ćukušića, A., Ivankovića, M., Fulgosi, H., Huzak, M., Smith, J.R., Rubelj, I., 2010. Abrupt telomere shortening in normal human fibroblasts. Exp Gerontol 45, 235-242.

von Zglinicki, T., 2002. Oxidative stress shortens telomeres. Trends Biochem Sci 27, 339-344.

Wang, C.W., Yao, D.S., Horng, S.G., Chiu, H.C., Chen, C.K., Lee, C.L., Huang, H.Y., Wang, H.S., Soong, Y.K., Pao, C.C., 2004. Feasibility of human telomerase reverse transcriptase mRNA expression in individual blastomeres as an indicator of early embryo development. J Assist Reprod Genet 21, 163-168.

Watson, J.D., 1972. Origin of concatemeric T7 DNA. Nat New Biol 239, 197-201.

Weinrich, S.L., Pruzan, R., Ma, L., Ouellette, M., Tesmer, V.M., Holt, S.E., Bodnar, A.G., Lichtsteiner, S., Kim, N.W., Trager, J.B., Taylor, R.D., Carlos, R., Andrews, W.H., Wright,

W.E., Shay, J.W., Harley, C.B., Morin, G.B., 1997. Reconstitution of human telomerase with the template RNA component hTR and the catalytic protein subunit hTRT. Nat Genet 17, 498-502.

World Health Organization, 1999. WHO laboratory manual for the examination of human semen and sperm-cervical mucus interaction, 4th ed. Cambridge University Press, Cambridge.

World Health Organization, 2010. WHO laboratory manual for the examination and processing of human semen, 5th ed. World Health Organization, Geneva, Switzerland.

Wright, D.L., Jones, E.L., Mayer, J.F., Oehninger, S., Gibbons, W.E., Lanzendorf, S.E., 2001. Characterization of telomerase activity in the human oocyte and preimplantation embryo. Mol Hum Reprod 7, 947-955.

Wright, W.E., Piatyszek, M.A., Rainey, W.E., Byrd, W., Shay, J.W., 1996. Telomerase activity in human germline and embryonic tissues and cells. Dev Genet 18, 173-179.

Wright, W.E., Tesmer, V.M., Huffman, K.E., Levene, S.D., Shay, J.W., 1997. Normal human chromosomes have long G-rich telomeric overhangs at one end. Genes Dev 11, 2801-2809.

Wright, W.E., Tesmer, V.M., Liao, M.L., Shay, J.W., 1999. Normal human telomeres are not late replicating. Exp Cell Res 251, 492-499.

Wu, L., Multani, A.S., He, H., Cosme-Blanco, W., Deng, Y., Deng, J.M., Bachilo, O., Pathak, S., Tahara, H., Bailey, S.M., Deng, Y., Behringer, R.R., Chang, S., 2006. Pot1 deficiency initiates DNA damage checkpoint activation and aberrant homologous recombination at telomeres. Cell 126, 49-62.

Wu, Y., Xiao, S., Zhu, X.D., 2007. MRE11-RAD50-NBS1 and ATM function as co-mediators of TRF1 in telomere length control. Nat Struct Mol Biol 14, 832-840.

Yan, L., Wu, S., Zhang, S., Ji, G., Gu, A., 2014. Genetic variants in telomerase reverse transcriptase (TERT) and telomerase-associated protein 1 (TEP1) and the risk of male infertility. Gene 534, 139-143.

Yang, Q., Zhang, N., Zhao, F., Zhao, W., Dai, S., Liu, J., Bukhari, I., Xin, H., Niu, W., Sun, Y., 2015a. Processing of semen by density gradient centrifugation selects spermatozoa with longer telomeres for assisted reproduction techniques. Reprod Biomed Online 31, 44-50.

Yang, Q., Zhao, F., Dai, S., Zhang, N., Zhao, W., Bai, R., Sun, Y., 2015b. Sperm telomere length is positively associated with the quality of early embryonic development. Hum Reprod 30, 1876-1881.

Yashima, K., Maitra, A., Rogers, B.B., Timmons, C.F., Rathi, A., Pinar, H., Wright, W.E., Shay, J.W., Gazdar, A.F., 1998. Expression of the RNA component of telomerase during human development and differentiation. Cell Growth Differ 9, 805-813.

Ye, J.Z., Hockemeyer, D., Krutchinsky, A.N., Loayza, D., Hooper, S.M., Chait, B.T., de Lange, T., 2004. POT1-interacting protein PIP1: a telomere length regulator that recruits POT1 to the TIN2/TRF1 complex. Genes Dev 18, 1649-1654.

Zalenskaya, I.A., Bradbury, E.M., Zalensky, A.O., 2000. Chromatin structure of telomere domain in human sperm. Biochem Biophys Res Commun 279, 213-218.

Zalensky, A., Zalenskaya, I., 2007. Organization of chromosomes in spermatozoa an additional layer of epigenetic information. Biochem Soc Trans 35, 609-611.

Zalensky, A.O., Allen, M.J., Kobayashi, A., Zalenskaya, I.A., Balhórn, R., Bradbury, E.M., 1995. Well-defined genome architecture in the human sperm nucleus. Chromosoma 103, 577-590.

Zalensky, A.O., Tomilin, N.V., Zalenskaya, I.A., Teplitz, R.L., Bradbury, E.M., 1997. Telomere-telomere interactions and candidate telomere binding protein(s) in mammalian sperm cells. Exp Cell Res 232, 29-41.

Zeng, S., Liu, L., Sun, Y., Xie, P., Hu, L., Yuan, D., Chen, D., Ouyang, Q., Lin, G., Lu, G., 2014. Telomerase-mediated telomere elongation from human blastocysts to embryonic stem cells. J Cell Sci 127, 752-762.

Zhao, F., Yang, Q., Shi, S., Luo, X., Sun, Y., 2016. Semen preparation methods and sperm telomere length: density gradient centrifugation versus the swim up procedure. Sci Rep 6, 39051.

Zhao, Z., Pan, X., Liu, L., Liu, N., 2014. Telomere length maintenance, shortening, and lengthening. J Cell Physiol 229, 1323-1329.

7. Appendices

Appendix A

Table A.1 – Summary of the results collected from studies assessing STL and stablishing positive or negative associations between STL and seminal parameters, DNA quality or clinical and embryological outcomes.

Ref	n	Patient age (years)	STL assessment	Statistically significant[a] STL-parameter associations													
				Positive										Negative			
				Age	Progressive sperm motility	Sperm concentration	Total sperm count	Sperm vitality	Sperm normal morphology	Sperm chromatin maturity	Good quality embryos	Fertilization rate	Pregnancy rate	ROS content	Sperm diploidy	Sperm aneuploidy	Sperm DNA fragmentation
Antunes et al., 2015	10	39.6 ± 6.0	SCT-pqPCR	Yes	Yes	Yes	-	-	No	-	-	-	-	-	-	-	-
Turner and Hartshorne, 2013	45	35.5 ± 0.99	Q-FISH	Yes	No	No	-	-	No	-	-	-	No (BP/CP)	-	-	-	No
Yang et al., 2015b	418	30.3 ± 4.0	Q-PCR	Yes	-	-	Yes	-	-	-	Yes	No	No (CP)	-	-	-	-
Ferlin et al., 2013	81	18–19	Q-PCR	-	-	-	Yes	-	-	-	-	-	-	-	-	-	-
Rocca et al., 2016	100	34.0 ± 8.6	Q-PCR	No	Yes	No	No	Yes	No	Yes	-	-	-	-	-	-	Yes
Thilagavathi et al., 2013a	57	-	Q-PCR	No	No	No	-	-	No	-	-	-	-	No	-	-	No
Yang et al., 2015a	105	31.2 ± 6.1	Q-PCR	-	b	Yes	-	-	-	-	-	-	-	-	-	-	c
Cariati et al., 2016	73	39.4 ± 5.5	Q-PCR	-	-	Yes	-	-	-	-	-	-	Yes (OP)	-	Yes	No	No
Santiso et al., 2010	27	-	Q-PCR	-	d	-	-	-	-	-	-	-	-	-	-	-	No
Zhao et al., 2016	150	31.76 ± 6.11	Q-PCR	No	Yes	No	Yes	-	No	-	-	-	-	Yes	-	-	Yes

STL: sperm telomere length; SCT-pqPCR: single-cell telomere length assay; Q-FISH: quantitative fluorescence in situ hybridization; Q-PCR: quantitative polymerase chain reaction. Patient age: mean ± standard deviation (range); BP: biochemical pregnancy; CP: clinical pregnancy; OP: ongoing pregnancy. a) $p<0.05$. b) Significant statistical increase of STL in sperm selected by density gradient centrifugation. c) Significant statistical decrease of DNA fragmentation in sperm selected by density gradient centrifugation. d) Significant statistical increase of STL in sperm selected by swim-up.

Appendix B

Table B.1 – Comparison of relative sperm telomere length in subgroups determined for sperm DNA fragmentation, **s**perm chromatin maturity, sperm chromosomic alterations, seminal parameters, male age, infertility factors and clinical parameters.

Relative STL's subgroups	n	Mean±SD	Median	Test	p
Seminal parameters					
Concentration ≤10 (×10^6/ejaculate)	7	6.03±2.06	5.00	Kruskal-Wallis	0.27
Concentration >10-<20 (×10^6/ejaculate)	9	5.03±1.57	4.99		
Concentration ≥20 (×10^6/ejaculate)	57	5.15±3.58	4.43		
Concentration <15 (×10^6/ejaculate)	11	5.38±1.90	4.99	Mann-Whitney *U*	0.367
Concentration ≥15 (×10^6/mL)	62	5.19±3.46	4.46		
Total sperm count <39 (×10^6/ejaculate)	9	5.50±2.09	4.56	Mann-Whitney *U*	0.397
Total sperm count ≥39 (×10^6/ejaculate)	64	5.18±3.41	4.63		
Total Motility <40%	9	5.29±1.83	5.48	Mann-Whitney *U*	0.465
Total Motility ≥40%	64	5.21±3.43	4.53		
Progressive Motility <32%	9	5.31±1.83	5.64	Mann-Whitney *U*	0.445
Progressive Motility ≥32%	64	5.21±3.43	4.53		
Progressive Rapid Motility ≤5%	7	5.23±2.37	6.16	Kruskal-Wallis	0.672
Progressive Rapid Motility >5- <15%	5	5.67±2.16	5.64		
Progressive Rapid Motility ≥15-<25%	19	4.60±2.08	4.01		
Progressive Rapid Motility ≥25%	41	5.48±3.95	4.83		
Normal morphology ≤1%	14	4.24±1.56	4.01	Kruskal-Wallis	0.471
Normal morphology >1-<4%	18	4.62±1.86	4.66		
Normal morphology ≥4-<10%	29	6.13±4.52	4.76		
Normal morphology ≥10%	10	5.45±2.38	5.03		
Sperm DNA fragmentation (%)					
TUNEL+ <30.6	30	5.78±4.50	4.80	*t*-test	0.71
TUNEL+ ≥30.6	8	4.64±1.83	4.54		
H+ <30.6	15	4.22±1.43	4.12	*t*-test	0.161
H+ ≥30.6	23	6.40±4.99	5.00		
AVR+ <30.6	34	5.69±4.29	4.80	*t*-test	0.619
AVR+ ≥30.6	4	4.25±1.39	4.57		
ER+ <30.6	30	5.95±4.45	4.92	Mann-Whitney *U*	0.259
ER+ ≥30.6	8	3.99±1.68	3.99		
PAR+ <30.6	28	6.00±4.62	4.95	*t*-test	0.294
PAR+ ≥30.6	10	4.24±1.51	4.44		
Sperm chromatin maturity (%)					
AB- <50	14	5.91±4.27	5.10	One-way ANOVA	0.231
AB- ≥50-<70	17	5.83±4.55	4.76		
AB- ≥70-<80	6	4.82±1.99	4.65		
AB- ≥80	3	2.64±1.22	2.29		
Sperm chromosomic alterations					
Euploidy rate	8	5.96±5.61	4.20	Mann-Whitney *U*	0.839
Aneuploidy rate	35	5.38±3.70	4.76		

Male age (years)					
Male age <35	17	4.86±2.29	4.96	Mann-Whitney *U*	0.857
Male age ≥35	64	5.31±3.39	4.66		
Infertility factors					
Male	28	5.13±3.34	4.33	One-way ANOVA	0.190
Female	30	5.93±3.74	4.94		
Female + Male	6	4.25±1.04	4.70		
Female + Female	9	3.76±1.34	3.62		
Clinical parameters					
OP	5	8.26±6.61	6.17	One-way ANOVA	0.172
CP	4	3.54±1.51	3.19		
BP	3	3.39±0.71	3.55		
NP (w/ ETC)	10	5.03±2.00	5.14		

STL: sperm telomere length; H: head; AVR: acrosomal vesicle region; ER: equatorial region; PAR: post-acrosomal region; OP: ongoing pregnancy; CP: clinical pregnancy; BP: biochemical pregnancy; NP: non-pregnancy; ECT: embryo transfer cycles.

Appendix C

Table C.1 – Correlation of relative sperm telomere length from the different clinical groups, according to WHO 2010 guidelines, with the sperm oxidative profile, sDNAfrag, sperm chromatin maturity, sperm chromosomic alterations, seminal parameters and male age, when the n was ≥3. P<0.05 is presented in bold.

Clinical subgroup	Parameter	n	r_p	r_s	p
NZ					
	Carbonylation (protein expression)	25	-0.072		0.731
	TUNEL+ (%)	22		0.025	0.913
	AVR+ (%)	22		0.053	0.814
	ER+ (%)	22	-0.251		0.26
	PAR+ (%)	22	-0.464		**0.03**
	H+ (%)	22	0.313		0.156
	AB- (%)	22		-0.027	0.905
	Euploidies (%)	25	-0.046		0.827
	Aneuploidies (%)	25		0.114	0.587
	Total sperm count (×10^6/ejaculate)	33	0.361		**0.039**
	Concentration (×10^6/mL)	33	0.188		0.294
	Total motility (%)	33	-0.176		0.328
	Progressive motility (%)	33	-0.113		0.53
	Progressive rapid motility (%)	33	0.285		0.108
	Normal morphology (%)	33		-0.053	0.768
	Male age (years)	33	0.153		0.394
OZ					
	Carbonylation (protein expression)	3	0.53		0.645
	Total sperm count (×10^6/ejaculate)	11	-0.42		0.199
	Concentration (×10^6/mL)	11	-0.574		0.065
	Total motility (%)	11	-0.252		0.454
	Progressive motility (%)	11	-0.38		0.249
	Progressive rapid motility (%)	11	-0.382		0.246
	Normal morphology (%)	11	-0.092		0.788
	Male age (years)	11	-0.328		0.326
AZ					
	Total sperm count (×10^6/ejaculate)	9	-0.409		0.275
	Concentration (×10^6/mL)	9	-0.428		0.251
	Total motility (%)	9	-0.265		0.491
	Progressive motility (%)	9		-0.894	**0.003**
	Progressive rapid motility (%)	9	-0.298		0.435
	Normal morphology (%)	9	-0.038		0.924
	Male age (years)	9	-0.939		**0.0002**
TZ					
	Carbonylation (protein expression)	18	-0.005		0.985
	TUNEL+ (%)	12	-0.199		0.535
	AVR+ (%)	12	0.085		0.792
	ER+ (%)	12	-0.539		0.071

	PAR+ (%)	12	-0.112		0.486
	H+ (%)	12	0.368		0.24
	AB- (%)	13	-0.74		**0.004**
	Euploidies (%)	15	-0.127		0.652
	Aneuploidies (%)	15		0.141	0.617
	Total sperm count (×10^6/ejaculate)	32	-0.217		0.234
	Concentration (×10^6/mL)	32	-0.288		0.11
	Total motility (%)	32		-0.299	0.097
	Progressive motility (%)	32	-0.393		**0.026**
	Progressive rapid motility (%)	32	-0.303		0.092
	Normal morphology (%)	32		0.189	0.3
	Male age (years)	32	-0.265		0.143
OA					
	Total sperm count (×10^6/ejaculate)	4	-0.931		0.069
	Concentration (×10^6/mL)	4	-0.946		0.054
	Total motility (%)	4	-0.734		0.266
	Progressive motility (%)	4	-0.999		**0.0005**
	Progressive rapid motility (%)	4	-0.299		0.701
	Normal morphology (%)	4	-0.317		0.683
	Male age (years)	4	-0.97		**0.03**
OT					
	Total sperm count (×10^6/ejaculate)	6	-0.867		**0.025**
	Concentration (×10^6/mL)	6	-0.86		**0.028**
	Total motility (%)	6	-0.57		0.238
	Progressive motility (%)	6	-0.718		0.108
	Progressive rapid motility (%)	6	-0.35		0.496
	Normal morphology (%)	6	0.067		0.9
	Male age (years)	6	-0.720		0.106
AT					
	Total sperm count (×10^6/ejaculate)	7	-0.494		0.259
	Concentration (×10^6/mL)	7	-0.586		0.167
	Total motility (%)	7	-0.505		0.247
	Progressive motility (%)	7		-0.778	0.057
	Progressive rapid motility (%)	7	-0.211		0.649
	Normal morphology (%)	7	0.199		0.669
	Male age (years)	7	-0.968		**0.0003**
OAT					
	Total sperm count (×10^6/ejaculate)	3		-1	0.333
	Concentration (×10^6/mL)	3		-1	0.333
	Total motility (%)	3		-1	0.333
	Progressive motility (%)	3		-0.866	0.667
	Progressive rapid motility (%)	3		0	1
	Normal morphology (%)	3		-0.5	1
	Male age (years)	3		-1	0.333

NZ: normozoospermia; OZ: oligozoospermia; AZ: asthenozoospermia; TZ: teratozoospermia; OA: oligoasthenozoospermia; OT: oligoteratozoospermia; OAT: oligoasthenoteratozoospermia; AT: asthenoteratozoospermia; H: head; AVR: acrosomal vesicle region; ER: equatorial region; PAR: post-acrosomal region